Titre: Title:	Physical Beneficiation of Rare Earth Elements by Pickering Emulsification
Auteur: Author:	Rahi Avazpour
Date:	2019
Type:	Mémoire ou thèse / Dissertation or Thesis
Référence: Citation:	Avazpour, R. (2019). Physical Beneficiation of Rare Earth Elements by Pickering Emulsification [Ph.D. thesis, Polytechnique Montréal]. PolyPublie. https://publications.polymtl.ca/3868/

URL de PolyPublie: PolyPublie URL:	https://publications.polymtl.ca/3868/
Directeurs de recherche: Advisors:	Louis Fradette, & Jamal Chaouki
Programme: Program:	Génie chimique

POLYTECHNIQUE MONTRÉAL

affiliée à l'Université de Montréal

Physical beneficiation of rare earth elements by Pickering emulsification

RAHI AVAZPOUR

Département de génie chimique

Thèse présentée en vue de l'obtention du diplôme de *Philosophiæ Doctor*

Génie chimique

Mai 2019

POLYTECHNIQUE MONTRÉAL

affiliée à l'Université de Montréal

Cette thèse intitulée :

Physical beneficiation of rare earth elements by Pickering emulsification

présentée par : **Rahi AVAZPOUR**

en vue de l'obtention du diplôme de *Philosophiæ Doctor*

a été dûment acceptée par le jury d'examen constitué de :

Oumarou SAVADOGO, président

Louis FRADETTE, membre et directeur de recherche

Jamal CHAOUKI, membre et codirecteur de recherche

Jean-Philippe HARVEY, membre

Gervais SOUCY, membre externe

DEDICATION

To NEDA, ASA, ARSHAN and my parents

They patiently supported my lifestyle as a PhD student!

CITATION

"They who know the truth are not equal to those who love it, and they who love it are not equal to those who delight in it." –Confucius

"The knowledge of anything, since all things have causes, is not acquired or complete unless it is known by its causes."- Avicenna

"Be happy for this moment. This moment is your life."- Omar Khayyam

"Imagination is more important than knowledge."- Albert Einstein

ACKNOWLEDGEMENTS

I would like to take this opportunity to express my gratitude to my supervisor Prof. Louis Fradette who fraternal supported me throughout the research project. I am deeply thankful for his aspiring guidance, encouragement and his kindly advice during the work.

In addition, I am sincerely grateful to my supervisor Prof. Jamal Chaouki for all his valuably guidance, paternal constructive criticism and all his kindly supports which bring me into the point.

Also I would like to express my appreciations to Dr.Mohhamad Latifi for his assistance and sharing their illuminating views on a number of issues and coordination related to this research project.

I am thankful to the professors of department of chemical engineering, graduate studies and laboratories' staff at the University POLYTECHNIQUE for all their support. The professors: Basil D. Favis, David Vidal, Fabio Cicoira, Gregory S. Patience, Jason R. Tavares, Jocelyne Doucet, Michel Perrier, Nick Virgilio, Oumarou Savadogo and Patrice Chartrand. The laboratory NAA Cornelia Chilian, Maryam A.Neysani and Darren Hall. The laboratory mixing and emulsification Dr.Emir Tsabet. the secretaries: Monique Malouin, Hélène Chatillon, Valérie Baudart, Kalonji Mblue, Yoan Ayassamipoullé, Brigitte Gagnon, Sophie Aure and laboratory technicians: Gino Robin, Robert Delisle, Martine Lamarche, Sylvie Taillon, Carol Savoie, Manon Leduc, Jérôme Leroy, Daniel Pilon, Matthieu Gauthier and, Wendell Raphael for their availability and continuous kindly helps.

Also, I would like to acknowledge The Natural Sciences and Engineering Research Council of Canada (NSERC) and NIOBEC Company for their financial and technical support.

I would like to express my appreciations to the professors, my friends, my colleagues, students of department of chemical engineering, PEARL and URPEI members for all their help and accompaniment (in an alphabetic order): Adrián C.Garcia, Afshin Fallahi, Alexandre Al-haiek, Amin Solouki, Bahman Yari, Bing Wan, Charles Bruel, Ehsan H.Nasab, El Mahdi

Lakhdissi, Gautier Houriez, Hamed N.Lari, Iman Soleimani, Jaber Shabanian, Jean-Philippe Laviolette, Jean-Michel Tucny, Liling Jin, Luc Charbonneau, Mai Attia, Majid Rasouli, Mohammad Khalil, Mohammad H.Monzavi, Mohammad J.D.Mahboub, Mojtaba Mokhtari, Navid Elahipanah, Odile Vekemans, Philippe Leclerc, Rouzbeh Jafari, Said Samih, Sepehr Hamzehlouia, Sherif Farag, Shuli Shu, Soumaya Benzennou, Yefeng Zhou,

I would also acknowledge my wife for her unwavering support and long patience and my dear parents who without their long-distance support the realization of this thesis would never have been possible.

In the end I would like to give sincerely thanks to merciful God.

RÉSUMÉ

L’émulsion stabilisée par solides (l'ÉSS ou l’émulsion de Pickering) à de nombreuses applications dans la production des matériaux et la synthèse dans différentes industries telles que le pétrole, la pétrochimie, polymères, produits cosmétiques, la transformation des aliments, la peinture, etc., et le plus récemment proposé dans cette étude, pour la séparation physique des minéraux. L'émulsion de Pickering n'utilise que des particules en tant qu'émulsifiant autour des gouttelettes, qui forment une barrière pour limiter la coalescence malgré d'autres émulsions qui utilisent des additifs surfactants pour stabiliser les gouttelettes dans la phase continue. La nouvelle technique utilise l’émulsion de Pickering pour séparer les particules contenant des métaux précieux et plus spécifiquement les minéraux porteurs d’éléments de terres rares (ÉTR) de leurs gangues associées dans le minerai. L’ÉSS peut être utilisée comme alternative à la flottation par mousse conventionnelle (FF) ou même en tant que complément à l'un des procédés en amont / aval dans l'étape d'enrichissement physique pour augmenter les performances de la séparation. Les problèmes économiques et environnementaux de la flottation sont brièvement discutées, au cours de laquelle les tensioactifs, les agents chimiques et les modificateurs de pH devraient être appliqués en plusieurs étapes et constituer de grands défis pour la durabilité du processus global. Il n'y a pas besoin d'agent tensio-actif ou de produits chimiques et donc les minéraux sont en leur surface naturelle dans le processus derrière SSE, ainsi, l'eau et l'huile peuvent être recyclée beaucoup plus facilement que FF. Par conséquent, l'ESS ouvre de nouvelles perspectives économiques et écologiques en vue d'une séparation physique durable des minéraux d’ÉTR. Dans le même temps, l’étude donne une idée d’une application similaire de la SSE dans la séparation des particules précieuses d’une poudre fine donnée dans de nombreuses industries.

Compte tenu de cette application de l'ESS et en raison des grands défis environnementaux liés à l’utilisation de la méthode FF, le projet de recherche vise à étudier d'abord la possibilité d'utiliser l'ESS dans une séparation physique des minéraux d’ÉTR à l'échelle industrielle. l'idée principale consiste à identifier les paramètres qui affectent la sélectivité du processus pendant la phase d’émulsification, y compris les propriétés des phases, la formulation et les conditions de fonctionnement. L'étape suivante consiste à obtenir les conditions optimales pour l'ensemble du processus et de développer un modèle semi-empirique pour le mécanisme derrière la sélectivité pour prédire la récupération et la qualité des produits. Ainsi, quatre sous-objectifs bien définis pour le travail comme articles des chapitres:

Le premier article est une étude de faisabilité pour un procédé SSE visant à produire un concentré de minéraux porteurs d'ÉTR provenant du mélange de minerais et de gangue. Nous avons utilisé le minerai original de la mine NIOBEC au Québec, sur lequel les minéraux les plus abondants porteurs d'ÉTR sont les types de carbonatite de bastnäsite ((Ce, La, Nd, Y) FCO_3) et de monazite ((Ce, La, Nd, Th) PO_4). Les résultats ont montré que les minéraux porteurs d'ÉTR avaient plus d'affinité à l'égard des gouttelettes d'huile que la gangue en raison de leur plus grand angle de contact. Ils ont attaché plus dans l'interface huile-eau que a gangue qui est restée plus dans la phase aqueuse. Le comportement du minerai d'ÉTR dans le système d'émulsion, les propriétés de surface des minéraux à l'interface huile / eau et leur interaction ont été étudiés. La teneur en TREO% (oxyde total de terres rares) dans les produits est calculée sur la base du TREE% total des terres rares obtenue par analyse d'activation neutronique. Nous avons pu démontrer la capacité de l'émulsion de Pickering à séparer et à concentrer les minéraux d'ÉTR, en tenant compte des effets des propriétés de minerai d'alimentation, tels que la taille des particules et la méthode de préparation. Le taux d'enrichissement (TE) après une étape d'émulsification à pH naturel a augmenté jusqu'à 290% avec une récupération supérieure à 50% sans utiliser aucun modificateur de surface, additif ou agent chimique.

Le deuxième article porte sur les effets des conditions de traitement telles que l'intensité du mélange (c.-à-d., la modification du régime vitesse de rotation par minute RPM) et l'uniformité du cisaillement (c.-à-d., la comparaison des turbine Maxblend et PBT) sur la récupération et la qualité du produit. La récupération et la qualité ont été améliorées en augmentant la vitesse de la turbine. En outre, la taille des gouttelettes d'émulsion a finalement été plus uniforme avec Maxblend ce qui conduit à un très meilleur de récupération et teneur de concentration. La récupération de l'émulsification en une étape est améliorée notamment en ajustant le régime RPM de Maxblend à 65% et un TE de 385%.

Le troisième article examine l'effet des propriétés physiques des phases pour améliorer le processus. La meilleure performance de séparation est obtenue par une amélioration de la formulation de l'émulsion et par la sélection de l'huile appropriée. Le travail se concentre sur la tension interfaciale (TIF) qui a finalement un effet significatif sur la récupération et le grade. TIF d'huiles alternatives modifiées avec des additifs (c.-à-d., la paraffine et le kérosène avec du 1-hexanol à 1%) et également une autre phase continue que l'eau (c.-à-d., l'éthylène glycol) et diverses viscosités ont été examinées. Une viscosité de 200 cSt, un rapport huile sur eau% 10 v /

v et une concentration de particules en 5% poids peuvent générer la meilleure sélectivité (c.-à-d., avec la récupération et le grade le plus élevé). Comme le PDMS est coûteux et qu'il n'est pas réalisable à l'échelle industrielle, l'huile de paraffine 100 cSt a été testée et a obtenu une meilleure sélectivité. Le récupération R et un TE sont encore améliorés jusqu'à 60% et 270% respectivement en choisissant l'huile de paraffine qui est une huile moins chère (comme le kérosène).

Le dernier chapitre porte un objectif très important pour une étude technico-économique sur les deux processus FF et SSE dans une échelle pilote avec une récupération de 75% et une TE de 200%. Les CAPEX, les OPEX et les impacts environnementaux ont été comparés distinctement pour les deux méthodes de séparation physique. Les résultats montrent la rentabilité économique et écologique significatives pour SSE par rapport FF conventionnel.

En conclusion, les concentrés d'ÉTR (une teneur plus élevée en bastnaésite et en monazite) ont été produits par SSE avec une économie raisonnable de processus et de nombreux avantages environnementaux. Comme aucun agent tensioactif n'est utilisée, les propriétés de surface naturelle des minéraux en particulier les différences de mouillabilité sont les paramètres clés qui contrôlent l'attachement sélectif et compétitif des particules aux interfaces des gouttelettes d'émulsion. Le modèle semi-empirique aide à déterminer rapidement les effets des paramètres principaux pour atteindre les conditions optimales. Pour compléter l'optimisation dans les travaux futurs, des sous-processus tels que la désémulsification et la séparation des phases devraient également être pris en considération.

ABSTRACT

Solid stabilized emulsions (SSE aka Pickering emulsions) have numerous applications in materials and synthesis in different industries such as petroleum, petrochemicals, polymer, cosmetics, food processing, paint, etc. and the most recently proposed in this study, for physical beneficiation of minerals. Pickering emulsion uses only particles as emulsifier around droplets which make a barrier to limit coalescence despite other emulsions which uses additive surfactants to stabilized droplets in the continuous phase. The novel technique uses Pickering emulsion for separation of precious metal bearing particles and more specifically, carrier minerals of rare earth elements (REE) from their associated gangues in the ore. SSE can be used as an alternative to the conventional froth flotation (FF) or even as a supplement with one of the up/downstream processes in physical beneficiation stage to increase the performance of separation. The economic and environmental nightmares of flotation are briefly discussed where the surfactants, chemical agents and pH modifiers should be applied in several stages and make big challenges for the sustainability of the overall process. There is no need for surfactant or chemicals and so the minerals are going with their natural surface into the process behind SSE, hence, water and oil can be recycled much easier than FF. Consequently, SSE opens new economic and green gate toward sustainable physical beneficiation of REE minerals. Meanwhile, the study gives an idea for a similar application of SSE in the separation of valuable particles from a given fine powder in many industries.

Considering this application of SSE and remarkably because of big environmental challenges come with FF, the research project aims to study first the feasibility of using SSE in physical beneficiation of REE bearing minerals at the industrial scale. The main propose is to identify the parameters affect the selectivity of the process during the emulsification stage including the properties of phases, formulation, and operating conditions. The next step is to obtain the optimal conditions for the overall process and develop a semi-empirical model for the mechanism behind the selectivity to predict recovery and grade of the products. Thus, four sub-objectives well defined for the work as the chapter articles:

The first paper is a feasibility study for a SSE process to produce a concentrate of REE carrier minerals from the ore mixture of gangue minerals. We used original ore from NIOBEC mine in Quebec on which the most abundant REE bearing minerals are the carbonatite types of bastnäsite

((Ce, La, Nd, Y) FCO_3) and monazite ((Ce,La,Nd,Th) PO_4). The results showed that the REE bearing minerals had more affinity to the oil droplets than the gangues due to their larger contact angle. They attached more into the oil-water interface and the gangues stayed more in the water phase. The behavior of the REE ore in the emulsion system, the surface properties of the minerals at the oil-water interface and their interaction were investigated. The grade of total rare earth TREO% in the products is calculated based on total rare earth TREE% which is obtained through Neutron activation analysis. We could demonstrate the ability of Pickering emulsion to separate and concentrate REE minerals, considering the effects of feed properties such as particle size and preparation method. The enrichment ratio (ER) after one stage emulsification at natural pH increased up to 290% with a recovery higher than 50% without using any surface modifiers, additives or chemical agents.

The second paper focuses on the effects of process conditions such as mixing intensity (i.e., changing RPM) and shear uniformity (i.e., comparing Maxblend and PBT impellers) on recovery and grade of product. Recovery and grade improved by increasing the impeller speed. Also, the emulsion droplet size was eventually more uniform with Maxblend which leads to higher recovery and grade. The recovery of one stage emulsification is enhanced notably by adjusting the RPM of Maxblend up to 65% along with an ER of 385%.

The third paper investigates the effect of the physical properties of the phases to improve the process. The best performance of separation is achieved through an improvement of the emulsion formulation and selecting appropriate oil. The work focuses on the interfacial tension which has eventually a significant effect on recovery and grade. IFT of alternative oils modified with additives (i.e., paraffin and kerosene with 1-hexanol 1%) and also another continuous phase than water (i.e. ethylene glycol) and various viscosities were examined. A sort of viscosity 200 cSt, oil to water ratio 10% v/v and mass particle concentration of 5%, can drive the best selectivity (i.e. with highest recovery and grade). Since PDMS is expensive and not industrially feasible, paraffin oil 100 cSt was tested and achieved a better selectivity. The R and ER are improved again up to 60% and 270% respectively by choosing paraffin oil which is less expensive oil (as kerosene).

The last chapter carries a very important objective for a techno-economic study on both FF and SSE processes into a pilot scale with 75% recovery and ER 200%. CAPEX, OPEX and environmental impacts were compared for two distinctive physical beneficiation methods. The

results show significant economic profitability and ecologic effectiveness for SSE vs. conventional FF.

As a conclusion, the REE concentrates (a higher grade of bastnaesite and monazite) were produced by SSE with reasonable process economy and many environmental advantages. Since no surfactants are used, the natural surface properties of minerals especially wettability differences are the key parameters which control selective and competitive particle attachment into the interface of emulsion droplets. The semi-empirical model helps quickly to find out the effects of the main parameters to reach the optimized conditions. To complete optimization in future works, sub-processes such as demulsification and phase separation should be also taken into consideration.

TABLE OF CONTENTS

LIST OF TABLES

LIST OF FIGURES

LIST OF SYMBOLS AND ABBREVIATIONS

Roman Letters

A_{cov} Coverage potential

A_{eff} Effectively covered interface

A_{gen} Generated interface

A_{Theo} Theoretical available interface

D_i Impeller diameter

D_p Particle diameter

D_{10} Diameter below which 10% of the overall droplet size is located

D_{90} Diameter below which 90% of the overall droplet size is located

D_{32} Sauter mean diameter

E_{sep} The total interfacial free energy when the particle is totally in the water phase

E_{min} The total interfacial free energy when the particle is attached to the droplet interface

E_{eng} The total interfacial free energy when the particle is totally engulfed by the droplet

E_{Col} Efficiency of collision

E_{TPCL} Efficiency of three phase contact line formation

E_{Att} Efficiency of attachment

E_{Cov} Efficiency of droplet interface coverage

E_{global} Global efficiency of attachment

$E_{Gangues}$ Gangues specific global efficiency

E_{REE} REE's minerals specific global efficiency

E_{Tot} Total efficiency

F_{Att} Attachment force

F_{Det} Detachment force

F_{col} Collision force

$Freq_{collision\ p/d}$ The particle/droplet collision frequencies

$Freq_{collision\ p/d}$ The droplet/droplet collision frequencies

G_F Grade of REE in the feed stream

G_O Grade of REE in overflow

G_U Grade of REE in underflow

I_{Att} Attachment efficiency index

m_F Mass of particles in the feed stream

m_O Mass of particles attached to droplets in overflow

m_U Mass of non-emulsified particles in underflow

M_t Theoretical mass of the system

N_p Impeller power number

Ni The impeller speed

n_s Selectivity factor

n_i Number of particles in size interval x_i

$N.total_{attached-REE}$ Total number of the attached REE' s mineral particles into the interface

$N.total_{REE}$ Total number of the REE' s mineral particles in the system

$N.total_{attached-Gangue}$ Total number of the attached gangue particles into the interface

$N.total_{Gangue}$ Total number of the gangues particles in the system

P Inlet power on the shaft

$P_{Att}(REE)$ Overall Probabilities of attachment for REE' s mineral particles

$P_{Att}(Gangues)$ Overall Probabilities of attachment for gangues particles

P_{REO} price of rare earth element oxide

q_i Numerical size distribution density in size interval x_i

t_c The contact time

t_d The drainage time

$t_{TPC_{cir}}$ TPC line expansion time

Greek Letters

γ_{wa} Water surface tension

γ_{oa} Oil surface tension

γ_{wo} Oil/water interfacial tension

θ_{sw} water-air-solid contact angle

θ_{so} oil-air-solid contact angle

$\theta_{o/w}$ water-oil-solid contact angle or particle contact angle

Δ_1 Interfacial energy preventing a particle to detach from interface

Δ_2 Interfacial energy needed for a particle being engulfed by the oil droplets

ρ_p Particle density

ε_{ave} Average turbulent energy dissipation rate

ρ_{Slurry} Density of suspension

ρ_p Particle density

ρ_S Solid bulk density

ρ_L Liquid density

τ Torque on the impeller shaft

Φ_d Dispersed phase volume fraction

Acronyms

BCO LEVEL OF BRIGHTNESS EMITTED FROM CONCENTRATED ORE

BEP BREAK-EVEN POINT

BFO LEVEL OF BRIGHTNESS EMITTED FROM FRESH ORE

BLR BRIGHTNESS LEVEL RATIO

BS LEVEL OF BRIGHTNESS EMITTED FROM THE SAMPLE

CAD$ CANADIAN DOLLAR

CAPEX CAPITAL EXPENSES

CSF CRUSHED SIEVED FEED

DSF DRY SIEVED FEED

ECO ELEMENTAL ASSAY OF CONCENTERED ORE

EDS ENERGY DISPERSIVE SPECTROSCOPY

EFO ELEMENTAL ASSAY OF FRESH ORE

EG90 ETHYLENE GLYCOL 90%

EMPA ELECTRON MICROPROBE ANALYSES

ER ENRICHMENT RATIO

ES ELEMENTAL ASSAY OF THE SAMPLE

FF FROTH FLOTATION

GB GLASS BEADS

GHG GREEN HOUSE GASES

HH HUMAN HEALTH

HREE HEAVY RARE EARTH ELEMENTS

HT HUMAN CARCINOGEN TOXICITY

IEP ISOELECTRIC POINT

IFT INTERFACIAL TENSION

IMGA IMAGE ANALYSIS

IRR INTERNAL RATE OF RETURN

LREE LIGHT RARE EARTH ELEMENTS

MD MIXING DURATION TIME

NAA NORTON ACTIVATION ANALYSIS

NEP NON-EMULSIFIED SEDIMENT PARTICLES

NPV NET PRESENT VALUE

NSD NUMERICAL SIZE DISTRIBUTION

O/W OIL IN WATER EMULSION (RATIO)

OPEX OPERATIONAL EXPENSES

OZP OZONE DEPLETION POTENTIAL

PBT PITCHED BLADE TURBINE

PDMS POLYDIMETHYLSILOXANE (SILICONE OIL)

PSD PARTICLE SIZE DISTRIBUTION

QEMSCAN QUANTITATIVE EVALUATION OF MINERALS BY SCANNING ELECTRON MICROSCOPY

R RECOVERY

RBM RARE EARTH BEARING MINERALS

REE RARE EARTH ELEMENTS

REO RARE EARTH OXIDES

RGB RED GREEN BLUE BRIGHTNESS LEVEL

RPM ROTATIONAL SPEED PER MINUTE

SCD STABILIZED CREAM DROPLETS

SEM SCANNING ELECTRON MICROSCOPY

SSE SOLID STABILIZED EMULSION

TPCL THREE PHASE CONTACT LINE

TREE TOTAL RARE EARTH ELEMENTS

TREO TOTAL RARE EARTH OXIDES

WSF WET SEIVED FEED OF FRESH ORE

LIST OF APPENDICES

CHAPTER 1 INTRODUCTION

This area of research considers physical beneficiation stage in the mining industry, and more specifically the early steps of recovery of the rare earth elements (REE) bearing minerals to separate them form their associated gangues in the ore mixture. Froth flotation (FF) is one of the most common methods in physical beneficiation that uses the surface properties of REE bearing minerals (RBM) to concentrate them form their ore mixture.

It is known (Bulatovic 2007) that many surfactants which are used in conventional physical beneficiation of the ore processing like in FF and they are very detrimental to the environment. This fact is more relevant in mineral processing where the separation of minerals of interest is very difficult and complicated, due to their very similar physicochemical properties to their associated gangues such as density, magnetic susceptibility and permeability, electrostatic and wettability. There are several physical separation methods such as FF, magnetic, electrostatic techniques, etc. which are used in physical beneficiation stage. Nevertheless, such physical methods result either in low beneficiation efficiency, limited tonnage feed rate or a complex and costly configuration of several physical processing units. Also, FF uses several of harmful and detrimental chemicals to the environment and human health such as pH modifier agents, surfactants including collectors, activators and stabilizers like frothers (Bulatovic 2007, Anderson, Taylor et al. 2016). The research project will evaluate the possibility of using the surface properties of RBM to separate them in an emulsification process. More specifically, adapted oil, water and solid particles of minerals to form a solid-stabilized emulsion (SSE) or Pickering emulsion in the early stages of the physical beneficiation of the mineral processing.

Therefore, in this study it is highly motivated to assess ability of Pickering emulsion to separate and concentrate REE minerals and furthermore to compare its ability with FF. Notably, one employs Pickering emulsion hopefully should have reasonable performance and it comes with less environmental impacts, more simple, cost-effective and safer along with high recovery yield and quality of product when compared with other conventional physical beneficiation methods.

A semi-empirical approach in this research will use to develop a model and more specifically to predict the performance of separation of the process. Beside all, research project obtains realistic processing conditions to form Pickering emulsion, demulsification and phase separation which can lead to have economic advantages over traditional separation methods such as FF. Also it can offer the basic guidelines and orientations for further development and noteworthy, to have the

state of the art knowledge in the application of Pickering emulsion in physical beneficiation of RBM.

Beforehand, a review about rare earth minerals specifications and some notions about physical beneficiation methods, especially about FF are given. Thereafter, main parameters about properties of an emulsion is explained where the critical notions will be addressed. The key point is to address the research main question and to introduce SSE technique as a novel solution in physical beneficiation stage. Regarding to the steps of this method, Pickering emulsification, phase separation and demulsification are explained.

In term of the scope of the project, the study consists of several approaches such as emulsification, stabilization, destabilization, physicochemical aspects and surface properties of REE bearing minerals, liquid phases and mixing conditions. The study focuses the activities on the following points during emulsification, demulsificaton and phase separation: the effect of the surface properties and size distribution of the solid fine particles and the emulsion droplets, the effect of the mixing and hydrodynamics, the effect of the other physicochemical parameters such as oil viscosity, polarity and interfacial tension on the performance of separation (Bulatovic 2010).

1.1 Rare earth elements

The rare earth elements (REEs) are the fifteen lanthanide elements in the periodic table which can be regrouped in two categories of light (LREE) with atomic numbers from 57 to 62 as well as scandium21 and yttrium39 and heavy rare earth elements (HREE) with atomic numbers from 63 to 71. REEs abundance in earth's crust for example varies from 64, 30 and 26 ppm for Ce, La and Nd to 3.8, 3.5 and 0.88 ppm for Gd, Dy and Eu respectively (Jones, Wall et al. 1996). The electron configuration is like [Xe] $5d^1 6s^2$ for La and like [Xe] $4f^x 6s^2$ for most of them which gives unique specification and similarity in physicochemical properties in their natural compounds (Gupta and Krishnamurthy 2004, Castor and Hedrick 2006). In addition REEs are abundant like many other elements on the earth's crust. The reason that REEs are called rare is not because of their abundance, but because of the difficulties with their beneficiation from the other conjunction minerals in the ore. The REEs have, in general, 3+ valences which can find in their compounds such as oxides, carbonates, phosphates and silicates (Jones, Wall et al. 1996). Their differences is in different ionic radius and the most important similarity is the nuclear

configuration of the three outer electrons. Given that, their electrons arrangement makes similar physicochemical property which in turn causes challenges in production of their oxides (REO) in pure forms. Hitherto, physicochemical properties of the rare earth elements and their applications in modern technologies are well described (Gupta and Krishnamurthy 2004). Each single element of the REEs has many applications in different sectors of industries and high technologies especially in the renewable energies and permanent magnets (Salazar and McNutt 2013). The other applications can be named here as catalysts, light devices, medical imaging, phosphors, UV resistant glasses, thermal control mirrors, ceramic, rechargeable batteries and etc., thus a fast growing global demands for applications of REEs is expected and finding substitutes for REEs producers is required in order to response to the policy driven demand-supply trends in the market. Almost 95% of the REE's are inherent in minerals such as Bastnaesite, Monazite, Xenotime and ion adsorption clay minerals which are the most economically feasible minerals for extraction of the REEs (Jones, Wall et al. 1996, Gupta and Krishnamurthy 2004, Zhang and Edwards 2012).

The Bastnasite (REE's)FCO_3 containing 67-73% REO's and the Monazite (REE's)PO_4 are the famous known minerals bearing REE's in the world which respectively contain LREEs and low amounts of HREEs. The recovery process of the REE's from the original deposit consist mineralogy, mining exploitation, physical beneficiation of the ore, concentration by various techniques such as thermal cracking, hydrometallurgy and separation of individual elements by refining. As previously mentioned, the physical beneficiation processes are the most difficult among mineral recovery because of the physicochemical similarities of the REE bearing minerals and their conjunction gangues in the ore. Whereby, several separation steps are required to concentrate REE bearing minerals such as magnetic, gravity, electrostatic and froth flotation in the complex network of unit operations. For example, the minerals in Bayan Obo deposit in China come with fluorite, magnetite, barite, calcite, quartz and feldspar which have very similar magnetic, specific gravity, electrical conductivity and floatability behavior to Bastnaesite and Monazite minerals. Thereupon, this challenge is more pronounced where the types and configurations of the unit operations depend on mineralogy, the grain sizes, versatility and composition of the minerals of the deposit. Furthermore, REE's bearing mineral composition varies from one deposit to another which makes more hurdles and their individual separation is

also very difficult regarding again to their similar physicochemical properties (Cheng, Hou et al. 2007).

1.2 Niobec REE deposit

Around 2011, IAMGOLD CORPORATION lunched the drilling reconnaissance campaign (29 drill holes) to a depth of 400 m in Niobec mine in Quebec with primary estimation of 466.8 million tons at a grade of 1.65% total rare earth oxides (TREO) which have reported in March 2012. The REE deposite consists of annular carbonatite type (Bastnaesite) and phosphate type (Monazite) corresponds to an enriched zone of LREE comprise 98.1% of the weight of the Total REEs and the rest of 1.9% HREE that have additional significant economic value. The estimation of Niobec deposit was a huge 1058.6 million tonnes at average grade of 1.64% TREO equal to 18.363 million tonnes to a depth of around 700 meters. Bastnaesite and monazite with almost a same mass ratio and gangues are including Carbonates (Dolomite, Calcite, Ankerite, Siderite) 65%, Silicates (Chlorite and Phlogopite, Feldspars, Quartz, Vermiculite)11%, Apatite 10%, Oxides (Magnetite, Hematite, Ilmenite, Rutile, Goethite, Pyrolusite ,Pyrochlore) 12%, Sulfides 1%, Fluorite, Baryte and Zircon 1 % collectively (Table 4.4) (Grenier and Tremblay 2013).

Table 1.1 Group of the consistent gangues in Niobec ore and weight percentage

Name	association (%wt)	Average grain Size (µm)	Category
Pyrochlore, Columbite, Fe-Oxides, Quartz, Rutile,Other Oxides	7.48	13.42	Oxide
Micas/Clays,Amphibole Chlorite, Plagioclase, K-Feldspar, Allanite	6.7	11.26	Silicate
Dolomite, Calcite, Ankerite, Siderite	77.22	16.85	Carbonate
Pyrite, Barite	4.92	21.81	Sulfide
Bastnaesite/Synchisite	1.96	14.34	Fluorocarbonate
Monazite/Th-Monazite	1.43	12.63	Phosphate
Other REE	0.01	6.84	Phosphate
Apatite	0.28	15.77	Phosphate
Total	**100**	**-**	**-**

1.3 Problem description

Considering the literature review, flotation has numerous environmental and viability issues. Given that, the big challenging of the conventional froth flotation raises up from chemical agents and surfactants due to recyclability of the surfactants and tailing water. The mineral particle's surface must be reacting with expensive organic chemicals to modify the surface into the desired wettability with higher contact angle for the minerals of interest to promote their attachment to the bubble interface. There are several types of surfactants used in the flotation which cannot also guarantee the reasonable efficiency, performances and viability of the process (Cheng, Hou et al. 2007).

Moreover, the required size treatment in case of REE bearing minerals is normally done by grinding. The ore size commonly known as P80 about 56 microns achieves liberation which is not ideal for optimal flotation performance. It more pronounced that above 50 microns the size locking between the Bastnaesite and Calcite is common. For lower than this size the treatment going to non-feasible zone in term of energy and cost. Thus, the effect of particle size on performance of flotation rate including recovery and grade is very complex (Bulatovic 2010).

In the other side, the grade yield of TREO after flotation could not be more than 45% where the recovery yield hardly acheives 75% (Bulatovic 2010, Jordens, Marion et al. 2014). It is important to note that a 100% recovery of monazite and bastnaesite from Niobec ore with theoretically 100% purity has 81% TREO, especially when we need to compare SSE vs. FF. Furthermore, in term of social impacts, some of the surfactants and chemicals which are currently used in the REE beneficiation have been investigated as hazardous for human health, especially for the process workers in mineral treatment plan. Also, economically the price of the surfactants are very high and affects operational cost of FF technique. Since it more pronounced at literature review, the environmental assessment from cradle to grave of the REE processing is recently studied and all the results show the high impacts in FF method itself mostly because of chemical reagents usage. They are also at the source of many problems downstream of the concentrator (Jordens, Cheng et al. 2013),(Castor and Hedrick 2006).

CHAPTER 2 LITERATURE REVIEW

A literature review conducted here to mostly focus on surface characterization of minerals, froth flotation, Pickering emulsion and demulsification. Thereafter, a critical review will come about mineral surface characterization, interfacial properties, particle selective attachment following the works related to phase separation and particle detachment. The review summarizes the most relevant works with respect to the solid particle as emulsifier, the generation of Pickering emulsions, fundamental phenomena to understand the stabilization/destabilization mechanisms, mixing conditions, and rheology of emulsions. The effects of the properties of Pickering emulsions and relevant phases on selective attachment are well reviewed. In the last part the bases of demulsification procedure and phase separation will come in review due to aim of separation of the mineral particles. Furthermore, the critical review highlight the capacity of the main mechanisms involved during the emulsification to selectively capture specific fine particles (i.e, REE bearing minerals) on which to explain the emulsified cream droplets render a higher concentration of REE's.

2.1 Surface characterization

Surface charge/ Zeta potential

All solid particles in aqueous phase will have a charge on their surface which is called surface charge. The surface charge is created by attachment of the various ions in electrolyte. Surface charge can govern the attachment/detachment of solid particles or emulsifier agents into surface site and hence this parameter directly has effects on physical beneficiation of a given system. Consequently in practice it is essential to consider its effects e.g. by measuring zeta potential. Zeta potential is one of the most important notions in a colloidal system. Zeta potential is a scientific term for electrokinetic potential in colloidal dispersions which can be define as the electric potential in the interfacial double layer around the particles or droplets from the slipping plane relative to a point of the bulk of electrolyte and away from the interface. In other words, zeta potential is the potential difference between the dispersion medium and the charged layer of attached ions to the surface. Based on this, zeta potential measurement can be used to investigate colloidal particle interactions regardless of its limitations for particle density and geometry. Zeta potential migh be measured by conventional electrophoresis zeta meter or electroacoustic

techniques. Surface charge varies by change of pH depending on the species which form on particles surface at a given pH. The charge might be positive or negative and there is a pH at which zeta potential is equal to zero (IEP isoelectric point). Thus, at pH values lower than IEP, zeta potential is positive and at higher than IEP is negative. Identifying IEP of minerals and knowing the ionization behavior allow one to predict the possible interactions in the mechanisms involved physical beneficiation (Liu, Zhou et al. 2002, Ofir, Oren et al. 2007, Jordens, Cheng et al. 2013).

Wettability / Surface energy / contact angle / hydrophobicity / Interfacial tension

Wettability is the tendency to wet a solid surface by liquid molecular of attraction force between the solid surface and liquid materials at contact pattern surface and in the presence of another immiscible fluid. The strength of attraction is determined by the surface energy of the materials or interfacial boundary tension. The surface energy can be defined as the energy differential at the surface of a material compared to the bulk of the material. The higher the surface energy leads to the greater the molecular attraction forces and the lower the surface energy gives the weaker attractive forces. In the other side, greater molecular attraction increase contact between the liquid and the solid surface. Indeed, on a high surface energy material, the liquid can wet better the substrate or liquid tends to spread on the solid surface at smallest contact angle. Contact angle is the angle at the surface point where the three phases meet each other on which the liquid–vapor interface meets the solid–liquid interface. If the liquid does not tend to contract, the liquid does not readily wet the solid then the contact angle is large (θ).

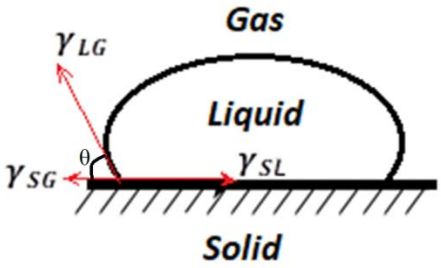

Figure 2.1 Graphical vector representation of contact angle and surface tension parameters (Kabza, Gestwicki et al. 2000)

Contact angle can be a measure scale for hydrophilicity which is the behavior of solid surface to be wetted by aqueous phase. Interfacial boundary tension is also defined by the energy per unit

area or force per unit distance at the contact surface between the phases. It is commonly expressed in milli-Newtons/meter or dynes/cm. The investigations show a meaningful correlation between hydrophobicity (wettability) and solid particle attachment into the liquid phase interface. A same manner reported for the mechanism behind the selective attachment of solid particles in the both FF and SSE process. Contact angle measurements on solid fine particles in a powder needs to be met by series of complicate methods. There are a few techniques for direct measurements of contact angle such as Young-Laplace method with goniometer which cannot work properly for powders. Another way is to measure the surface energy of the solid particles (minerals) to calculate the contact angle. An important aspect of this last measurement is to compare degree of reactivity of minerals with different oil types in contact with aqueous phase especially in case of Pickering emulsion and also in case of surfactants in FF. The wettability of REE bearing minerals is based on analysis of the surface chemistry of their pure form samples with their complex composition (Kabza, Gestwicki et al. 2000, Binks and Clint 2002, Yuan and Lee 2013).

2.2 Physical beneficiation

In order to separate Bastnaesite and Monazite from the associated gangues in early stages of mineral processing, physical beneficiation take place using several techniques such as magnetic, gravimetric, electrostatic, froth flotation. In this manner, the effects of the physicochemical properties such as density, magnetic susceptibility and permeability, electrostatic and wettability of the REE bearing minerals and associated gangues are extremely important on the processing of separation. Among these, FF has applied as high tonnage capacity and effective technique for separation of bastnaesite and monazite. However a proper design that employs multiple integrated unit operations such as one employing sizing, gravity, magnetic, can outperform alternatively the separation, compare to one that use the only FF technique. Whereby, physical beneficiation can be defined as separation of minerals base on differences in physical properties. Although, bastnasite and monazite are accompanied with gangue minerals which have very slight differences in physical properties, and more specifically in wettability. Therefore, FF as a separating technique requires providing of delicate conditions (Gupta and Krishnamurthy 2004, Zhang and Edwards 2012).

2.2.1 Electrostatic separation

Indeed, electrostatic separation is a beneficiation technique which exploits the differences in electrostatic charge ability between the minerals and gangues where alternative treatment techniques are not enough. Considering that dry minerals before electrostatic separation is required and products unit operations in mineral processing plant are mostly wet, thus the energy consumption to dry minerals before electrostatic separation is significant. However, this method could be valuable enrichment technique due to usage in heavy metal bearing minerals. Electrostatic separator with high tension is used in electrostatic separation which works with an ionizing electrode and variable applied charge. The material with low ability to release charge, remain on the rotating roll while the particles which lose their charge by applied electric field are thrown from the roll (Gupta and Krishnamurthy 1992).

2.2.2 Gravity concentration

In fact, REE bearing minerals are good candidates for gravity concentration since they have relatively large specific density (mostly above 4 gr/cm^3). They are typically associated with gangues minerals that have significantly lower density. The approach uses gravity force in dynamic rotary mechanisms to separate particles base on their specific density, especially this technique can be used successfully for monazite enrichment. There are spiral concentrators and centrifugal concentrators which work base on density differences of the minerals in the ore. In general, size of the particles is important factor to design equipment plan where the finer mineral particles have more optimal size for gravity concentration (Gupta and Krishnamurthy 1992).

2.2.3 Magnetic separation

Magnetic separation is based on response to an applied magnetic field by minerals which might have differences in magnetic susceptibility. In general, minerals show three distinct behaviours while exposed to a magnetic field: Ferromagnetic, paramagnetic and diamagnetic particles which respectively will be attracted to the magnets and the last will be repelled. In fact, the magnetic properties of the mineral can be determined using a vibrating sample magnetometer. One of the important results for REE bearing minerals is that magnetic susceptibility of bastnaesite is lower than fergusonite and allanite which are gangue minerals. Magnetic separation can be done both in wet or dry streams. In order to have maximum performance, preparations of data sheets for the

magnetic properties of the individual minerals and a tailored magnetic separation protocol are essential(Dobbins, Dunn et al. 2009, Jordens, Sheridan et al. 2014).

2.2.4 Froth flotation

FF is the most famous conventional method among other physical beneficiation, especially in case of recovering rare earth minerals from their associated gangues. On the other hand, the composition and diversity of REE minerals are varied a lot and every deposit has its own characteristics which lead to specific processing strategies. The challenges in physical beneficiation of REE bearing minerals are mentioned before. Some of these difficulties and lack of information include: adequate characterization of physicochemical properties of individual REE mineral, suitable reagents to selectively separate minerals from ore body, how to reach highest separation performance with minimum reagent and chemical usage, sustainability aspects, water, energy and capital consumption. Indeed, the ultimate goal of FF or other physical beneficiation methods is to economically produce a concentrate with high quality and minimum ecologic impacts and in order to be well suited for leaching (i.e., to reduce acid and other chemicals consumption) in downstream processes (Zhang and Edwards 2012, Jordens, Cheng et al. 2013).

The FF process of separating targeted mineral in the ore depends on the relative wettability of the particles of interest. Indeed, the more hydrophobic particles are attached to the bubbles and in turn induced a froth carrying the particle into top of the pulp. Once a particle and bubble get in contact, the bubble must be large enough for its buoyancy to lift the particle to the surface. The froth layer must resist enough to either flow over the discharge of the cell by gravity or mechanical froth scrapers. Since, most of the minerals are hydrophilic, thus their surface must be treated by a surfactant reagent. The interactions of reagents with mineral surface in the electrolyte depend on the chemistry of the mineral surface and the solution. The interaction changes the surface either more hydrophobic or hydrophilic. As it mentioned before, hydrophobic surface has more affinity to attach into interface (i.e., bubbles) and this is the main property governing the phenomenon. The aim of additive reagents usage is to selectively float the targeted minerals while the gangue minerals are rejected (Jordens, Cheng et al. 2013).The flotation in laboratory scale tests can be carried out in a micro cell made of glass and a fritted disc installed at the bottom of the cell where the gas is pumped. A Denver cell is employed for batch flotation tests.

Some of the most important parameters that should be controlled during the tests are air rate, impeller speed, froth depth, froth scraping rate, surfactants, pH, temperature, concentrations and particle size distribution (Figure 2.2). In general, air rate should be high enough to maintain a fluid froth depth and to avoid collapsing froth. Also impeller speed should be sufficiently controlled to maintain solid particles in suspension whereas a constant and fairly fast scraping rate is required. Since a slow floating mineral will take longer to reach completion, the time interval between each concentrate collection should be controlled. Given that, it is required more information to simulate the results for batch flotation tests. FF will be performed on fresh ore samples provided by company at realistic conditions, e.g. particle size which plays an important role in many separation processes. In the other side, the recovery yield of monazite in total REO entire beneficiation accomplished with flotation could not be more than 80% (Figure 2.3).This last is important especially when we are looking for an alternative to flotation itself which has many environmental side effects due to usage of huge amount of surfactant and many difficulties due to recyclability of these surfactants (Bulatovic 2010), (Bulatovic 2010, Jordens, Marion et al. 2014).

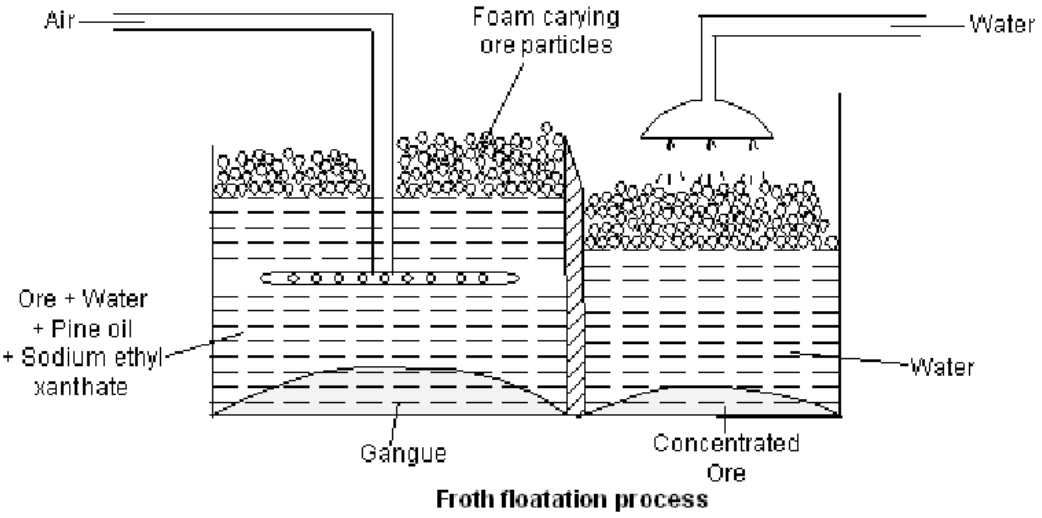

Figure 2.2 Schematic of froth flotation (Bulatovic 2010)

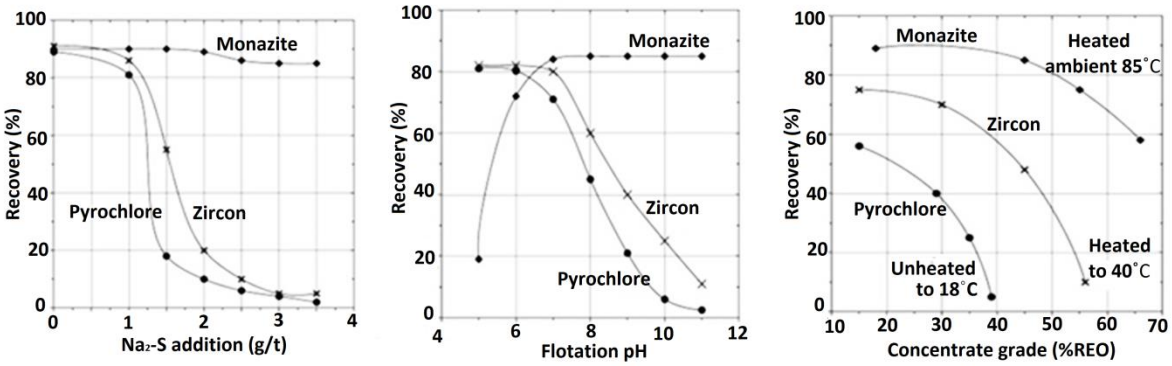

Figure 2.3 Effects of surfactatnts concentration, temperature and pH on recovery of Monazite (Bulatovic 2010)˚

For example, in the Bayan Obo mine, there are mainly six different beneficiation processes being used. A general processing route is shown in Figure 2.4 for REE ores but as each site have different composition, the process routes deviate to different extents (except for purification step 5). Also, in term of liberation size, at least 90% of the ore being ground to less than 74mm to be prepared for the froth flotation process. Na_2CO_3 (2.5–3.3 kg/ton) is used as a pH regulator with Na_2SiO_3 (2.5–3.3 kg/ton) as the depressant agent of associated iron minerals and silicate gangues and paraffin soap as a collector. The depressed iron minerals and silicates will be remained at the bottom of the flotation cells, thus they are going for iron beneficiation and niobium recovery. After eliminating the surplus fatty acid collector by thickening and desliming treatment, selective REO flotation is completely carried out. The following accomplishment is done with Na_2CO_3 as the pH regulator, Na_2SiO_3 and Na_2SiF_6 as gangue depressants, and hydroxamic acid as the collector. The depressed calcite, fluorite and barite remain at the bottom of the cell. After the flotation, the rougher concentrate contains around 45% REO consist both monazite and bastnaesite. The recovery of REO at this stage is approximately 80%. The final treatment includes cleaning with high intensity magnetic separators. These results have two concentrate fractions with the primary bastnaesite having 68% REO concentrate and the secondary monazite containing 36%REO. The total recovery rate of REOs from the ore is around 61%. After the flotation process, it is estimated that 80.63% of Thorium as a radioactive element remains in the tailings and it might be 1.83% in the REE concentrate (Jordens, Cheng et al. 2013), (Castor and Hedrick 2006, Navarro and Zhao 2014).

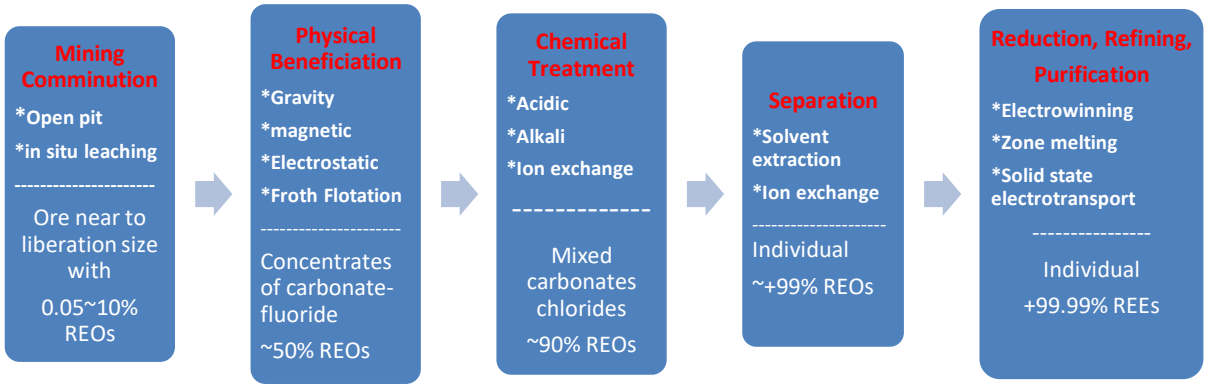

Figure 2.4 General processing routes for REE ore (Navarro and Zhao 2014)

In practice, more than one flotation step, commonly 3 to 5 cascade cells in series for each one of three main steps including thickening, cleaning and scavenging are required to reach a typical 50 % yield recovery and a concentrated ore with a grade seldom above 60%. The water used in the process cannot be recycled simply as a result of presence of numerous additives (Table 4.1) and chemicals, hence, a large tailings ponds are accumulate beside every FF processes (Bulatovic 2007, Bulatovic 2010, Sprecher, Xiao et al. 2014). There are different values of recovery and quality of products is being reported after FF of REE bearing ores. (Bulatovic 2010, Jordens, Cheng et al. 2013, Xia, Hart et al. 2014, Liu, Wang et al. 2016).The REE recovery from a three stage micro-flotation applying Hydroxamate as collector is around 15% and the enrichment ratio for average REE bearing minerals is around 6 (Xia, Hart et al. 2014, Xia, Hart et al. 2015). In FF the surfactants are employed to modify the minerals surface wettability, interfacial tension and create froth with controlled properties, (i.e., size of bubbles, stability, lifespan, and etc.). The pH of the aqueous phase (slurry) should be controlled very well. The chemical reagents and additive molecules are in overall expensive and extremely detrimental to the environment (for soil, surface and subterraneous water) (Sprecher, Xiao et al. 2014). Moreover in case of particle size, for those deposit that have a very small grain size of RBM (Bastnaesite and Monazite in Niobec fresh ore has -14 microns average grain size) first the size reduction in upstream processes (Comminution) to reach a desirable liberation takes more energy and cost. The second, to reach a desirable recovery and grade during FF there are various series of surfactants should be applied in a flotation tank for different purposes such as frothers, collectors and depressants (Mittal and

Shah 2013, Anderson, Taylor et al. 2016). An estimation for the OPEX relevant to the chemicals and additives on the final concentrate would be around 1.35 USD per kg of REO only in FF stages (Mittal and Shah 2013). Using this and the average global price of rare earth oxide, a techno-economic analysis can be driven for a given flow rate into FF processes including annual cash flow diagram, net present value (NPV), internal rate of return (IRR) and payback period [CostMine2014] (Ulrich 1984, Schena, Villeneuve et al. 1996, Gorain, Franzidis et al. 2000, Rinne and Peltola 2008, Yang, Satur et al. 2015). The total energy consumption, average labor for installation and maintenance of FF process per normalized kg TREO is also investigated and reported as well and can be used in the common model for economic evaluation (Peters, Timmerhaus et al. 1968, Ityokumbul, Bulani et al. 1987, Schena, Villeneuve et al. 1996, Rinne and Peltola 2008, Safari, Harris et al. 2016, Tabosa, Runge et al. 2016, Mankosa, Kohmuench et al. 2018, Zhang and Zhang 2019). The environmental impact datasheets of an industrial FF facilities in a REE beneficiation site are categorized such as human health, carcinogen, ODP, smog, CO_2eq GHG are also reported (Navarro and Zhao 2014, Sprecher, Xiao et al. 2014, Izatt, McKenzie et al. 2016, Jin, Park et al. 2017, Arshi, Vahidi et al. 2018). The pH adjustment agents (i.e., acids or bases) must be applied which makes the processing more costly and hurdles to recycling the water and surfactants, thus, a large tailings ponds are being created at the mining site (Bulatovic 2007, Bulatovic 2010, Sprecher, Xiao et al. 2014).These have pointed out as slower throughput and much intensive environmental footprints for FF (Yang, Lin et al. 2013) vs. SSE that offer recovery of monazite and bastnaesite with a simpler process along with minimum tailing and waste generation.

2.3 Pickering emulsion

In chemical process engineering, numerous fields use emulsification including the cosmetics (Frelichowska, Bolzinger et al. 2009), food (Dickinson 2010), paint (Cauvin, Colver et al. 2005), petroleum, petrochemicals (Frelichowska, Bolzinger et al. 2009) etc. The common emulsions are stabilized by surfactants, but Pickering emulsion is been developed since last century for sustainable alternatives such as solid particles that act in many manners like as emulsifiers (Binks 2002). Noteworthy, this work also considers application of solid particles and taking advantage of their natural surface properties (i.e., the REE ore particles) in SSE, but to separate them

afterward. First time, solid particles had been studied to produce very stable emulsions by the pioneering work of W. Ramsden and S. U. Pickering (Ramsden 1903).

First of all, Pickering emulsion will be described and followed by definitions and notions. Pickering emulsion is one kind of emulsions that one of two immiscible liquid disperse as droplets in another e.g. oil droplets in water and then the droplets are stabilized by solid particles as emulsifier. There is a big advantage to use solid particles as emulsifiers instead of common surfactants, especially where the solid particles are the mineral particles. Indeed, mineral particles which are adsorbed at interfaces of water/oil, forms a steric barrier around the droplets and prevent coalescence. These kind emulsions commonly called Pickering emulsions (Figure 2.5) are more stable than those stabilized by surfactants but may be destroyed by the application of an external force such as centrifugation, magnetic field, etc., or by alternating of particle surface properties like as changing their wettability (Langevin, Poteau et al. 2004). These emulsions were discovered in the early 20th century (Ramsden 1903, Pickering 1907). The idea of this thesis is to prepare a Pickering emulsion by a mixture of solid particles, some of the specific particles with most similar surface properties selectively and competitively attached more into the interface of dispersed phase (i.e., droplets) and the rest remain in continuous phase. Then the separation of the oil droplets can lead to selectively separation of the specific fine particles from the mixture and in our case the REE bearing minerals from the ore. Since, the oil-water interfacial tension (IFT) is much higher than air-water IFT, thus we expect that Pickering emulsion is more sensitive to the wettability differences than the FF.

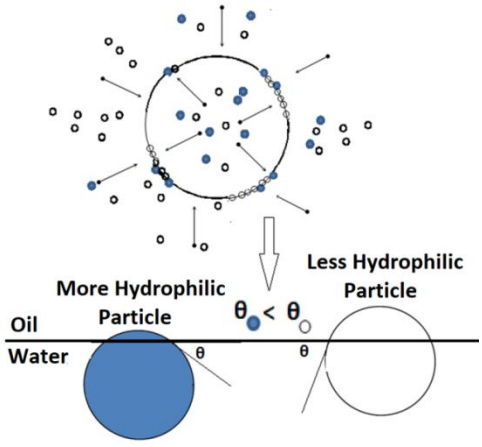

Figure 2.5 Representation of solid particles adsorbed at the interface

Pickering emulsions are controlled by several phenomena and physicochemical interactions. For example, an interfacial phenomenon is controlled by the interfacial tension between the solid and liquid phases. It is originated in molecular interactions and particularly dominated by Van Der Waals forces resulting from molecular permanent and/or induced dipoles. In this manner, the immiscibility of water and oil phases come from the fact that the polar phase cannot establish hydrogen bonds (permanent dipoles) with the oil phase whose attractive interactions are mainly composed by induced dipoles. This phenomenon creates appearance of interface with different properties from those of the bulk of two phases. Unlike the molecules of the core phase, the surface molecules are thus subjected to an asymmetrical intraction that attracts them towards the interior of the liquid and makes a tendency of the surface toward center and minimize the volume which explains the spherical shape of drops. On the other hand, creating the interface requires an input energy in the system, this energy per unit area is used for the work that must be performed to extend the interface and commonly known as surface tension or stress, it is expressed in milli-joules per square meter or milli-newton per meter (e.g., the surface tension of water /air at ambient temperature is around 73 mJ / m^2). It is defined as the change of the free energy of the system at constant composition and temperature. J.W. Gibbs developed the thermodynamic theory of surface tension based on the idea of surfaces of discontinuity where surface tension equals to Gibbs free energy G per surface area A: $\sigma = (\frac{\partial G}{\partial A})_{T,P,}$ at constant temperature and pressure. The tendency of the surface to spherical shape of droplets is balanced by the incompressibility of the liquid and by the internal pressure of the droplet and the interfacial tension. This is in particular given by the equation of Young-Laplace which is characterize the pressure difference between both sides of the interface. Furthermore, the equilibrium can be achieved thermodynamically by minimizing the Gibbs free energy which can be achieved by the reduction of the interface area or by reducing the interfacial tension for example by reducing the temperature of the system or reduction of the surface tension by manipulation (Ramsden 1903, Pickering 1907, Tsabet 2014).

2.3.1 Characterization of an emulsion

Hereafter, some of the notions and characterization parameter would be introduced. According to the related literature different properties might be used for characterization of emulsions and their

importance depend on objective of application where the process is used. Whereby, emulsion can be characterized by its type, size distribution, stability or life time, its rheological behavior etc.

2.3.1.1 Type of emulsion

An emulsion can be a simple water as dispersed phase in oil as continuous phase (W/O) or inversely oil dispersed in water (O/W) or even multiple emulsion (W/O/W or O/W/O) where a droplet itself can be a continuous phase dispersed in another and some part of the continuous phase dispersed inside the droplets. However, the objective of most emulsification processes is to produce a simple emulsion that means in most of the case, the multiple emulsions are undesirable. Indeed, the type of emulsion is directly related to the type and physicochemical properties of the stabilizing agents (in SSE i.e., the solid particles) , two phases, formulation such as order of mixing and preparation (Tadros 2009).

2.3.1.2 Volume fraction of the dispersed phase

These proportions are often represented by the volume fraction of the dispersed phase:

$$\Phi_d = \frac{V_D}{V_D + V_C} \qquad (2.1)$$

Where V_D and V_C are volume fractions of the dispersed phase and the continuous phase. An emulsion can be named diluted when Φd <0.01, slightly concentrated for 0.01 <Φd <0.2 and concentrated when Φd> 0.2 as these values are very examined. If we are considering the emulsions as a bulk where the same size spherical droplets dispersed in, the maximum Φd would be limited by 0.74, however it is possible to reach a higher value by producing droplets with different sizes (Ramsden 1903, Pickering 1907, Tsabet 2014).

2.3.1.3 Mean diameter and droplet size distribution

An emulsion can also be characterized by their size distribution or droplet average diameter. The Sauter diameter D_{32} is defined bellow and most frequently used as average diameter:

$$D_{32}(m) = \frac{\sum_1^m n_i {d^3}_i}{\sum_1^m n_i {d^2}_i} = \frac{6V_D}{A_{gen}} \qquad (2.2)$$

Where V_D is the total volume of droplets and A_{gen} is the total interface area generated and $d_i$is the diameter of droplet in the interval (i) and n_i is the total number of drops in the interval (i).

For a dimensionless volume format, the generated interface in a dimension of (m^{-1}) is calculated as follows:

$$A_{gen}(m^{-1}) = \frac{6\Phi_D}{D_{32}} \ or \ A_{gen}(m^2) = \frac{6V_D}{D_{32}} \tag{2.3}$$

The droplet numerical size distribution is generally represented by a histogram in terms of frequency number of drops at the same size class:

$$q_{ni} = \frac{n_i}{\sum_1^m n_i} \tag{2.4}$$

Or can sometimes represent by volumetric distribution frequencies:

$$q_{vi} = \frac{n_i {d^3}_i}{\sum_1^m n_i {d^3}_i} \tag{2.5}$$

The distribution of droplet sizes can also be presented in a cumulative form:

$$Q_{vi} = \sum_1^m q_{vi} = \sum_1^m \frac{n_i {d^3}_i}{\sum_1^m n_i {d^3}_i} \tag{2.6}$$

2.3.1.4 Emulsion stability

As we need to manipulate emulsions in the upstream phase separation, thus we should have a desirable stability of an emulsion or producing substantially a stable dispersion of two immiscible liquids. However, all kind emulsions are often subject to destabilization phenomenon that can be categorized in three groups (Figure 2.6) (Ramsden 1903, Pickering 1907, Tadros 2009, Tsabet 2014):

- The migration of droplets mechanisms (flocculation, sedimentation and creaming).
- The droplets size variation mechanisms (d'Ostwald ripening and coalescence).
- Phase inversion mechanisms.

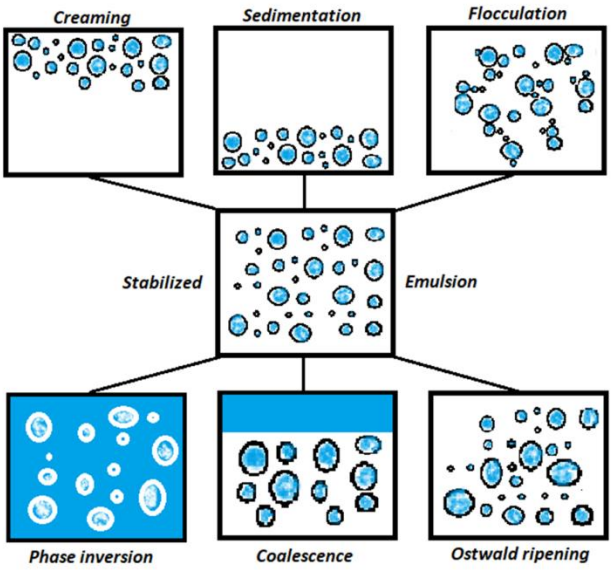

Figure 2.6 Schematic representation of various breakdown processes in emulsion or mechanisms of destabilization of an emulsion (Khatri 2010)

2.3.1.5 Flocculation

Flocculation is the agglomeration of droplets with each other and forming bigger size in batch or clusters which may lead to creaming or sedimentation. This phenomenon can have different interaction causes. For instance, flocculation is caused by interaction of attractive forces between particles/particle and particles/droplet according to their surface charge (in the case of the minerals is often repulsive, thus flocculation is limited). These forces are described by the theory DLVO including Van der Waals, electrical double layer and other forces such as hydration forces, steric strength ... etc. As a result, flocculation happens by the dominance of attractive forces which is often attributed to Van der Waals forces at the atomic scale (Lifshitz and Hamermesh 1992, Tsabet 2014).

2.3.1.6 Sedimentation and creaming

Sedimentation and creaming is appeared when we have difference in density between the continuous phase and dispersed droplets. Indeed, when the dispersed droplets are denser than the continuous phase, they tend to migrate downward by the influence of gravity (sedimentation) or otherwise upward (creaming). The migration speed of droplets might be obtained by Stokes Law for dilute emulsions:

$$V_{sed/cer} = \frac{g{D^2}_d(\rho_c - \rho_d)}{18\mu_c} \quad (2.7)$$

Where g is the gravitational acceleration, D_d is the droplet's diameter, ρ is the density of the droplet or continuous phase and $\mu_c$is the dynamic viscosity of the continuous phase.

The maximum total amount of solid mass of particles that can be attached to the creamed droplet and carried to the top of emulsion is calculated according to the buoyancy force balance:

$$M_{solid-max}(attached\ with\ cream\ droplets) = V_D(\rho_c - \rho_d) \quad (2.8)$$

2.3.1.7 Coalescence and the phase inversion

This phenomenon has been described for the first time in 1896 by Ostwald. It consists of an increase in the droplet size of an emulsion by the time span. It follows the Laplace pressure difference between the droplets with different sizes and therefore depends on the size distribution as well as the solubility of the dispersed phase in the continuous phase. Indeed, diffusion may cause larger droplets from smaller. This phenomenon is also due to the fact that the Laplace pressure is higher in the smaller drops. The coalescence is the main mechanism that makes emulsions unstable. It occurs in three steps:

- Droplets approaches stage and the frequency of collision between the droplets which are controlled by the hydrodynamics in the system.
- The film drainage during the collision of droplets and corresponds to the thinning of the interface film due to mobility and deformability of the droplets until it breaks.
- Film breakage phase where the film reaches a minimum thickness locally and lead to form a larger droplet.

Also, there are two types phase inversion. The transitional phase inversion can be caused by the change of the temperature or the concentrations of electrolyte system that may influence the particular surface properties. The catastrophic phase inversion is induced by the increase of the concentration of the dispersed phase. The inversion limit depends on droplet size distribution, system properties, type, shape, and, size distribution of the other emulsifier agents (Arditty, Whitby et al. 2003, Tadros 2009, Wan and Fradette 2017)

2.4 Stabilisation of Pickering emulsion

Notably, in the recent years, many studies have been conducted on emulsion properties including stability, type, size, and more recently the rheological behaviour. Particularly, the formation of a steric particle barrier around the droplets prevents coalescence and makes stability. In general, solid stabilized emulsification could be explained by these phenomena: 1) In term of hydrodynamics: phase breakage and droplet formation, Particle/droplet approach and collision. 2) In term of formulation: particles attachment into the interface. 3) Both hydrodynamics and formulation: network formation and droplet stabilization. The effects of formulation phenomena on final emulsion properties have been widely studied. However, the effects of hydrodynamics phenomena in emulsification process itself are very rare (Tsabet 2014, Tsabet and Fradette 2015).

2.4.1 Particle/droplet interactions

In an overall view, Pickering emulsification of oil, water and solid particles can be attributed to the formation of particle network around the droplets which can stabilize droplets. This process happens in three stages: 1) the particles approach and collide to the fluid/fluid interface. 2) the particles are captured and attached into the interface. 3) The adsorbed particles form a packed network around droplets that protects them from coalescence and stabilizes the emulsion. To investigate the phenomenon involved during approach and adsorption, The DLVO theory can be used. In this theory which is named after Boris Derjaguin and Lev Landau, Evert Verwey and Theodoor Overbeek, the interaction of two colloidal particles explains quantitatively based on the forces between charged surfaces interacting through the liquid medium. It investigates the effects of the van der Waals attraction forces due to the molecular structure interactions and the electrostatic repulsion forces due to the generation of double layer of counter ions around the surfaces. The approach is to use force analysis. The forces include DLVO forces such as attractive van der Waals forces and repulsive electrostatic double layer forces, and also non-DLVO forces such as repulsive hydration forces and attractive hydrophobic forces. By analysing their amplitude, is deduced that capillary force is the dominating force compared to other involved forces which is in turn governed by the contact angle (Table 2.1) (Yan and Masliyah 1994, Yan and Masliyah 1995, Binks and Fletcher 2001, Yan, Gray et al. 2001, Fournier, Fradette et al. 2009, Tsabet 2014).

Table 2.1 Force analysis during adsorption (Tsabet and Fradette 2016)

Force	Nature	General expression	Order of magnitude
Viscous	*Repulsive*	$6\pi\eta V_p R_p$	~ 10 nN
Buoyancy	*Repulsive*	$4\pi R_p^3 \rho_w g/3$	~ 1 nN
Gravity	*Attractive*	$4\pi R_p^3 \rho_p g/3$	~ 3 nN
Hydrostatic pressure	*Attractive*	$\pi R_p^2 L\, \rho_w g$	~ 50 nN
Capillary	***Attractive***	$\boldsymbol{2\pi R_p \gamma}$	**~ 10000 nN**

2.4.2 Particle/interface approach and collision

Many research projects have been granted recently to investigate the particle/fluid interface approach and collision process, particularly in flotation processes. Most of them have focused on a global approach based on film drainage flow analysis and forces analysis (DVLO theory) including van der Waals, electrical double layer, and, other forces such as hydration, hydrodynamic, hydrophobic, and steric forces (Tsabet 2014). The force analyzing can be deuced by force-distance curves using AFM (atomic force microscopy) techniques (Ducker, Xu et al. 1994), (Fielden, Hayes et al. 1996).

DLVO Forces

Among DLVO forces such as van der Waals, London dispersion, Debye forces and electrostatic double layer forces, the last one is more pronounced in emulsification of mineral particles. It occurs between surfaces with relatively high dielectric constants. These forces mainly related to the formation of charge layers at the mineral surface or interfaces through the adsorption of free ions in the slurry. A repulsive force occurs due to the formation of double layer of similar charges. Sometimes especially in the case of minerals and air bubbles, when the free ions concentration is increased in the system, coagulation happens between colloidal droplets due to the effect of all attractive dipole interactions including van der Waals forces (Ducker, Xu et al. 1994, Gillies and Prestidge 2005, Liang, Hilal et al. 2007).

Non DLVO Forces

One of these forces is hydration forces that their mechanism has been attributed to the formation of water molecular layers at particle interfaces. They are mostly bigger than DLVO forces and are associated with the higher energy required to remove the water molecular layer adsorbed with hydrogen bonds at the interface. Many studies have been devoted to repulsive nature of hydration forces, especially during interactions between solid particles and interfaces. Hydration forces can be described by exponential decaying evolution with the separation distance and will be classified as part of detachment force (Pashley and Israelachvili 1984, Drelich, Nalaskowski et al. 2000, Gillies and Prestidge 2005). Another is hydrodynamic repulsive forces which are induced during the drainage of the thin liquid film between surfaces and arise at very short distances. Like as the drag force, hydrodynamic forces for the sphere shapes depend on the separation distance. The liquid slippage at boundaries requires a corrective factor to a non-slippage condition (Chan and Horn 1985, Craig, Neto et al. 2001). The steric forces arise when the particles attach to interface and form an overlapping network structure that prevents the approach of other particles due to a repulsive entropic interaction. Steric forces depend on the nature of the liquid media, the surface and ionic properties of the adsorbed particles, and the adsorption time but, it is the main reason of minimizing covered interface (Tsabet 2014).

2.4.3 Particle adsorption dynamic and equilibrium conditions

There are two approaches to assess the particle stability at interface. The first considers that stability occur when the system reaches its minimal energy based on a free energy analysis. The second considers that the particle equilibrium is reached when the forces are balanced at the point based on a force analysis. The free energy approach supposes that the adsorbed particles at the interface are going to stabilize when the interfacial energy balance reaches to the minimum level.

$$E_{particle\ at\ interface} < E_{dispersed\ particle} \qquad (2.9)$$

$$E_{droplet\ with\ particle} < E_{droplet\ without\ particle}$$

In other word, the minimum value of the interfacial energies is attained while the particle stabilized in the equilibrium position at the interface (Binks and Horozov 2006):

$$\frac{dE_{particle\ at\ interface}}{d\theta} = 0 \qquad (2.10)$$

$$\frac{dE_{droplet\ with\ particle}}{d\theta} = 0$$

Where $E_{p/disp}$, $E_{p/interf}$, $E_{d/with\ p}$ and $E_{d/without\ p}$ are the interfacial energy of the particle in the bulk aqueous phase, at the interface, the droplets with adsorbed particles and without adsorbed particles and θ is the contact angle. A thermodynamic equilibrium including the adsorption energy or work is used to deduce stability of the system. The interfacial energy balance for the adsorption of silica particles at a planar interface has also been deduced (Levine, Bowen et al. 1989):

$$E = 4\pi r^2\gamma_{ws} - \pi r^2\gamma_{ow}(1 - cos\theta)^2 \quad \text{for} \quad \theta < 90^\circ \qquad (2.11)$$

$$E = 4\pi r^2\gamma_{os} - \pi r^2\gamma_{ow}(1 + cos\theta)^2 \quad \text{for} \quad \theta < 90^\circ$$

Where, γws is the water/solid interfacial tension, γow is the oil/water interfacial tension, γos is the oil/solid interfacial tension, r is the particle radius, and θ is the contact angle.

The first two terms describe the interfacial energy of the particle in the bulk (Oil or water) phase while the second term describes variations of the interfacial energy when the particle captured and stabilized at the interface. Since, the capillary forces are the main interaction between particles at the interface and concerning the stability of huge number of particles N_p at the interface, there is a good assumption that the interfacial energy variation must be balanced by only particle interactions at the interface which in turn concluded from contact angle or wettability differences for variety of mineral particles in the system. (Levine and Bowen 1991, Aveyard, Binks et al. 2003). In the force balance approach, it is assuming that the sum of external forces on particles is equal to zero at the equilibrium position. Thus, the stability conditions of the particles at interface by a good assumption are deduced again mainly from capillary forces and more relevant to the contact angle (Rapacchietta and Neumann 1977, Levine, Bowen et al. 1989, Fielden, Hayes et al. 1996, Tsabet 2014)

2.4.4 Formation of particle network

The third step is the formation of the particle network around the droplets and to stabilize them depends on particle compactness and configuration. In general, the particles form at least one layer of strike barrier, however, by increasing the layer number the coalescence rate reduces. In the other hand, it is also possible to stabilize Pickering emulsions without covering the entire interface with particles (Binks and Horozov 2006). Ordered hexagonal networks are one of the most common particle configurations at fluid interfaces and monolayer hexagonal structures have also been observed. There are many parameters that affect the network formation, for instance, the presence of a repulsive interaction between the attached particles at the interface, the particle size, adsorption level and ionic concentration (Tarimala and Dai 2004). Furthermore, for a network cohesion, the repulsive forces must be balanced by the attractive forces such as lateral capillary which is caused by particle surface wettability or contact angle (Horozov, Aveyard et al. 2005). Particle adsorption at the interface is surrounded by a meniscus curvature around the particle while the expansion of the three contact lines (TCL) reach to the equilibrium position by the amplitudes of capillary forces at the interfaces (Rapacchietta and Neumann 1977). Thereupon, the mineral particles with irregular shape (i.e., sphericity <<1) and a high aspect ratio increase the deformation of the interface and the amplitudes and magnitude of attractive capillary forces, and, more distortions at the interface (Loudet, Yodh et al. 2006). In the other hand, the asymmetry of the dipolar electrical field on charged particles at the interface, causes the difference in dielectric constants between the two immiscible liquids, and makes the electrostatic stresses which act as the third source of capillary forces (Nikolaides, Bausch et al. 2002). Furthermore, electrolyte concentrations have a significant effect on electrostatic double layer forces. In other side, van der Waals Forces have intermediate values ranging and less significant than capillary forces. They are relatively important and lead to prove the importance of wettability differences to control the emulsion properties and particle/droplet selective and competitive attachment (Midmore 1998, Pichot, Spyropoulos et al. 2012). Particle dynamics at the interface have been attributed to thermodynamic equilibrium and the inter-particle force balance. The studies report the particle diffusion coefficient at the interface with the same order of magnitude at the bulk of liquid media (around $5\times10^{-9}\ cm^2$/s) and it can decrease considerably by increasing the oil viscosity limited to zero (i.e., no diffusion) and thus the stability, network

formation and selective attachment relatively have been attributed to the characteristic of the oil viscosity and the particle size (Vignati, Piazza et al. 2003).

2.4.5 Properties of Pickering emulsion

The stability is one of the important properties of an emulsion. In terms of time, it can be defined as the ability of droplets covered by solid particles to be remained dispersed in the continuous phase. Destabilization can be promoted by droplets contact and thus increase the probability of coalescence, which lead emulsions into demulsification and phases separation. Hereafter, other properties of a Pickering emulsion can be divided into parameters (Tsabet 2014) affect the particle selective attachment such as properties of phases (aqueous, oil, solid particles), droplet size distribution, creaming behaviour, and other parameters. In case of emulsions prepared by REE minerals, the droplet size was around 12 times larger than the average size of the associated particles. The emulsion size (i.e. droplet size), grow slowly by increasing the size of the feed particles. A similar behavior observed with different type of particles in the fundamental literature (Tambe and Sharma 1994) mostly due to the fact that the oil droplets in a Pickering emulsion have tendency to get stabilized with smaller particles which have larger coverage potential (Tsabet and Fradette 2015).

2.4.6 Formulation (parameters of solid, aqueous and oil phases)

As previously mentioned, wettability of the solid particles has the most significant effect on SSE stability and there are many studies to investigating the roles of particle, water, and oil properties in emulsion stability. In order to describe the effect of contact angle, the energy required to attach or remove a particle from the interface the following expression has been proposed (Fournier, Fradette et al. 2009):

$$\Delta E = \pi R^2 \gamma_{ow} (1 \pm cos\theta)^2 \qquad (2.12)$$

Where E is the detachment energy (J), R is the particle radius (m), γ_{ow} is the oil/water interfacial tension (J/m^2), and θ is the contact angle.

The contact angle can be calculated from interfacial tensions at three contact lines between the different phases by applying the Young equation:

$$Cos\theta_{aw} = \frac{\gamma_{sa}-\gamma_{sw}}{\gamma_{wa}} \ , \quad Cos\theta_{ao} = \frac{\gamma_{sa}-\gamma_{so}}{\gamma_{oa}} \tag{2.13}$$

$$Cos\theta_{OW} = \frac{\gamma_{wa}Cos\theta_{aw}-\gamma_{oa}Cos\theta_{ao}}{\gamma_{wo}} = \frac{\gamma_{so}-\gamma_{sw}}{\gamma_{wo}}$$

Where θ and γ are respectively the contact angle and the interfacial tension (J/m^2) for oil/water, solid/oil and solid water.

Moreover, the particles with more hydrophobicity (i.e., large contact angles) form a compact layer at the interface while the particles with small contact angles flocculate and thus, create less compact layer at interface, a promoting factor for a selective attachment (Yan and Masliyah 1994). However, the emulsions can be destabilized using specific mixtures of particles with different wettability due to the inability of the network to prevent coalescence (Binks 2002, Whitby, Fornasiero et al. 2010). On the other hand, amphiphilic particles, or Janus particles, with different wettability around their surface area such as locked grain mineral particles generate considerably more stable emulsions (Binks and Fletcher 2001). It is also important to know that O/W emulsions can be produced by the use of particles with the contact angle lower than 90 such as the REE ore particles. Notably, this behaviour is according to Bancroft rule, whereby the particles are initially wetted and dispersed in the continuous phase which they have higher affinity (water) and while the dispersed phase (oil) fraction is smaller or equal to the continuous phase fraction (Binks and Lumsdon 2000, Yan, Gray et al. 2001, Binks, Philip et al. 2005, Binks and Horozov 2006). The studies show that the droplets should be completely covered by at least one particle layer to ensure emulsion stability. Thus the demulsification rate is reduced when the particle concentration is increased. However, the increase of particle concentration in the system will decrease the emulsion droplet size slightly and also has a negative effect on the particle attachment efficiency. Thus, increasing feed mass ratio would not be always a good idea to improve the process efficiency (Binks 2002). However, in some cases, it is possible to stabilize emulsions without covering the entire droplet surface where the particles are partially flocculated at the interface or has significant dynamics at the interface. This is more pronounced on the REE minerals in the slurry with significant surface charges and flocculation behaviour. Also, emulsion stability can be increased by decreasing the size of the particles which lead to a close-packed network formation (Yan and Masliyah 1994, Yan and Masliyah 1995, Vignati, Piazza et al.

2003). The smaller in size cut in the upstream mineral treatment process makes more uniformity and higher grade of liberated REE bearing minerals due to the maximum liberated surface of targeted minerals would be available towards the selective interface. However, the smaller cut sizes need more cost and energy to be performed. The smaller particle size also leads to a better stabilization by maximizing the stabilized interface in the system which can in turn lead to smaller droplet size (Binks and Lumsdon 2001, Tarimala and Dai 2004, Wills and Finch 2015). The effect of particle shape generally describe by aspect ratio, sphericity, morphology and surface roughness where the emulsion stability can be enhanced by increasing the aspect ratio, less sphericity and higher roughness mostly due to formation of a denser packed-layer network at the interface and stronger capillary forces (Tsabet 2014). Thereafter, the properties of emulsions are very sensitive to hydrogen potential (pH) variations which can also affect the surface charges of particles (zeta potential) and ionic species in the system especially in the case of REE minerals, consist of both hydrophobic and hydrophilic groups (Yan and Masliyah 1996, Yan and Masliyah 1997, Owens, Nash et al. 2018). Thereupon, particle flocculation has been occurred in presence of electrolytes ions or salts in the aqueous phase mostly because of the particle interactions with higher repulsive double layer DLVO forces (Binks and Lumsdon 1999, Yang, Liu et al. 2006, Horozov, Binks et al. 2007). the fact that the emulsion size enlarge with the higher capillary number or number of viscosity (Tsabet and Fradette 2015). Thereinafter, the properties of emulsions are affected by oil viscosity where an increase (limited) η_{oil}/η_{water} ratio decreases the emulsified oil volume fraction and reduce stability until the emulsification cannot be achieved for a given process condition (Fournier, Fradette et al. 2009). The oil-to-water volume ratio Φ_d should be adjusted for an appropriate interface generation always more than coverage potential of available particles in the system. An adequately low amount of Φ_d leads to smaller emulsion size (Binks and Whitby 2004, Tsabet and Fradette 2015). Polar oils such as fatty alcohols, esters, and triglycerides contain heteroatoms in one side with differential electronegativity between the two bonded atoms (e.g., oxygen) vs. single bonded atoms (e.g., hydrogen) which form a dipole molecular structure. Polar oils have lower IFT versus water comparing to non-polar oils such as mineral oils (Binks and Lumsdon 2000, Binks 2002, El-Mahrab-Robert, Rosilio et al. 2008).The oil polarity with electrical properties of heteroatoms composed of (O, N, and S) can also affect emulsion stability due to modifying particle/particle/interface interactions. Oil polarity enhances oil/particle affinity and thus a

smaller contact angle while reduce interfacial tension (Binks and Lumsdon 2000, Binks 2002, Tsabet 2014). Oil/particle affinity, wettability and emulsion conductivity which is good indicator to determine emulsion's types will change with polar oils (Binks and Lumsdon 2000).There are interfered interactions with the polar oils and the surface charges of the particles in aqueous phase (Danov and Kralchevsky 2006). Both interfacial tension and contact angle as the physical properties of phases have significant effect on the competitive attachment of the mineral particles at the interface. There are parameters that particularly affect the contact angle and IFT such as temperature, aging, salinity and double layer formation (Pichot, Spyropoulos et al. 2012). The most polar oils made most stable O/W emulsions and it is mainly due to the particles remaining at the interface rather than the water phase. However, the effect of polar oil on the selective attachment is every complex due to the completely changes on the wettability ragnges and interfacial tensions (Binks and Lumsdon 2000, Binks 2002, Tsabet 2014). Indeed, particles become more hydrophobic with polar oils and more hydrophilic with nonpolar oils (Tsabet and Fradette 2015).

2.4.7 Effect of temperature and surface modification

Some of the emulsion properties are influenced by temperature through its effect on interfacial tension and oil viscosity (i.e., decline by increasing temperature) such as stability, particle selective attachment. Also, increasing the system temperature might promote the coalescence and thus emulsion destabilization or phase inversion might be happen (Binks, Murakami et al. 2005, Ngai, Behrens et al. 2005). Surfactants adsorb on particle surfaces and modify particle wettability. Also, the presence of surfactants in the process can influence the properties of generated interface by reducing the interfacial tension. The surfactants can be classified into natural or synthetic base and four categories based on their structure of hydrophilic head: non-ionic (uncharged functional groups), cationic (ionizable at acidic PHs), anionic (ionizable at basic pH), and zwitterionic (both cationic and anionic groups). The act of surfactants are very sensitive to pH and thus pH variations are using to control the particle-interface infarctions (Yan and Masliyah 1996, Binks, Murakami et al. 2006).

2.5 Minerals characterization

The surface chemistry aspects of bastnaesite and monazite are significantly related to their semi-solubility and chemisorption in aqueous phase. The conjunction gangues in the REE ore have also chemisorption interactions at different pH. Several studies dedicated to their surface charge which is commonly explained with zeta potential, point of zero charge (PZC) (Cheng 2000) and isoelectric point (IEP). It seems that a pH around 9 is near to the nature of the ore slurry in aqueous phase where there are many alkali ions e.g. Ca++, Mg++…after partially dissolution of minerals even with very low solubility. This pH gives also the best differences in zeta potential for the REE bearing minerals and the rest of the major gangues which in turn promote their selective attachment into the interface (Herrera-Urbina and Fuerstenau 2013, Jordens, Marion et al. 2014, Owens, Nash et al. 2018). A QEM-Scan analysis of the ore is provided in appendix including mass fraction and grain size of the associated minerals (Lafleur, Eng et al. 2012). The ore minerals can be categorized in four main groups of carbonates, silicates, oxides and phosphates. Bastnäsite and monazite are the most abundant REE bearing minerals in the Niobec ore. On the other hand, calcium carbonate minerals such as calcite, dolomite and ankerite constitute the main mass fraction of the gangue. It is notably, the abundance of minerals varies from one location of the deposit to another. However, the ingredients of the ore follow a similar pattern in the Niobec's deposit (Lafleur, Eng et al. 2012).

2.5.1 Grade of Niobec's ore

The electron microprobe analyses (EMPA) of elemental assay on pure bastnaesite and pure monazite from Mountain pass USA are indicated respectively in Table 4.5 for the most abundant elements including Cerium, Lanthanum and Neodymium. The minerals model from Mountain pass USA will be used to characterize the wettability of REE bearing minerals. However, the crystal structure and composition have effect on the surface properties. Since the TREO in the composition is very similar for both Niobec and Mountain pass model minerals, the surface properties and wettability should be similar (Jordens, Cheng et al. 2013).

2.5.2 Minerals Contact angle

A single particle of ore could be composed of more than one grain mineral. As it mentioned, the wettability is the most important parameter to control selectivity of SSE during particle attachment into the interface (Hey and Kingston 2006). Thus, small enough particles in favour to liberate the encapsulated grains of monazite and bastnäsite should be provided. Otherwise, contact angle of the complex Janus surface of mineral particle governs their selective attachment into the interface (Rezvantalab and Shojaei-Zadeh 2013). The average water-solid contact angle of the most pure minerals was measured directly on their clean and polished flat surface with a goniometer (Kabza, Gestwicki et al. 2000, Azimi, Dhiman et al. 2013) that employed the sessile drop technique for intermediate equilibrium contact angle. The water-air-solid contact angle could be simply linked to the oil-water-solid contact angle in Young equation which is briefly called contact angle (Hey and Kingston 2006). Since some of pure samples of monazite and bastenaesite were obtained in powder form, the oil-water-solid contact angle of these minerals was estimated from the Blake–Kozeny equation based on a capillary rise in a capillary tube filled with the powder (Fournier, Fradette et al. 2009). The literature reported contact angle between water and pure monazite was above 49° and the values of contact angle indicate wettability difference between the REE bearing minerals (i.e., a larger contact angle with water or more hydrophobic) and their associate gangues (i.e., more hydrophilic). (Abaka-Wood, Addai-Mensah et al.). Notably, the contact angle values change in different conditions and more pronounced at different aqueous conditions such as pH, presence of different ions, crystal structure, surface roughness, oil molecular interaction, chemisorption of the free ions and double layer formation (Kvítek, Pikal et al. 2002, Thompson, Lombard et al. 2012, Zhang 2014). According to the literature, bastnäsite and monazite tend to either attach more into the interface of the oil droplets and conversely the more hydrophilic particles such as dolomite and calcite tend to remain in water phase (Binks and Lumsdon 2000, Hey and Kingston 2006, Tadros 2009, Tsabet and Fradette 2015). Since the contact angles are not absolute values, we could assign a mineral surface if it is more hydrophilic or less hydrophobic when compared with other minerals. The contact angle of minerals is affected by the wetting characteristics, electrokinetic features and surface charge in conjunction with the oil and it is significantly related to their semi-solubility and chemisorption behaviour in the aqueous phase (Castor and Hedrick 2006, Li and Fuerstenau 2013, CH Li and W. Fuerstenau 2015).

2.6 Pickering emulsification

Three different mechanisms can be identified to describe solid stabilized emulsification process: Droplet generation or breakage, droplet stabilization and droplet coalescence. In a standard emulsification, breakage and coalescence are often studied because the stabilization can be achieved very fast especially by reducing the interfacial tension using surfactant. Nonetheless, the stabilization mechanisms are significantly affected by surface properties while the generation of the interface and coalescence are controlled through particles interactions and hydrodynamic in the system. In general, the particles do not change interfacial tension during the stabilization step because solid particles do not act as amphiphile molecules and also their size is much higher than the surfactant, henece, the stabilization time would be much longer (Arditty, Whitby et al. 2003, Binks and Whitby 2004, Tsabet and Fradette 2015). Whereby, depending on the particle properties the emulsion might flocculate, cream or settle as sediment. Hence, a complex interaction between the involved mechanisms and the emulsification hydrodynamic should be considered in term of system analysis. In general, droplets are firstly generated then stabilized by the fine particles adsorption into their equilibrium position, assuming that the only droplet breakage and coalescence are involved in Pickering emulsification. However, the particles affect the system through their effect on the phases, rheology and thus stabilization mechanism. In such a system, an interface generation potential can be deduce from the Sauter mean diameter and the system characteristic and capacity to produce droplets (Tadros 2009, Simon, Theiler et al. 2010, Tsabet 2014).

On the other hand, a coverage potential of the system can also be calculated as follows:

$$A_{cov} = N_p \times A_{cov/1p} \tag{2.14}$$

Where, A_{cov} is the coverage potential and, $A_{cov/1p}$ is the covered surface by one particle of D_{32p} and N_p is the number of total particles in the system. The first aim in Pickering emulsification of REE bearing minerals is to promote mineral particle/droplet contact and maximize the adsorption force and droplet coverage (Tsabet 2014).In general, the stabilization can be achieved when the coverage rate (a mean diameter size of stabilized droplet covered by certain amount of particles) overcome the overall coalescence rate. Coverage rate of particles can be formulated by particles/droplet collision frequency and the stabilization efficiencies applied for each single

particle. As previously mentioned, particle attachment includes three main steps including the approach, film drainage and the adsorption which are mostly governed by DLVO and capillary forces (Tsabet 2014). In another side, the solid particles with wettability differences adsorbed on the interface have been investigated in few literature, a decrease in concentration of the particle with larger contact angle will reduce the inter-particle distance, and thus lead to aggregated particles and a transition from ordered hexagonal network to a disordered structure configuration (Horozov, Aveyard et al. 2003). It has been shown that using extreme hydrophobic and hydrophilic particles can lead to the least stable emulsions, whereas the most stable emulsions are generated using particles of intermediate hydrophobicity (Binks and Lumsdon 2000, Yan, Gray et al. 2001). Whenever a mixture of solid particles have a relatively a range of wettability, the property of the emulsion produced will depend on the order of mixing, the phase in which the powder mixture will be initially mixed or wetted and the proportions of the three phases (Vignati, Piazza et al. 2003).

2.7 Demulsification and phases separation

In order to separate the mineral particles, we need to destabilized emulsion by a demulsification process. Several applications and methods are used for demulsification design and normally followed by a phase separation process in the related industry. Some of these are applying magnetic or electric field to generate a force greater than the capillary force responsible for the detachment of particles from the interfaces (Yan and Masliyah 1995). The magnetic field separators are likely exist in the industry among different technologies which have been developed for demulsification. The various breakdown methods can destabilize emulsion through simultaneously or consecutively processes (Jordens, Cheng et al. 2013). The gravitational and centrifugal forces are also using in demulsification processes and act on the density difference between the continuous and dispersed phases. The size distribution of the emulsion droplets does not change during natural creaming and sedimentation and so they are independent from droplet-droplet interactions (Binks and Horozov 2006). Creaming/sedimentation can be results of an external force such as the gravitational and centrifugal forces. Creaming/sedimentation are limited by reducing the density difference between two phases or by thickening the continuous phase or by reducing the droplet size (Yan and Masliyah 1995). There is no changing in the original size of the droplet during flocculation and it is just the aggregation of droplets.

Flocculation occurs only by enough strong attraction between the droplets to overcome the repulsive forces. Indeed, it is partially reversible depending on the magnitude of the forces between the droplets (Tadros 2009). The Figure 2.7 depicts the net interaction energy between the droplets resulting from the balance between attractive forces (van der Waals) and repulsive forces (electrostatic double layer). a) Attractive forces overcome the repulsive forces and thus the rest of the interaction energy is negative. This condition is a required step towards the coalescence of the droplets and most favorable for destabilization. b) The interaction energy reaches a minimum at large separation distances and a maximum at relatively at very small separations related to flocculation, a metastable emulsion. c) The interaction energy is positive for entire the separation distances, illustrating that the repulsive forces are stronger than the attractive forces between the droplets and prevent droplets to form coagulation, very stable emulsion which is generally observed in the case of REE minerals (Yan and Masliyah 1995, Yan and Masliyah 1995, Khatri 2010, Tsabet 2014). An increase in free ions made e.g. by a part of soluble salts in the associated REE minerals gangues, will enhance surface charges effect on droplets and lead to less repulsive double layer forces which in turn lead to higher stability. Also the multiple ion valences like as disassociated REE mineral free ions in aqueous phase, promote the particle flocculation rate and thus better coverage potential and stability (Binks and Lumsdon 1999, Yang, Liu et al. 2006, Horozov, Binks et al. 2007). In the slurry, REE minerals and their associated gangues may change pH (the reported IEP values for bastnaesite ranges from 4.6 to 9.5 and for monazite from 1.1 to 9, they reported the particle adsorption rate at the bubble interface decreases when the pH is very increased and thus a modification of particle wettability and interfacial tension is essential to improve performance of separation (Cheng 2000). Also, demulsification rate increases when pH is very increased due to the particles flocculation (Yan and Masliyah 1996, Yan and Masliyah 1997).

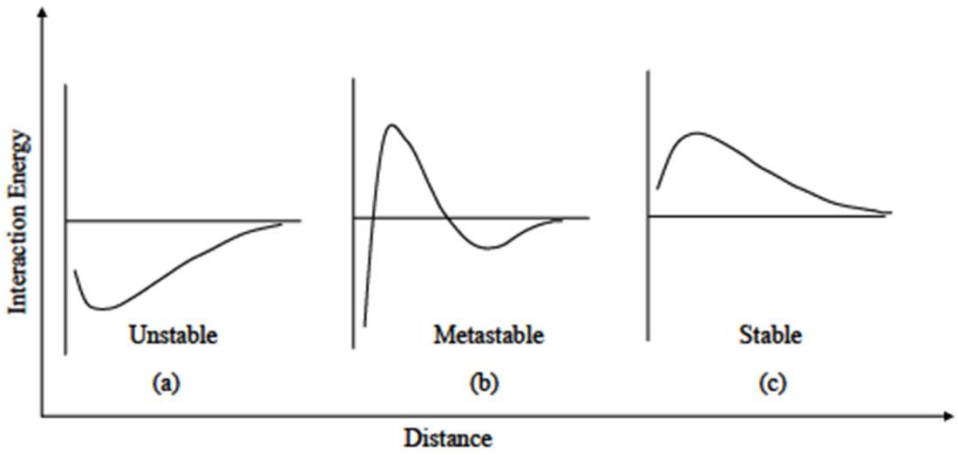

Figure 2.7 Potential energy curves for the interaction of two colloidal bodies. Negative values correspond to attraction and positive values correspond to repulsion: (a) Attractive forces overcome the repulsive forces; (b) repulsion and attraction are comparable in magnitude and amplitue; (c) repulsive forces are stronger than the attractive forces (Khatri 2010)

Coalescence is the thinning and drainage of liquid films between a pair of droplets as it is shown in Figure 2.8 and following fusion of the droplets. The coalescence is an irreversible process and more pronounced during demulsification resulting a complete phase separation into three distinct phases (Yan and Masliyah 1996, Tuinier and De Kruif 1999, Tadros 2009).

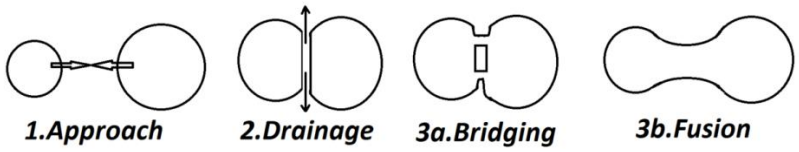

Figure 2.8 Schematic representation of coalescence process

There are also other external factors to promote demulsification rate and can be categorized in such chemical, thermal, mechanical, electrical and magnetic factors. Among them, the mechanical g force by centrifugation are more feasible at industrial scale (Hirajima, Sasaki et al. 2005, Tadros 2009). During phase inversion process there are the particles exchange between the dispersed and the continuous phases over time. By doing so, type of emulsion may change from O/W to W/O and reverse versa. In some cases multiple emulsions (O/W/O or W/O/W) have also been observed (Yan, Kurbis et al. 1997, Wan and Fradette 2017).

2.8 Rheology and mixing conditions

Hereafter, the significant effect of emulsion rheology is reviewed due to its effects on the particles attachment and detachment. The rheology of Pickering emulsion exhibit like shear-thinning fluids over yield stress especially at turbulent regime and high concentration of particles and thus its viscoelasticity is tend to the continuous phase in the case of REE bearing mineral separation. Thereupon, the power low for shear-thinning of a non-Newtonian Pickering emulsion is deduced where the model parameters are very sensitive to the particles concentration (Midmore 1998, Simon, Theiler et al. 2010, Tsabet and Fradette 2015):

$$\tau = \tau_0 + k_{HB}\dot{\gamma}^{\alpha} \tag{2.15}$$

Where, τ is the shear stress, τ_0 is the apparent yield stress, k_{HB} is the consistency, α is the power low index and γ dot is the shear rate.

The dissipation energy in an emulsification system equipped with agitator comes from mixing. The particles attachment rate for smaller particles is more dominant than for larger particles, an indication for the selective attachment of the particles. Because, at the similar mixing conditions, the smaller particles need less energy to be dispersed and smaller detachment forces (i.e. higher attractive force versus repulsive forces). In same manner, the particles with more affinity to the droplets or larger contact angle need less energy to be attached into the interface (Coulaloglou and Tavlarides 1977, Tsabet and Fradette 2015). The average turbulent energy dissipation rate can be deduced by the inlet power over the total theoretical mass of the system includes solids and liquids in the slurry (Paul, Atiemo-Obeng et al. 2004). Thus, the higher average turbulent energy dissipation rate, up to certain values, enhances the particle selective attachment and has a positive effect on the selectivity of the overall process (Tsabet and Fradette 2015).For small batch emulsification, the impeller should be installed off-centre to avoid vortex formation and to generate turbulence in the flow field. This setup is equivalent to a centered impeller with baffles in term of mixing performance (Karcz, Cudak et al. 2005, Gingras, Tanguy et al. 2012). Maxblend impeller can generate uniform shear rate in the emulsification tank compared to a same proposed PBT impeller. In another word, the difference between the maximum and minimum shear rate in the system equipped with Maxblend is much lower (Leng and Calabrese 2004, Paul, Atiemo-Obeng et al. 2004, Hashem 2012).Aslo, Maxblend setup provides lower average

turbulent energy dissipation rate beside a uniform and a lower shear rate when compared with PBT at a similar We number (Paul, Atiemo-Obeng et al. 2004, Hashem 2012). The “just suspended” speed (Njs) is the minimum agitation speed at which all particles reach a complete suspension. In an emulsification system, the rotational speed should be always above Njs to ensure there is an effective particle-droplet interaction and maximum selective attachment in case of the REE minerals. Many correlation is being proposed for Njs such as Zwietering model (Paul, Atiemo-Obeng et al. 2004). However, there is no correlation for Njs in the stirred tank equipped with Maxblend; thus Njs should be defined experimentally (Jafari 2010, Hashem 2012, Jafari, Chaouki et al. 2012).

2.9 Selective attachment

Indeed, the effects of applying particles with different wettability on SSE repoted that there might be produced a multiple emulsions. However, in the case of REE ore particles, all of them classified as hydrophilic surface. Thus, O/W emulsions would be generated, but the droplet gets mainly stabilized with those particles that has larger contact angle. This is so called the partially selective adsorption of the particles into the interface (Binks 2002, Aveyard, Binks et al. 2003, Binks and Whitby 2005, Whitby, Fornasiero et al. 2010). To investigate the selectivity, a global attachment efficiency of targeted minerals is being compared to the rest of gangue particles in the system and regarding the wettability differences (Abaka-Wood, Addai-Mensah et al. , Zhang 2014). The properties of an O/W emulsion made by mixtures of particles with slightly different wettability are similar to those one use hydrophilic particles alone. This is likely due to the fact that in O/W emulsions hydrophilic particles flocculate at the interface, whereas hydrophobic particles are preferentially dispersed all around the interface of droplets. Moreover, depends on particles interactions with the droplets at the interface, the emulsification behaviour vary mostly relevant to those of hydrophobic alone and more complicated when hydrophilic particles presence flocculated at the network configuration. Regarding to competitive attachments, the performance of separation could be defined as function of interface generation potential, coverage potential and selective attachment/detachment efficiencies (Braisch, Köhler et al. 2009, Pichot, Spyropoulos et al. 2009, Simon, Theiler et al. 2010, Pichot, Spyropoulos et al. 2012, Tsabet 2014). The diffusion coefficient is hindered when the oil shows elastic behaviour and it decreases with lower particle size. The hydrophobic particles are more immersed in the viscous

oil phase than hydrophilic particles, a better selective attachment for the REE bearing minerals with the viscous oil. (Binks and Lumsdon 2000, Fradette, Fournier et al. 2008). Indeed, the particle stabilization at the droplets interface have been reported with four steps as collision, attachment, three phase contact line (TPCL) development and network formation. According to the literature, we have specific efficiencies for each one of these steps, regarding an effective coverage during stabilization and selective particle adsorption at the interface. The literature mostly for the interaction of particles-bubble interface, give fundamentals behind the stabilization phenomena, these efficiencies can be assessed by free energy or even force analyses (Tsabet 2014). Hereafter, we provide the general formula and the sources of correlation for calculating these efficiencies.

$E_{Col} = exp(-C_1 \frac{t_d}{t_c})$, C.A. Coulaloglou (1975) (2.16)

$E_{TPCL} = 1 - exp(-\frac{t_c}{t_{TPC_{cir}}})$, H.J. Schulze et al. 1993

$E_{Att} = 1 - exp(1 - C_{Att} \frac{F_{Att}}{F_{Det}})$, H.J. Schulze et al. 1993

$E_{Cov} = exp(-\frac{Freq_{collision\ d/d} \times E_{Coalescence}}{Freq_{collision\ p/d}})$, A.K.Chesters (1991)

Where E_{Col},E_{TPCL},E_{Att}, $E_{Cov}$and $E_{Coalescence}$ are efficiencies of collision, three phase contact line formation, attachment, droplet interface coverage and coalescence respectively, t_c is the contact time, t_d is the drainage time, $t_{TPC_{cir}}$is TPC line expansion time, C_1 and C_{Att} are the constants, F_{Att} is the attachment force, F_{Det} is the detachment force, $Freq_{collision\ p/d}$ and $Freq_{collision\ p/d}$ are the particle/droplet and droplet/droplet collision frequencies (Coulaloglou and Tavlarides 1977, Tsouris and Tavlarides 1994, Nguyen, Schulze et al. 1997). As an example for the theoretical efficiencies, they are relatively lower for larger particles, and thus the overall efficiency to cover the interface would decline by increasing the particle size. In other words, the selectivity of emulsification declines for larger particles. Indeed, the larger particles cover smaller interface or have fewer coverage potential, and thus, a lower recovery and grade of the REE bearing minerals with larger particle size cut is expected (Binks and Lumsdon 2001, Tsabet and Fradette 2015).

CHAPTER 3 OBJECTIVES, RESEARCH FOCUS AND COHERENCE OF THE CHAPTERS

Regarding to this literature review, our research project aims to develop, for the first time, the application of SSE in physical beneficiation of REE bearing minerals and its feasibility at the industrial scale. This approach has been patented (US62793848) as a novel technique. There are also four article papers according to the exact sub-objectives titles.

3.1 Research questions

The specific main questions of the research project are listed as bellow:

1- Could the droplets in SSE be able to selectively capture the monazite and bastnaesite and concentrate them from the gangues?
2- How RBM mineral's surface property (i.e., wettability) promote their competitive attachment into the droplets and eventually their selective separation?
3- Is the SSE technique industrially feasible and viable to be applied instead of conventional FF methods?

Directions of achievements:

The SSE process can be compared with other physical beneficiation processes such as froth flotation. Although, eliminating the impact of chemical reagents or surfactants, reducing the water, chemicals and energy consumption and tailing ponds are the other important achievements.

3.2 Original solution and the main objective of the thesis

The Pickering emulsion will be used as an application for the REE bearing minerals beneficiation (i.e., mostly known in Niobec ore bastnaesite and monazite). Noteworthy as an alternative to flotation process, separation of bastnasite and monazite minerals from gangue minerals could be carried out through the solid-stabilized emulsions. It is important to note that no surfactant or emulsifier is used to generate such solid-stabilized emulsions. Therefore, the technique must be investigated to reach optimum condition at which bastnaesite and monazite will be recovered at maximum possible concentration. The principe is to make a stable emulsion with mixture of ore,

water and oil. However, the emulsion must have enough stability to go through the phase transfer separation process.

The main objective is to separate bastnaesite and monazite coming with individual physicochemical properties from the ore by emulsifying the mixture and generate a solid stabilized emulsion. Also, to develop the method and to identify the mechanisms involved in the emulsification phase separation and demulsification. The objectives follow to evaluate the separation performance quantitatively and compare with other physical beneficiation technique (i.e., froth flotation achieves recovery about 55% (Xiong, Deng et al. 2018)) and to define the optimal operating conditions in term of formulation and process parameters. The research hypothesis associated with these objective states correspond to introduce Pickering emulsion as a novel technique that it is quite possible to replaced or placed in the physical beneficiation of mineral processing without using any chemical reagents or surfactants. Th main objective of the research project is followed with the main title of the research project.

3.3 Hypothesis, specific objectives

In order to accomplish the main objective, the justification and hypothesis of the work consist of specific objectives as follows (Coherence of the chapters-articles):

1. Develop a novel approach for physical beneficiation of rare earth bearing ores: Pickering solid-stabilized emulsification. In addition, we improve the performance of separation of the process by adjusting the processing conditions to a comparable recovery and enrichment with FF (next objective):
2. Investigate the effect of mixing intensity and shear uniformity on enhancing recovery of monazite and bastnaesite through Pickering emulsification. In the next objective, We find an economic and cheaper formulation with comparable recovery and enrichment to FF:
3. Investigate the effect of the properties of oil on recovery of monazite and bastnaesite through Pickering selective emulsification. Finally, we analyze the feasibility of the process (next objective):
4. Evaluate techno-economic aspects of the recovery of rare earth bearing minerals by Pickering selective emulsification vs. FF;

CHAPTER 4 ARTICLE 1: A NOVEL APPROACH FOR PHYSICAL BENEFICIATION OF RARE EARTH BEARING ORES BY PICKERING EMULSIFICATION

Rahi Avazpour, Mohamamd Latifi, Louis Fradette, Jamal Chaouki[1]

Department of Chemical Engineering, École Polytechnique de Montréal, c.p. 6079, Succ. Centre-ville, Montréal, Québec, H3C 3A7, Canada

(Journal of MINERALS ENGINEERING, Date submitted: 15/04/2019)

4.1 Abstract

A solid stabilized emulsification (SSE) process was developed to produce a concentrate of the rare earth element (REE) bearing minerals, i.e. bastnäsite and monazite, from an ore that included gangue minerals such as dolomite, calcite, ankerite, silicate, quartz, pyrite, mica, hematite, and barite. The results showed that the liberated REE bearing minerals had a better affinity to the oil droplets than the gangues due to their surface wettability differences; therefore, they eventually attached more into the oil-water interface whereas the gangues stayed in the water phase. We studied the behaviour of the REE ore in the emulsion system along with the surface properties of the minerals, water and the employed oil to demonstrate the ability of Pickering emulsion to separate and concentrate the REE bearing minerals. The enrichment ratio after one stage emulsification increased up to 290% with a recovery higher than 50% without even manipulating the pH and/or applying any surface modifier.

Keywords: Pickering emulsion, Rare earth elements, Minerals recovery, Physical beneficiation

[1] Correspondence concerning this article should be addressed to L. Fradette at Louis.fradette@polymtl.ca

4.2 Introduction

Physical beneficiation is the upstream process to produce a concentrate of the desired mineral(s) from an ore with a low concentration. Magnetic, gravity and electrostatic separation are some known physical beneficiation methods. Given the fact that rare earth element (REE) bearing minerals are usually adjacent to gangue minerals of similar physical properties, e.g. magnetic susceptibility, density and electrostatic properties, such physical methods result either in poor beneficiation efficiency or a complex and costly network of physical processing units (Castor and Hedrick 2006, Jordens, Cheng et al. 2013).

One way to overcome the challenge of similar physical properties is to modify surface property of ore particles and apply the separation based on wettability of minerals. The froth flotation is the conventional surface chemistry based process that relies on the attachment of grinded ore particles with modified surface hydrophobicity to air bubbles that lift them to the top of the flotation tank followed by a foam scrubbing. The overflow hence contains a higher concentration of the targeted minerals to recover. However, sometimes the particles attaching to the air bubbles are not of interest, i.e. particles mainly containing gangue minerals; Such a flotation process is called reverse flotation (Bulatovic 2007).

Surfactants are employed to create froth with controlled properties, i.e. size of bubbles, stability, lifespan, and etc. to modify the surface of minerals of interest that are most often in combination with pH control of the aqueous phase. The employed surfactant molecules are in overall costly while they are detrimental to the environment. Moreover, there are normally various sorts of surfactants in a flotation tank for different purposes such as frothers, collectors and depressants to reach a desired recovery and grade (Table 4.1) (Mittal and Shah 2013).

Table 4.1 Common surfactants and pH reagents for REE minerals flotation (Anderson, Taylor et al. 2016)

Collectors		**Depressant**	**Activators, Flocculant, Frother**
Cationic	**Anionic Oxhydryl-Sulfhydryl**		
Primary, secondary and teriary amines, Quaternary ammonium compounds (Dodecylammonium chloride)	Carboxylates (Fatty acids and their salts, Oleats, tall oils F4286, Sodium oleate), Phosphoric acid ester (Flotinor SM15 1682) ,Dithiophophates, Hydroxamates (Benzohydroxamic acid,Flotinor V3759), Sulfates, Sulfonates, Benzoic acid	(Sodium Silicate Na_2SiO_3) ,(Sodium Sulphide Na_2S), Starches, Sodium Hexametaphosphate $(NaPO_3O3)_6$, Quebracho, Amylopectin, Potasium alum, Sodium silicofluoride, Lignin sulfonate	Fluorosilicic Acid H_2SiF_6, Magnafloc156, Ferric Chloride $FeCl_3$, Disponil SLS 101/103, MBC F150, Acumer 9400, Witcomul 3251

Table 4.2 presents an approximate cost for a mining capacity rate of 1000 tons/day inlet to flotation:

Table 4.2

Approx. quantity fed of reagents (kg/ton)	Average approx. Price USD per kg	Total cost USD/day	OPEX USD/year
50 Per overall flotation process	0.4	4000	1460k

Thus, we have a portion of OPEX around 4000 USD/day. If the recovery of overall beneficiation be considered around 50% from a grade up to 60%TREO, thus the expense on the final concentrate would be around 1.35 USD/kg of REO only for the reagents used in flotation (Mittal and Shah 2013).

Environmental problems associated with the flotation surfactants are doubled felt due to the lack of promising surfactants for a desired recovery and grade. Beside surfactants, numerous pH

tuners, either acidic or basic, should be used. This is because the surface chemistry aspects of bastnaesite and monazite are significantly related to their semi-solubility, surface behaviour and chemisorption in aqueous phase. Their conjunction gangues have also chemisorption interactions at different pH which is commonly explained with surface charge (zeta potential), point of zero charge (PZC) and isoelectric point (IEP) (Herrera-Urbina and Fuerstenau 2013, Jordens, Marion et al. 2014, Owens, Nash et al. 2018).

Furthermore, more than one flotation step, namely 3 to 5, is required followed by washing and separation steps to reach a typical 50 % recovery and a concentrated ore with a grade seldom above 60 %. Another serious drawback of the flotation process is that the water used in the process can hardly be recycled as a result of presence of numerous additives. Large tailings ponds are hence built up beside every flotation facility (Bulatovic 2007, Bulatovic 2010, Sprecher, Xiao et al. 2014).

It is also noteworthy that the gangue minerals with similar floatability usually accompany REE bearing minerals causing selection of surfactants even harder. Moreover, given the fact that selection of flotation surfactants is empirical, their response to variation of ore composition might yield in very poor separation efficiency. This is because composition of the ore differs from one place to another in the same deposit of REE.

On the other hand, the water/oil/particles based Pickering emulsions or solid stabilized emulsifications (SSE) (Ramsden 1903) with an eco-friendly oil recycling process could be an alternative or a supplementary technique in physical beneficiation of the REE bearing minerals. The solid particles play the role of the emulsifiers that can stabilize droplets of an appropriate oil in the aqueous phase (Binks 2002). Taking advantage of the natural surface properties of the solid particles, e.g. the REE ore particles in this research, this is because the SSE process does not require the surface modifying as in the flotation process, and as a consequence, the SSE process would be superior in terms of cost and environment protection (Figure 4.1).

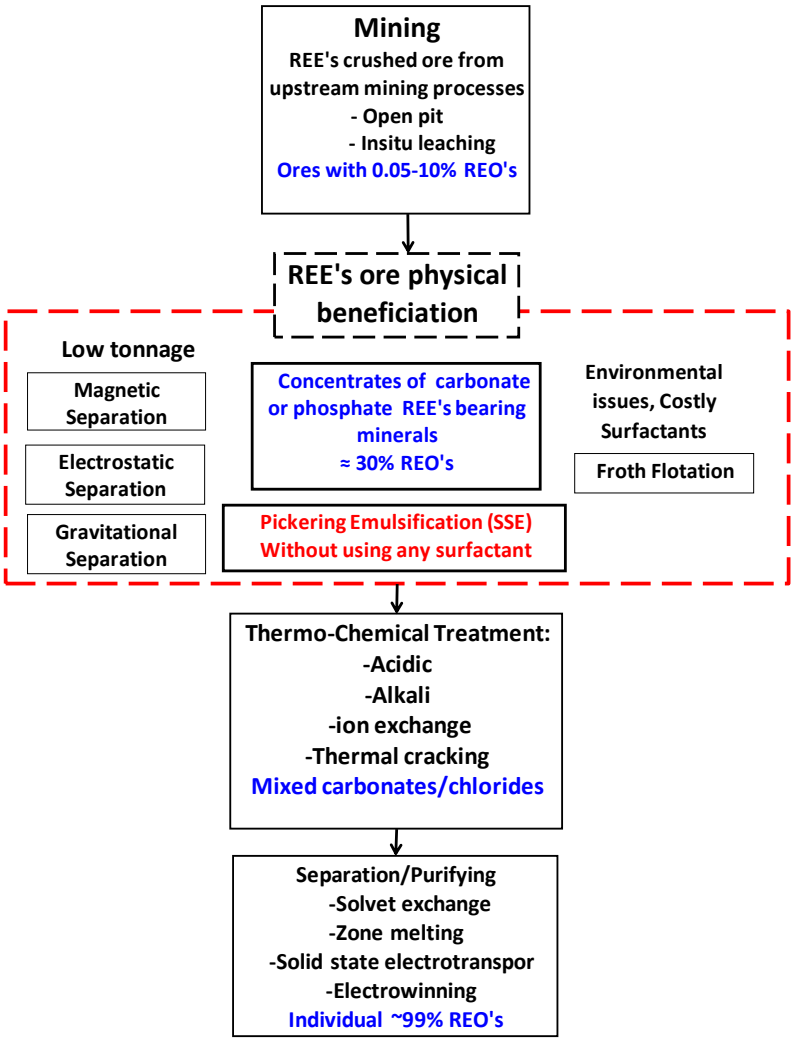

Figure 4.1 Schematic rout of REO's production from excavation to physical beneficiation including flotation, Pickering emulsification, magnetic, gravitational ad electrostatic methods and other alternatives in upstream processes.

It is expected in a SSE system that majority of the mineral particles with a relatively lower level of hydrophilicity as opposed to hydrophobicity attach into the interface of oil droplets, whereas majority of relatively hydrophilic minerals remain in the continuous water phase. Particle size distribution of particles, physical properties of the oil, oil to water (O/W) ratio and mixing condition in the tank are some influential parameters that govern the efficiency of the SSE process. Figure 4.2 presents a schematic of attachment of two spherical particles with different wettability into the interface of oil droplet in a SSE process. One is relatively more hydrophilic and the other one is relatively more hydrophobic. It is noteworthy that the mineral particles has

low sphericity and irregular shape. Also, one single particle may contain at least two minerals with different levels of hydrophilicity; this is why a relative wettability of the mineral particles is usually considered. It is very likely that a particle with one single grain mineral would exist in the system provided the particles were grinded to a size under the liberation size of the mineral (Castor and Hedrick 2006). The wettability is directly described by measuring the contact angle θ.

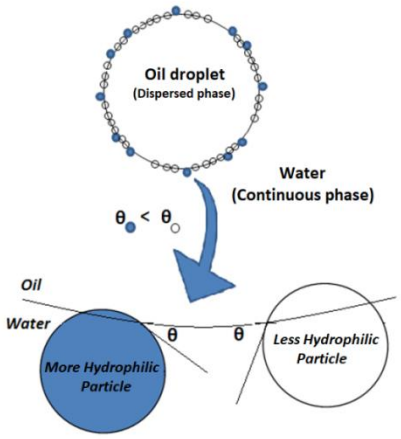

Figure 4.2 Schematic of particles attachment to the oil droplet to make the barrier around interface and to prevent coalescence of droplets, Pickering emulsification with fine particles functioning as emulsifiers, θ is solid-oil-water interface contact angle

Pickering emulsification has versatile and efficient applications in various industries such as cosmetics (Frelichowska, Bolzinger et al. 2009), food (Dickinson 2010), paint (Cauvin, Colver et al. 2005), petroleum, petrochemicals (Frelichowska, Bolzinger et al. 2009) etc. We employed the solid-stabilized emulsification technique and developed a process to separate and concentrate valuable REE bearing minerals such as bastnäsite ($REE.FCO_3$) and monazite ($REE.PO_4$) from the associated gangues of a fresh ore, i.e. a grinded ore that has not underwent any physical and chemical separation process. In this article, the feasibility of the developed process in favor of the REE bearing ore concentration is presented for some fixed operating conditions such as mixing criteria, the O/W ratio and the oil type. In addition, effect of particle size and concentration of the upstream feed on the performance of the processes is discussed in detail.

4.2.1 Pickering emulsification fundamentals

As a matter of the fact, the REE bearing minerals such as bastnäsite and monazite has higher oil-water contact angle than the gangue (Abaka-Wood, Addai-Mensah et al. , Zhang 2014), so their affinity to attach into the interface of oil droplets is higher than the gangue minerals that tend to stay in water phase. By properly selecting an oil, adjusting the W/O ratio, and providing appropriate hydrodynamic conditions, it is possible to selectively capture the ore particles of interest at the O-W interface while the undesired ore particles settle at the bottom of the processing tank.

The particles attached to the oil droplets can be collected downstream of the emulsification tank and subsequently separated from the oil droplets, for instance, by centrifugation. A single particle of the ore may contain both types of hydrophil and hydrophobe minerals, so an optimized particle size as close as possible to the liberation size of the REE bearing minerals should be selected in favour of maximum attachment of REE bearing minerals to the oil droplets.

The wettability differences of the targeted mineral particles and the gangues in their conjunction with the tailored oil and water interface govern their competitive attachment and consequently the selective separation of the REE bearing minerals.

To describe the SEE mechanism in a micro scale, M.J.Hey et al. (2006) have shown that the maximum stability of a spherical particle attached into the interface of an oil droplet is controlled by interfacial energy which is in turn affected by contact angle or influence of wettability on the capillary force (Figure 4.2). In this micro scale consideration, the maximum stability of the attached particle into the interface is dedicate to contact angle. The capillary force is the dominant force during the approach and the absorption steps of the particles with the order of magnitude of 200 times higher than the hydrostatic force, 1,000 times higher than viscous force and a 10,000 times higher than buoyancy and gravity force (Tsabet 2014).

At the equilibrium, the balance of interfacial energy preventing a particle from interface to detach and move into the water phase (Δ_1 in *4.2*) is exactly equal to the one needed in order for the particle being engulfed by the oil droplets (Δ_2 in *4.1*). This is the main rule behind the stabilization of a particle at the interface governed by contact angle or wettability. Thus, those particles with a contact angle nearby the maximum stability are better stable at the oil droplet

interface in opposite to the particles with smaller contact angle, i.e. lower hydrophobicity, during emulsification in a competitive attachment.

The parameters Δ_1 and Δ_2 are defined in equations 4.3. E_{sep} is the total interfacial free energy when the particle is totally in the water phase, E_{min} is the total interfacial free energy when the particle is attached to the droplet interface with the Young's contact angle, and E_{eng} is the total interfacial free energy when the particle is totally engulfed by the droplet (Hey and Kingston 2006).

$$\Delta_2 = \pi b^2 \gamma_{ow} (1 + COS\theta)^2 \qquad 4.1$$

$$\Delta_1 = \pi b^2 \gamma_{ow} (1 - COS\theta)^2 \qquad 4.2$$

$$\Delta_1 = E_{eng} - E_{min} \quad , \quad \Delta_2 = E_{sep} - E_{min} \qquad 4.3$$

We employed this principle to explain separation of REE bearing minerals from their associated gangues in the ore. Even though, the REE ore particles were not spherical, the equations 1 and 2 are still applicable by considering a shape factor, i.e. relative sphericity, for the particles.

The REE ore particles which have more water affinity or lower contact angle on the oil-water interface remain mainly in water (continuous phase) and sediment after emulsification. On the other hand, the particles which have superior oil affinity or higher contact angle attach to the oil droplets (dispersed phase). Therefore, the attached particles can be easily separated along with the creamed droplets. In fact, after the emulsification step, the stabilized droplets are creamed at the top of the emulsification tank following a long enough creaming time. The creaming occurs because density of the stabilized droplets is close to or lower than water density. The rest of the gangue particles which have higher density than water, sediment at the bottom of the emulsification tank (Figure 4.3).

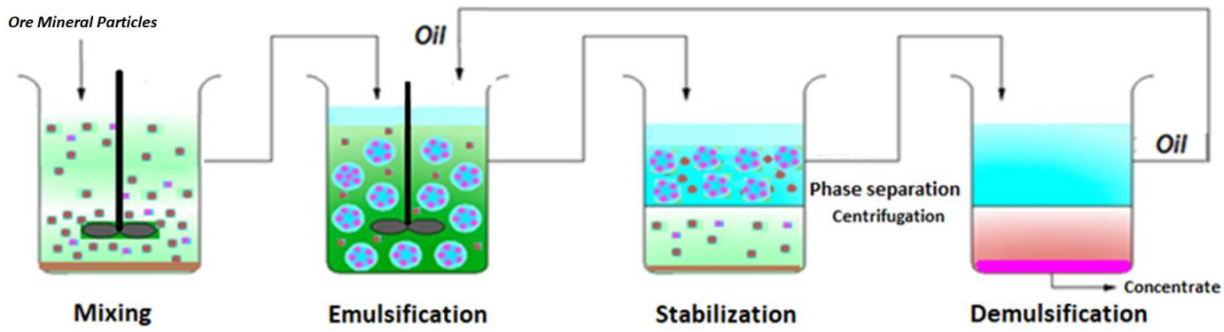

Figure 4.3 Schematic of emulsification and separation steps

4.3 Materials and methodology

4.3.1 Liquid phases

The Pickering emulsification employs essentially two immiscible liquids, normally an oil along with water, to generate a continuous phase and a dispersed phase. Herein, a typical silicone oil of poly dimethyl siloxane (PDMS) (from CLEARCO Inc.) was employed as for the dispersed phase. Some related physical properties of this oil are presented in Table 4.3. Distilled water with surface tension of 72.6 mN/m at 22 ºC was utilized as the continuous phase.

Table 4.3 Silicon oil PDMS properties

Silicone oils	Density (kg/m^3)	Dynamic viscosity (mPa.s)	Surface tension (mN/m)
S50	960	48.0	20.8

4.3.2 Niobec's ore

Minerals of Niobec's ore

The raw grinded ore was supplied from Niobec's rare earth elements deposit located in St-Honore in province of Quebec of Canada. A QEM-Scan analysis of the ore is provided in Table 4.4 including mass fraction and grain size of the associated minerals. The ore minerals can be categorized in four main groups of carbonates, silicates, oxides and phosphates. While with a very low quantity, Bastnäsite and monazite are the most abundant REE bearing minerals of this

ore. On the other hand, calcium carbonate minerals such as calcite, dolomite and ankerite constitute the main portion of the gangues.

It is noteworthy though that the abundance of minerals varies from one location of the deposit to another. However, the ingredients of the ore follow a similar pattern in the Niobec's deposit.

Table 4.4 Group of the consistent gangues in Niobec ore and weight percentage (Lafleur, Eng et al. 2012)

Name	**association (%wt)**	**Calculated grain Size (µm)**	**Category**
Pyrochlore	0.12	10.93	Oxide
Columbite	0.17	18.29	Oxide
Bastnaesite/Synchisite	1.96	14.34	Fluorocarbonate
Monazite/Th-Monazite	1.43	12.63	Phosphate
Allanite	0.13	7.02	Silicate
Other REE	0.01	6.84	Phosphate
Fe-Oxides	5.85	21.43	Oxide
Ilmenite	0.07	6.88	Oxide
Rutile	0.20	9.98	Oxide
Other Oxides	0.15	12.33	Oxide
Plagioclase	0.06	11.33	Silicate
K-Feldspar	0.15	19.70	Silicate
Quartz	0.92	14.13	Oxide
Micas/Clays	1.15	10.32	Silicate
Amphibole	0.75	8.83	Silicate
Sphene	0.00	12.84	Silicate
Chlorite	4.43	18.37	Silicate
Other Silicates	0.00	6.90	Silicate
Dolomite	50.00	27.23	Carbonate
Calcite	13.16	20.21	Carbonate
Ankerite	13.72	21.96	Carbonate
Siderite	0.21	7.09	Carbonate

Pyrite	2.86	24.76	Sulfide
Other Sulphides	0.07	14.32	Sulfide
Zircon	0.03	6.05	Silicate
Apatite	0.28	15.77	Phosphate
Barite	1.99	26.36	Sulfate
Other	0.13	7.78	-
Total	**100.00**	**-**	**-**

Grade of Niobec's ore

Table 4.5 illustrate respectively the results of NAA in the fresh ore and electron microprobe analyses (EMPA) of elemental assay for pure bastnaesite and monazite from Niobec when compared with model minerals of pure monazite and pure bastnaesite from Mountain pass USA resulted by NAA. The most abundant elements including Cerium, Lanthanum and Neodymium are presented. The model minerals will be used to characterize the wettability of REE bearing minerals. However, the crystal structure and composition have effect on the surface properties. Since the TREE in the composition is very similar for both Niobec and Mountain pass model minerals, we assume that the surface properties could be similar.

Table 4.5 La, Ce and Nd abundant in fresh ore, pure bastnaesite and pure monazite from NIOBEC resulted by NAA and EMPA comparing to the model pure monazite and pure bastnaesite from Mountain pass USA resulted by NAA (Lafleur, Eng et al. 2012).

	NAA Niobec fresh ore	**EMPA Niobec pure bastnaesite**	**EMPA Niobec pure monazite**	**EMPA Mountain Pass pure Bastnaesite**	**EMPA Mountain Pass pure monazite**
La	4412	137700	104500	131290	118270
Ce	9816	261700	269200	278970	243730
Nd	4525	89800	99500	83860	107010
TREE (ppm)±10%	18753	489200	473200	494120	469010

Minerals Contact angle

A single particle of ore could be composed of more than one mineral. Whereas, the wettability is the most important parameter to control selectivity of Pickering emulsion during particle attachment into the interface of oil droplets (Hey and Kingston 2006). Thus, small enough particles in favour of liberation of the target monazite and bastnäsite minerals should be selected; otherwise, contact angle of the complex minerals on the surface of a particle governs its affinity to either oil or water phase.

Therefore, a true understanding of contact angle of the REE bearing minerals as well as the gangue minerals help gain an insight into the separation mechanism. To do so, constituting minerals of the Niobec's ore were purchased in almost pure form: calcite from Morocco, dolomite from Teruel Spain, bastnäsite and monazite from Mountain Pass USA and pyrite from La Rioja Spain and others from Vizcaya Spain.

The average water-solid contact angle of the minerals was measured directly on their clean and polished flat surface with a goniometer (Data Physic OCA, SCA20 software) that employed the sessile drop technique. An intermediate equilibrium contact angle was obtained by the release of a water droplet from the syringe-needle tip after falling on the surface.

The water-air-solid contact angle could be simply linked to the oil-water-solid contact angle in Young equation (4.4 and 4.5) which is briefly called contact angle. In other words, we assumed that the oil-air-minerals contact angle tend to near zero which is almost valid for all minerals.

$$Cos\theta_{o/w} = \frac{\gamma_{wa}Cos\theta_{sw} - \gamma_{oa}Cos\theta_{so}}{\gamma_{wo}} \quad 4.4$$

$$\theta_{so} \to 0 \Rightarrow Cos\theta_{so} \approx 1 \Rightarrow Cos\theta_{o/w} = \frac{\gamma_{wa}Cos\theta_{sw} - \gamma_{oa}}{\gamma_{wo}} \quad 4.5$$

Contact angle measurement was repeated three times for each individual mineral. The average values are presented in Figure 4.4. The uncertainty of measurements was ±5°. Since pure samples of monazite and bastenaesite were obtained in powder form each with D32 of about 20µm, the oil-water-solid contact angle of these minerals was estimated from the Blake–Kozeny

equation, and based on a capillary rise in a capillary tube that was filled with the powder (Fournier, Fradette et al. 2009). Our estimation resulted in the contact angles of 54±5º and 60±5º, respectively, for bastnäsite and monazite; this is consistent with literature that reported contact angle between water and pure monazite was above 49°(Abaka-Wood, Addai-Mensah et al.). However, they reports higher value of air-water contact angle for hematite which may had a different crystalline surface property than our sample. It should be noted that the contact angle values will change in different system conditions and more specifically at different aqueous phase conditions such as pH, presence of different ions, crystal structure, surface roughness, oil molecular interaction, chemisorption of the free ions and double layer formation of polar species (Zhang 2014). It is advantageous that the values of contact angle indicate wettability difference between the REE bearing minerals and their associate gangues.

The results indicate that REE bearing minerals were relatively more hydrophobic when compared to their associated gangues (Figure 4.4). It should be mentioned that the natural pH of slurry of Niobec's ore in water is around 9 where there are many alkali ions e.g. Ca++, Mg++…after partially dissolution of minerals even with very low solubility such as calcite, dolomite, silicate, and etc. Contact angle of calcite and dolomite that exist significantly in Niobec's ore are less than 50°. Such contact angle differences imply that the REE bearing minerals could be selectively captured through the oil droplets of the emulsion. According to the fundamental studies in literature, bastnäsite and monazite tend to either attach into the interface or immersed into the oil droplets of the Pickering emulsion and conversely the more hydrophilic particles such as dolomite and calcite tend to remain in water phase (Simon, Theiler et al. 2010) (Hey and Kingston 2006, Tadros 2009).

Since the contact angles are not absolute values, we could assign a mineral surface if it is more hydrophilic or less hydrophobic when compared with other minerals. The contact angle of minerals is affected by the wetting characteristics, electrokinetic features and surface charge in conjunction with the oil and it is significantly related to their semi-solubility and chemisorption behaviour in aqueous phase. (Li and Fuerstenau 2013) (Castor and Hedrick 2006)

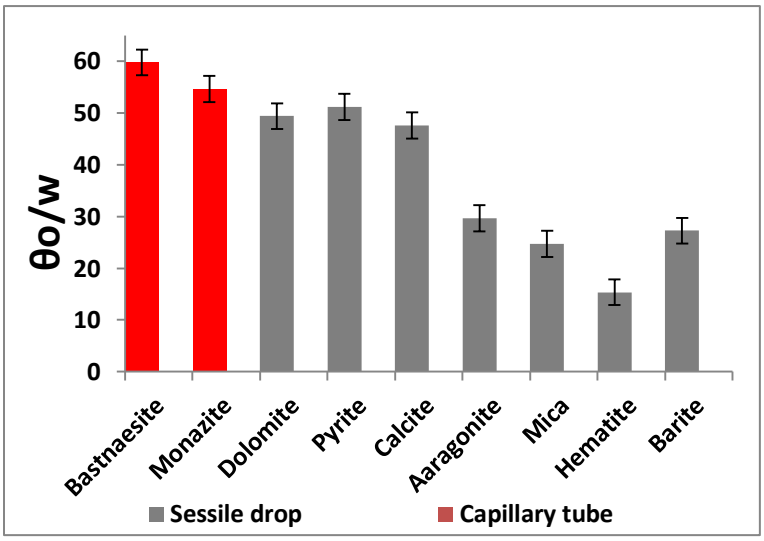

Figure 4.4 Average contact angle of pure minerals were measured directly on Crystalline pure minerals by sessile drop technique and capillary tube filled with powder

4.3.3 Dry and Wet Sieving for feeds preparation

A QEMScan analysis helped identify grain size of the minerals associated with the Niobec's ore. According to Figure 4.5, the grain sizes of more than 94% of monazite and of 86% of bastnaesite were under 63 µm. Therefore, we targeted to maximize recovery of REE bearing minerals by preparing the feeds of less than 63 µm size; this was to achieve maximum available surface of the monazite and bastnaesite.

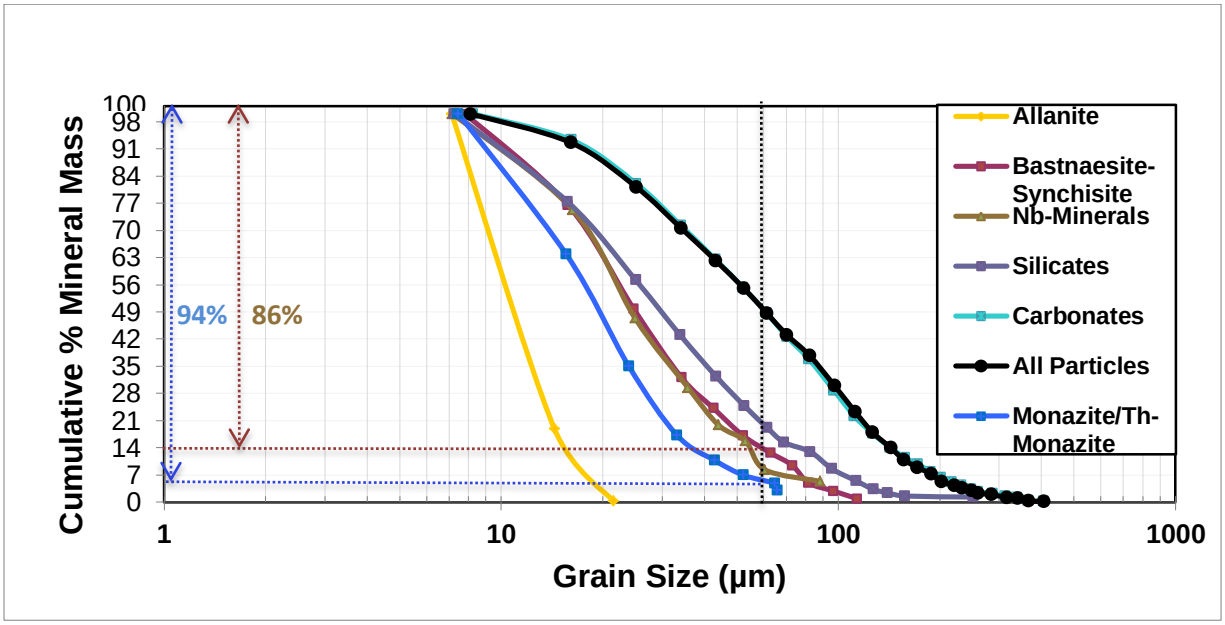

Figure 4.5 Cumulative grain size distribution of Niobec ore REE minerals from QEMSCAN analysis

Size distribution of some samples from the bags of the received ore is depicted in Figure 4.6. Even though there are some minor shifts between the size distributions, it seems reasonable to say that they follow a similar trend within the shown range of the sizes . Having said that, contents of the bags were compiled and mixed to obtain an inventory for the rest of the research.

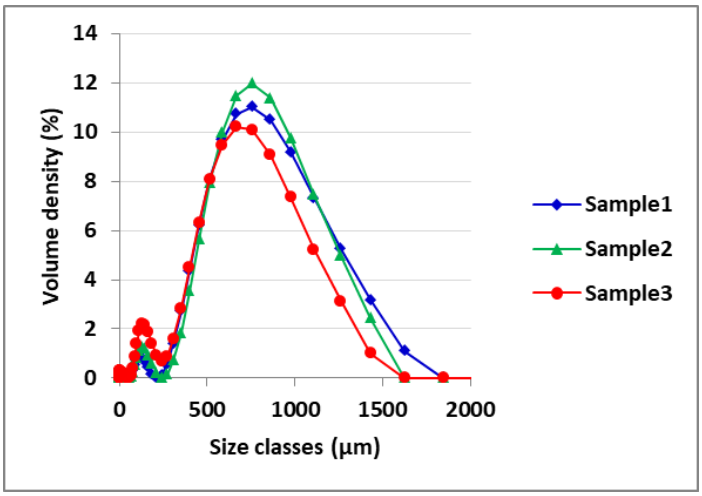

Figure 4.6 Particle size distribution of the received ore

Dry sieving and wet sieving methods were applied to the inventory of the ore to select the required feeds (Lafleur, Eng et al. 2012). The dry sieved feed (DSF) is the collected particles of -63 µm size following a dry sieving. Further grinding was applied to the particles of +63 µm size from the remainder of the preceding dry sieving, and then another dry sieving was applied; the collected -63 µm particles were assigned as the crushed sieved feed (CSF) feed.

The wet sieved feed (WSF) corresponds to the -63 µm particles collected after a wet sieving was applied to a new sample of the ore inventory. To execute the wet sieving, a flow of distilled water flew from the top of the piled sieves down to the lowest one on a shaking machine.

Despite the need for water, and consequently, the higher OPEX and CAPEX attributed to the sieving process, there are some important advantages associated with wet sieving (Wills and Finch 2015). As a matter of the fact, it is expected that a considerable amount of the very fine particles, generated during grinding process, stick onto the surface of the larger particles due to the inter particle forces such as electrostatic and Van der Waals forces. Such fine particle most

likely include liberated REE bearing minerals whereas undesired minerals, for instance calcite, ankerite and dolomite, exist in the larger particle. Thus, a concentrate of REE bearing minerals might be attainable inside the tray below the lowest sieve. Having said so, we will show that both recovery and grade of REE bearing minerals would rise in the overall Pickering emulsification process over DSF, CSF and WSF feed.

The Figure 4.7 illustrates the PSD of the feeds indicating that the fine particle sticking to the larger particles were washed away by applying the wet sieving.

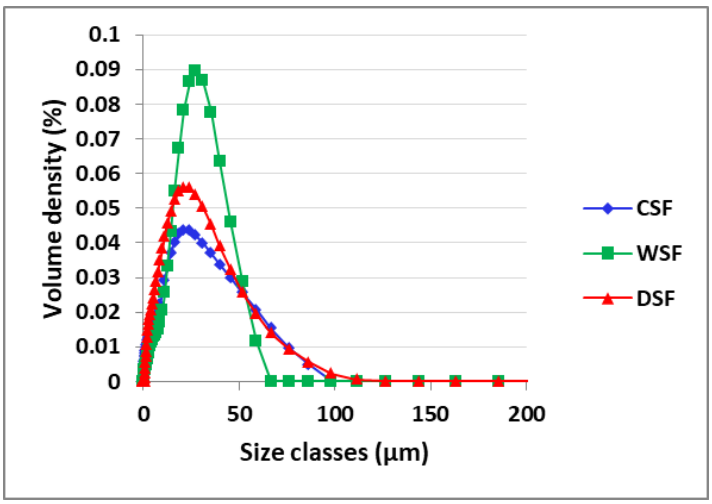

Figure 4.7 Particle size distribution of three prepared feeds DSF,CSF and WSF

Scanning Electron Microscopy (SEM EDS TM3030 Plus Hitachi) was applied to the 45 to 63 µm size cut of dry and wet sieving processes at two zooms of X500 and X1500 (Figure 4.8). Particles smaller than 45 µm down to 1 µm were present around larger particles according to the scales of SEM images concerning the dry sieving sample. On the other hand, particles of less than 45 µm size were not identified on the wet sieving sample confirming superior efficiency of wet sieving when compared with dry sieving in term of separation of fine particles.

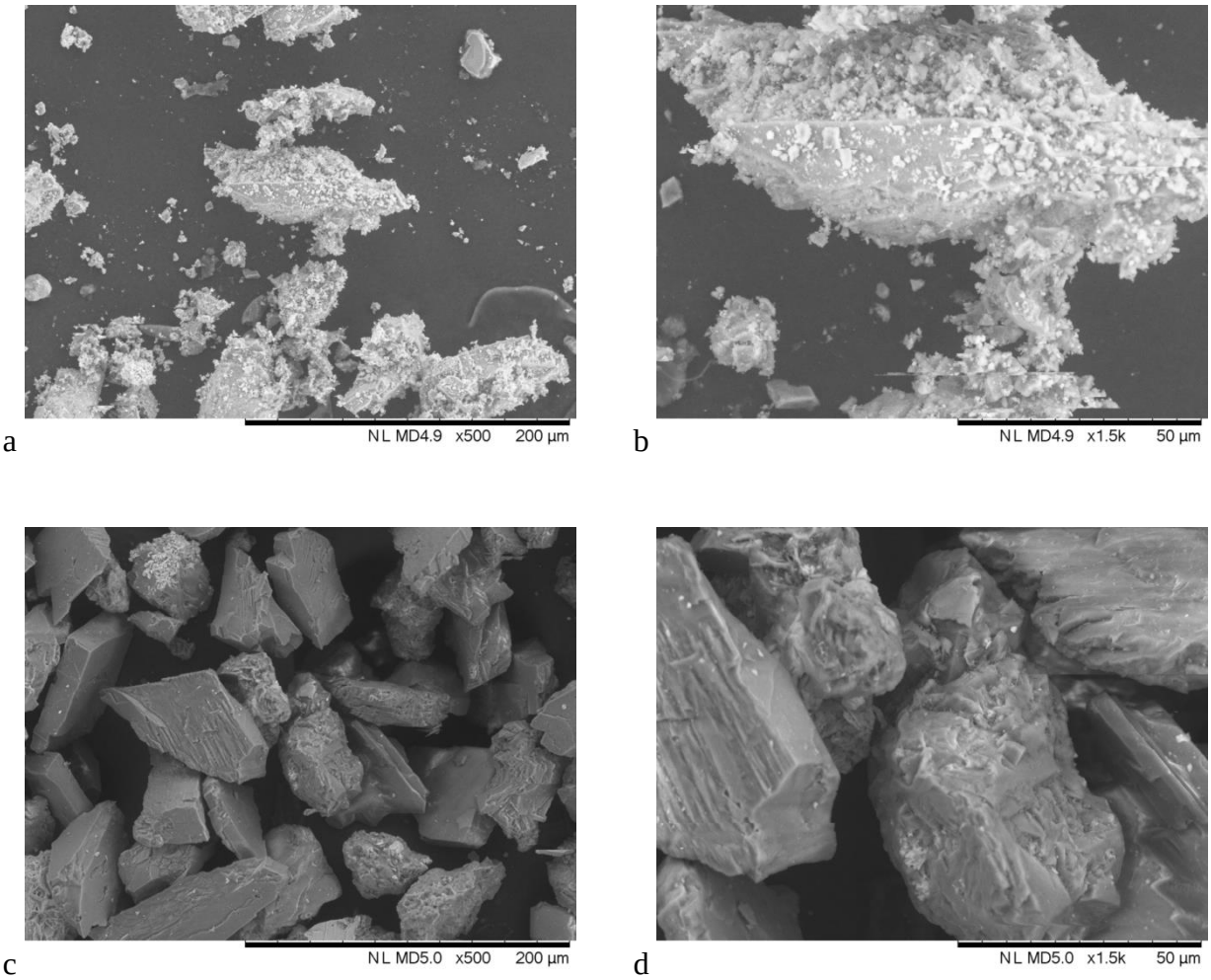

a b c d

Figure 4.8 SEM image of dry (a and b) and wet (c and d) sieved fresh ore; cut size: 45-63µm

Comparison of the mass fractions of each size cut of the dry and wet sieving processes also certifies the applied wet sieving process washed away the very fine particles and accumulated in the lower size cuts (Figure 4.9). On the other hand, the dry sieving resulted in a heavier mass in upper sieve cuts, larger than 125 µm. It was necessary for this solid emulsification research to ensure the fine particle were well separated from the larger particles to illustrate the performance of this novel physical beneficiation is based on wettability of the solids rather than on their size.

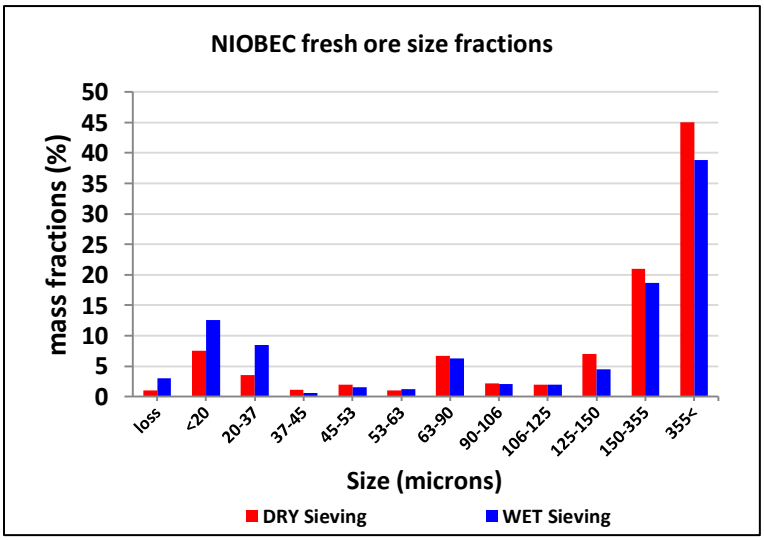

Figure 4.9 Mass fractions of size cuts following dry and wet sieving processes

Figure 4.10 and Figure 4.11 confirm that higher grade and recovery of total rare earth oxides were obtained in the size cut of less than 37 µm. Comparison of TREO grade of the feeds DSF and WSF reveals that majority of the fine particles collected in the lowest size cut upon applying the wet sieving belonged to REE bearing minerals. Consequently, as Figure 4.11 displays, the wet sieving process enriched the Niobec's ore up to 190% (Figure 4.10) by a mass recovery of 21% in sieving size cut under -37 µm. Taking TREO grade of the feeds CSF in addition to DSF and WSF into consideration, it is concluded that REE bearing minerals break relatively faster than the gangue minerals during the grinding process; hence, a well-controlled grinding process followed by a wet sieving process would produce a valuable concentrate of the rare earth elements upstream of any other physical beneficiation.

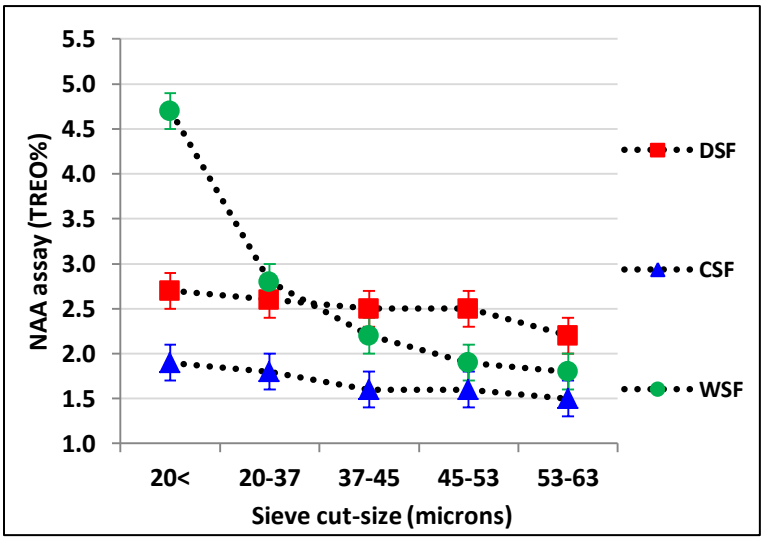

Figure 4.10 TREO grade versus sieving size cuts, Head grade of different feed sizes

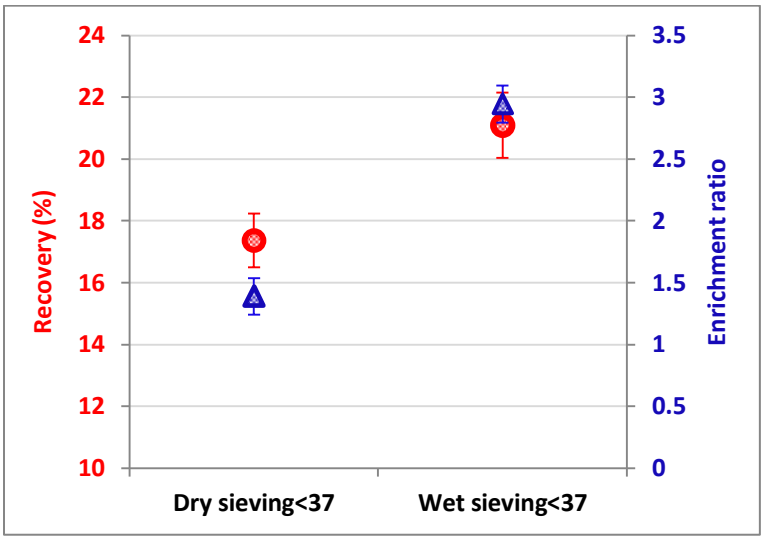

Figure 4.11 Recovery and the enrichment ratio of dry and wet sieving -37µm cut size

4.3.4 Experimental setup

The experimental setup included an agitation tank (H=T, C=0.5 cm) of 0.5 L volume equipped with a controllable pitched blade turbine (PBT) impeller (D=3cm) that was installed off-centre to avoid vortex formation and to generate turbulence in the flow field (Figure 4.12). This setup is equivalent to a centered impeller with baffles in term of mixing performance (Gingras, Tanguy et al. 2012) (Karcz, Cudak et al. 2005).

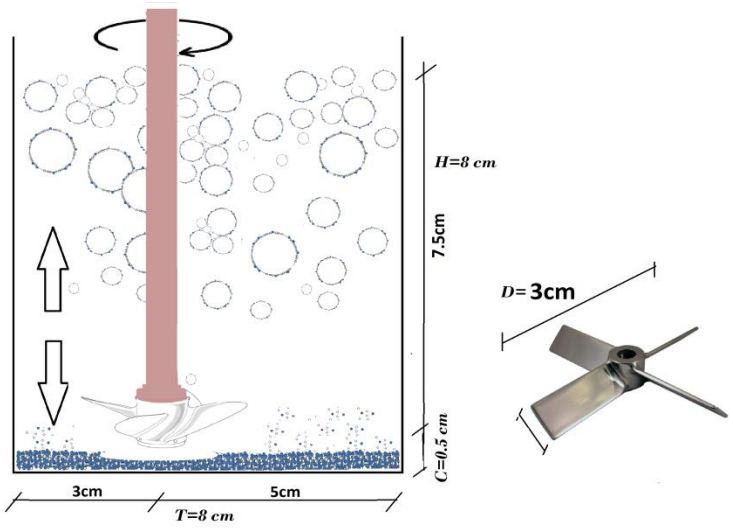

Figure 4.12 Stirrer tank installation configuration

Volume fraction of PDMS oil in the oil-water formulation was adjusted at Φ= 9 wt% to make a dilute emulsion with an appropriate interface generation. In addition, mass fraction of the feed, i.e. ore particles, in the solid-oil-liquid formulation was set at 5 wt%. Stirring speed of the PBT impeller was 1000 rpm in all experiments (Tsabet 2014). To consider the impact of stirring on the particles breakage, we tried stirring the ore in water and compared PSD of particle before and after stirring and did not observe big change in PSD even in higher rpm up to 1600.

4.3.5 Experimental procedure

A typical experiment started with adding 300 g mass of water to 16 g mass of feed followed by mixing at 1000 rpm for 3 minutes to homogenize particles dispersion, and to break down the possible aggregates of the particles. Once reasonable dispersion of the solids was reached, mixing was stopped, and then a 30 g mass of PDMS oil was added. Subsequently, the mixing continued for another 15 minutes at 1000 rpm to reach a state of emulsion homogeneity and stabilized equilibrium. The mixing time should be long enough to allow the selective attachment of the desired particles to the oil-water interface formed by the impeller. As discussed in preceding sections, ore particles must have a certain size allowing for the liberation of the desired mineral(s) in favour of recovery and selectivity.

Once agitation is stopped, creamed droplets (at the top) typically contain higher concentration of REE bearing minerals. The remaining mineral particles settled in the bottom contain lower

concentration of REE bearing minerals. The mixture is left for 15 minutes to stabilize resulting in two distinguishable overflow (cream droplets) and underflow (sediment) phases. In fact, the overflow contains particles attached into the interface and extracted with oil droplets, and the underflow consists of the rest of the particles remained as non-emulsified sediments (Figure 4.13).

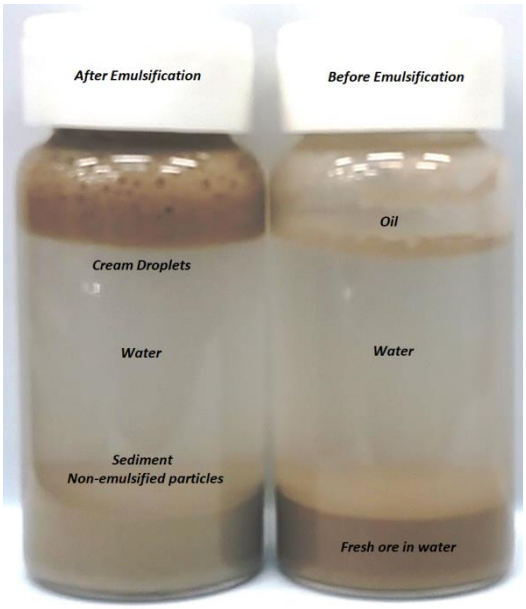

Figure 4.13 Ore particles in the experimental vial before and after emulsification

A separation funnel or decanter was employed to trap the creamed droplets from the top of the emulsion. Subsequently, centrifuge was applied on the collected creamy phase to separate the solid particles from the oil. Particles of the sediment phase that mainly contained water were also dried. A schematic of the overall experimental procedure, i.e. from emulsification step through to phase separation and products analysis is depicted in Figure 4.14.

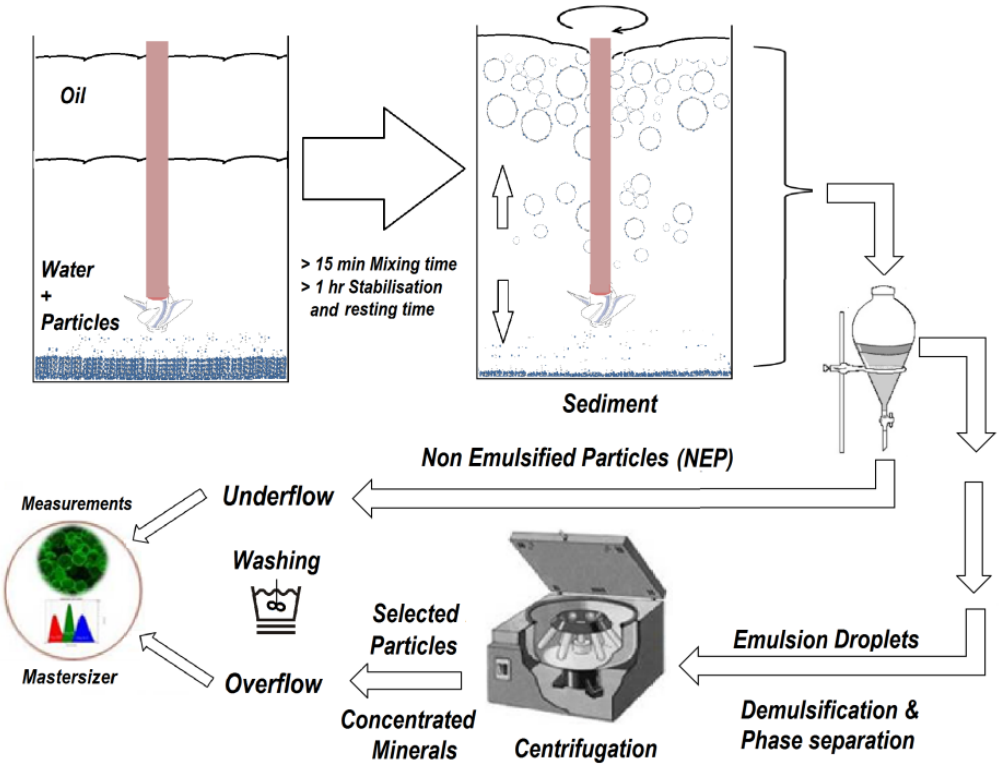

Figure 4.14 Schematic of the Pickering emulsification procedure

4.3.6 Analysis of overflow and underflow

Ideally, there are three streams of particles in a SSE system, as shown in Figure 4.14, such as the feed of raw ore, the emulsified minerals which are attached to droplets (overflow) and the non-emulsified sediment minerals (underflow). It is noteworthy that the emulsion had to be washed carefully to prevent non-emulsified particles get trapped between droplets, and consequently, come into the overflow. To do so, water was injected on top of the creaming droplets while agitating the emulsion with a very moderate stir speed.

A Mastersizer 3000 (Malvern Inc.) instrument was employed to obtain the size distribution of the particles and the droplets. Where applicable, the mean diameters such as D_{10}, D_{90}, and D_{32} (Sauter mean diameter) of either particles or droplets were analyzed.

4.3.6.1 Mass balance calculations

The nuclear Slowpoke reactor of the Ecole Polytechnique de Montreal was employed for detecting the elemental composition of the collected solid samples associated with the overflow

and the underflow of each test by the Neutron Activation Analysis (NAA) (M. Abdollahi Neisiania 2017).

Since lanthanum (La), cerium (Ce) and neodymium (Nd) constitute more than 95 wt% of the REE bearing carriers in Niobec's fresh ore, the mass of the total rare earth oxide (TREO) in a sample, either a feed or a product sample, was assumed to be the total mass of these three elements.

As discussed later, we have observed that the rare earth bearing minerals tend to attach to the oil droplets; thus, recovery, grade and enrichment ratio of the total La, Ce and Nd were evaluated based on their abundance in the overflow by equations 4.6 to 4.8. The enrichment ratio can also be calculated based on TREE% or TREO% as the same.

$$\%Recovery = \frac{Grade\ in\ product\ (Overflow) \times mass\ flow\ of\ product\ stream}{Grade\ in\ feed \times mass\ flow\ of\ feed\ stream} = \frac{G_O \times M_O}{G_F \times M_F} \quad (4.6)$$

$$\text{Grade TREO\%(wt)} = \sum \frac{\%Elemental\ assay}{2 \times REE's\ Atomic\ weight} \times (\ Molar\ mass\ of\ ((REE)_2O_3) \quad (4.7)$$

$$\text{ER\%(enrichment ratio)} = \frac{\text{Overflow or products (TREO\% or TREE\%)}}{\text{Feed garde or head grade (TREO\% or TREE\%)}} \quad (4.8)$$

4.3.6.2 Grade estimation by image analysis

As a matter of the fact, several samples of SSE were generated during this research. However, elemental analysis by NAA not only takes at least ten days, but also it is a costly analysis. Therefore, it was mandatory to develop a quick screening technique to select the most suitable samples for elemental analysis. Having said that, we developed an image analysis (IMGA)

method experimentally to obtain a preliminary and quick estimation of the grade of rare earth elements on either overflow or underflow stream.

Details of the IMGA method and the calibration curve is provided in the appendix A. Based on this method, the equations 4.9 and 4.10 were developed that estimate the TREO of an unknown sample by a parameter called BLR, brightness level ratio. The overall validation results are presented in Figure 4.16.

$$\frac{(\mathrm{B.F.O.}-\mathrm{B.S.}) \times (\mathrm{E.C.O.}-\mathrm{E.F.O.})}{\mathrm{B.F.O.}-\mathrm{B.C.O.}} + \mathrm{E.F.O.} = \mathrm{E.S.} \qquad 4.9$$

$$\frac{\mathrm{B.F.O.}-\mathrm{B.S.}}{\mathrm{B.F.O.}-\mathrm{B.C.O.}} = \text{Brightness level ratio "BLR"} \qquad 4.10$$

Where B.F.O. is level of brightness emitted from fresh ore, B.S. is level of brightness emitted from the sample, B.C.O. is level of brightness emitted from calibrated sample ore, E.C.O. is elemental assay of calibrated sample ore, E.F.O. is elemental assay of fresh ore and E.S. is elemental assay of the sample.

4.4 Results and discussion

4.4.1 PSD of overflow vs. underflow

Figure 4.15 displays a typical unimodal volumetric PSD of a WSF with particles of -20 μm size as well as the PSD of the associated overflow and underflow after an emulsification was applied. As expected, the PSD of the overflow had a trend toward smaller particles in opposite to the PSD of the underflow. There are two reasons to explain this observation. First, the oil droplets in a Pickering emulsion have tendency to get stabilized with smaller particles due to the larger coverage potential (Tsabet and Fradette 2015). Second, given the fact that the WSF was prepared under a wet sieving, the abundance of the relatively liberated hydrophobic REE bearing minerals in the size cut of -20 μm was more than in bigger size cuts. In other words, the wettability difference between the REE bearing minerals and the associated gangues governed the selectivity of Pickering emulsification.

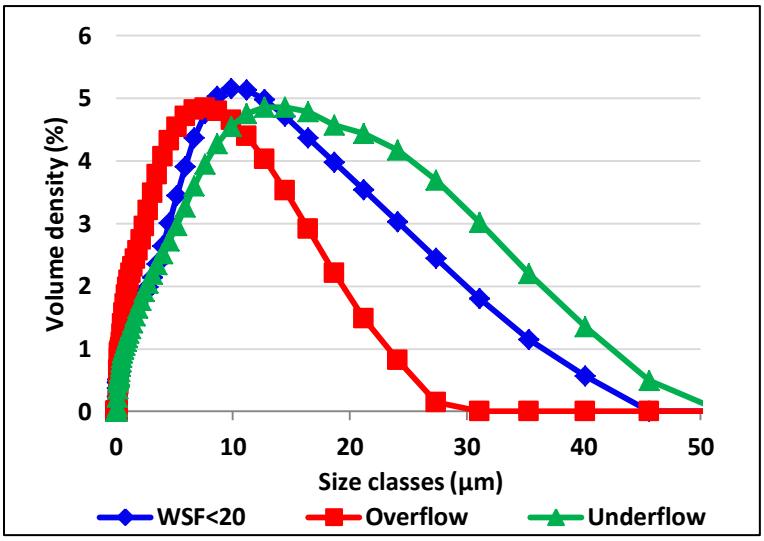

Figure 4.15 Particle size distribution of WSF <20 µm and its associated product streams, (Φ_d=9%, PDMS oil 50 cSt, Ms=5%, 15minPBT@1000 rpm)

The Pickering emulsification was also applied on a DSF and a CSF with particles of -20 µm size to investigate whether separation efficiency follows a similar behavior as observed for the WSF. Accordingly, the D_{10}, D_{50}, D_{90} and D_{32} mean diameters were measured. As illustrated in Table 4.6, regardless of the feed, smaller particles were collected in the overflow whereas the courser ones remained in the underflow. Taking the Sauter mean diameter, $\frac{D_{32,overflow}}{D_{32,underflow}}$ ratio of the CSF, DSF and WSF were, respectively, 0.62, 0.67 and 0.82. This confirms that the abundance of the relatively liberated REE bearing minerals versus the feed followed the order of WSF > DSF > CSF for the selected -20 µm size cut.

Table 4.6 Particle mean sizes of three streams: feed, overflow and underflow, Feed <*20 μm* ,PDMS 50 cSt, PBT@1000rpm , Φ_d=9%, Ms= 5%

Stream	D10	D50	D90	D32	Span
DSF<*20 μm*	4	22	40	13	1.64
Overflow	3	14	23	10	1.43
Underflow	5	29	51	15	1.59
CSF<*20 μm*	3	21	38	11	1.67
Overflow	2	13	21	8	1.46
Underflow	4	27	48	13	1.63
WSF<-*20 μm*	3	18	32	10	1.61
Overflow	1	12	18	9	1.42
Underflow	4	23	44	11	1.74

Uncertainty ±15%

4.4.2 Effect of feed PSD on SSE separation performance

The three feeds, i.e. DSF, CSF and WSF, each with five particle size distributions of -20 µm, 20 to 37 µm, 37 to 45 µm, 45 to 53 µm and 53 to 63 µm underwent the Pickering emulsification to investigate an optimum particle size required for the best separation performance in terms of recovery and enrichment ratio. Figure 4.16 a and b display recovery and enrichment ratio of the rare earth elements in the overflow of each experiment. Enrichment ratio of a size cut was calculated based on TREO grades of the feed within that size cut and its associated overflow.

Recovery and enrichment ratio of the REE bearing minerals were between 25 to 50 % and 140 % to 295 %, respectively. It is noteworthy, regardless of the upstream sieving method, the maximum recovery and enrichment ratio were found at the smallest size cuts so that they decreased versus larger size cuts. For instance, the highest selectivity, i.e. enrichment ratio, of 295 % associated with WSF was achieved with the size cut of -20 µm. This was expected

because of the size uniformity and higher grade of liberated REE bearing minerals in smaller feed cuts where the maximum liberated surface of targeted minerals were available towards the selective interface. Also, as discussed in the preceding section, the smaller particle size leads to a better stabilization. In other word, a smaller PSD increases the probability of emulsion stabilization by maximizing the stabilized interface in the system which can in turn lead to smaller droplet size, and consequently higher achievable recovery (Binks and Lumsdon 2001, Tarimala and Dai 2004).

The experimental data concerning the particles size classes obviously demonstrated that a larger size would lead to a lower selectivity due to the need for a higher energy for the attachment, and consequently, to low attachment efficiencies. In fact, the particle stabilization at the droplets interface includes successive steps such as collision, attachment, three phase contact line (TPCL) development and network formation. Each one of these steps has a specific efficiency regarding an effective coverage during stabilization of the droplets. According to the literature and fundamentals behind the stabilization phenomena, these efficiencies can be assessed by free energy or force analyses (Table 5.5 chapter 5) (Tsabet 2014).

Among these efficiencies, the efficiency of collision, attachment and TPCL are always low for relatively large particles, and thus the overall efficiency to cover the interface would decline by increasing the particle size (Tsabet and Fradette 2015).

The energy in the SSE system comes from mixing, and thus a higher dissipation energy can enhance particle attachment to the oil droplets, i.e. selectivity enhancement. The selective attachment efficiency, which is linked to the overall probability of the particles attachment, is higher for smaller particles than for larger particles; this is because, at similar conditions, the smaller particles need less energy to be dispersed and less force for attachment, i.e. much higher attractive capillary force versus repulsive forces (Tsabet and Fradette 2016).

4.4.3 Effect of upstream sieving process on SSE separation performance

Following the discussion in the previous section, comparison of recovery/enrichment ratio versus particles size cut of the DSF and the WSF reveals that the WSF resulted in higher REE recovery and enrichment ratio than the DSF as long as particles were less than 37 µm; this trend was reciprocal for larger particles sizes. This is due to the presence of very fine liberated REE

bearing minerals sticking to surface of coarse particles in the DSF. Regardless of this observed behavior, it is concluded that wet sieving may not be required upstream of the SSE process provided there is no need to a preliminary concentrate production before emulsification.

From another point of view, it is understood from the CSF data in comparison with the DSF and the WSF data that excess grinding of larger particle, i.e. > 63 µm, resulted in an undesired situation. That is, the liberated gangue minerals those with a contact angle close to of bastnäsite and monazite competed with the REE bearing minerals and eventually attached to the oil droplets. Thus, recovery and enrichment ratio of REE declined from 47 % to 35 % and from 280 % to 190 %, respectively, when particles of feed were smaller than 37 µm. Such performance of separation are still considerably high; however, a secondary SSE process with optimized operating conditions would help remove the gangues from the REE bearing minerals in the overflow of the primary SSE process.

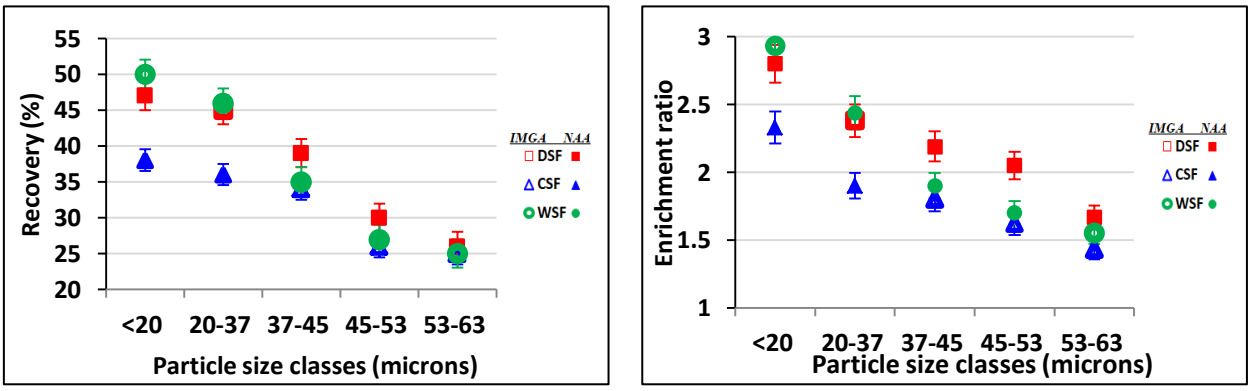

a b

Figure 4.16 a) TREO recovery from different feeds b) TREO enrichment ratio from different feeds (Φ_d=9%, PDMS oil 50 cSt, Ms=5%, 15 min PBT at 1000 rpm)

4.4.4 Emulsion (droplet) size

The mean sizes of the droplets corresponding to emulsification of five size cuts of the DSF are presented in Figure 4.17. Size of the droplets was almost 12 times larger than the average size of the associated particles of -20 µm cut; this ratio was smaller concerning the larger size cuts; for instance, it was almost 5 for the size cut of 53 to 63 µm. However, it is evident that the emulsion size, i.e. droplet size, grew slowly by increasing the size of the feed particles. A

similar behavior but to do with different type of particles is reported in the fundamental literature (Tambe and Sharma 1994) (Tsabet and Fradette 2015).

This trend provides another insight to explain why selectivity of emulsification declines for larger particles. In other words, larger particles generate larger droplets that provide smaller interface for attachment of the particle, and therefore, lower recovery of the REE bearing minerals is achieved (Binks and Lumsdon 2001).

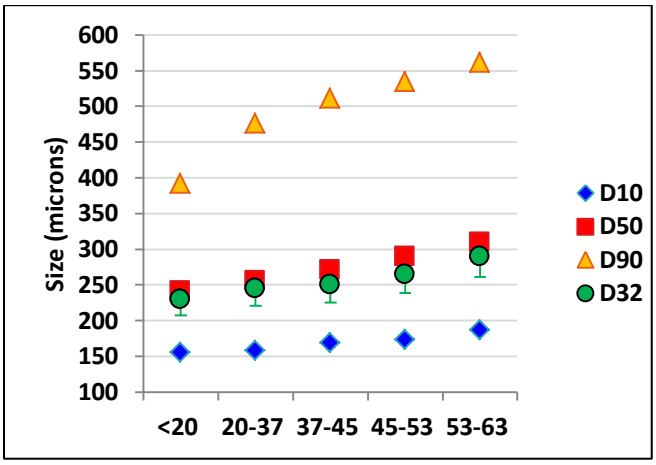

Figure 4.17 Droplet mean sizes from emulsification of DSF, (Φ_d=9%, PDMS oil 50 cSt, Ms=5%, 15 min PBT at 1000 rpm)

Figure 4.18 illustrates D32 of the generated droplets for the DSF, the CSF and the WSF. A similar trend to the ones in Figure 4.16 a and b is deduced. It is because WSF for those size classes lower than -37 µm included a larger mass of the relatively more hydrophobic REE bearing minerals and also correspondent PSD was sharper toward smaller particles. Therefore, the associated oil droplets were smaller than of DSF and CSF. With a similar explanation to do with the size cuts of +37 µm, the WSF generated larger bubbles than DSF and CSF because there was no presence of the very fine particles sticking onto the surface of the larger particles.

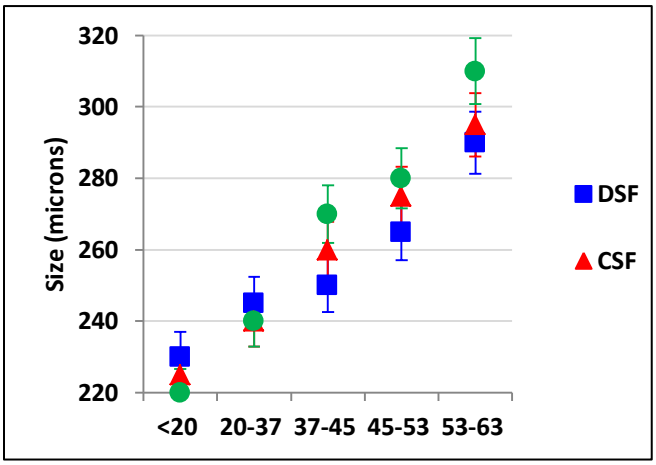

Figure 4.18 Sauter mean diameter of emulsion droplets (Emulsion size) from DSF,CSF and WSF, (Φ_d=9%, PDMS oil 50 cSt, Ms=5%, 15 min PBT at 1000 rpm)

4.4.5 REE's mineral attachment efficiency index

We defined an attachment efficiency index to make a link between the REE recovery and the emulsion properties. This index is related to multiplication of the efficiencies related to particle stabilization at the oil droplet interface: collision, attachment, TPCL development and effective interface coverage (Tsabet 2014), i.e. a total efficiency according to 4.11. By defining a total efficiency for attachment of the REE bearing minerals $(E_{Tot})_{REE}$ as well as for the attachment of the gangue minerals $(E_{Tot})_{Gangue}$, the index is estimated from 4.12.

We assumed that the fundamental correlations behind the efficiencies could be valid for the non-sphere ore particles. However, a shape factor could be applied to correct the deviation from sphericity. The average contact angle for gangues is around 45º and for REE bearing minerals is around 60º. By this assumption, we are able to use the index as a qualitative indicator to compare the effect of different parameters such as particle size and grade of the feed on the separation performance, i.e. recovery and grade.

$$E_{Tot} = E_{col} \times E_{TPCL} \times E_{Att} \times E_{cov} \quad 4.11$$

$$I_{Att} = \frac{(E_{Tot})_{REE}}{(E_{Tot})_{Gangue}} \quad 4.12$$

Figure 4.19 illustrates that the attachment efficiency index had a maximum at -37μm particle sizes. The index thus indicates that lower in size will lead to higher beneficiation of REE bearing minerals through Pickering emulsification. The index shows a substantial reduction at larger particle sizes that corresponds to a lower performance of separation or selectivity. This is consistent with the experimental results discussed in the preceding sections.

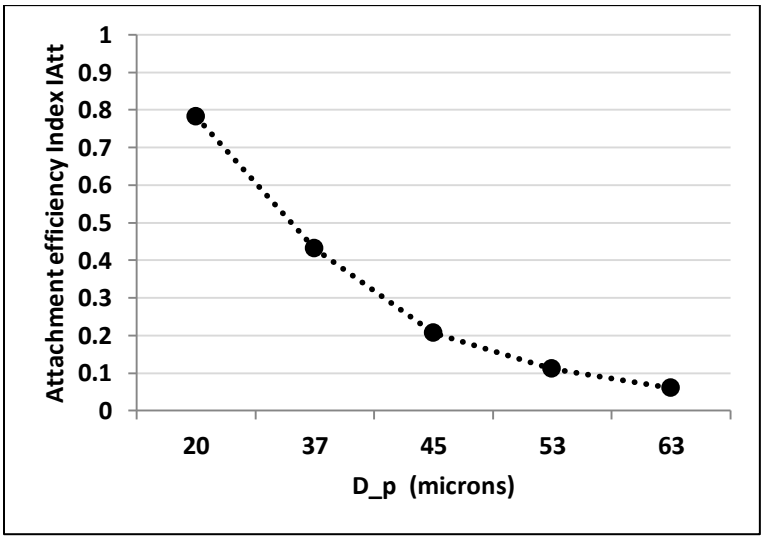

Figure 4.19 Selective attachment index for REE bearing minerals versus particle sizes

4.4.6 Pickering emulsification vs Froth flotation

There is limited technological information concerning froth flotation of the REE bearing minerals. Two known flotation processes are from Bayan Obo China and Nechalacho located at Thor Lake in Canada processing carbonatite and phosphate REE bearing minerals. However, there are differences and similarities in their associated gangues and composition when compared with Niobec's ore. The REE recovery from a multi stage micro-flotation applying Hydroxamate as collector is around 15% and the enrichment ratio is around 8 (Xia, Hart et al. 2014, Xia, Hart et al. 2015). Our work reports a feasibility of REE bearing minerals recovery through Pickering

emulsification at their natural condition without using any pH or surface modification. The enrichment ratio and recovery of one stage Pickering emulsification process were, respectively, 2.9 and 50%. Regarding the current environmental standards and economic viability, the SSE approach provides new prospects but like many others, must be optimized in favor of the highest feasibility and performance. So, two approaches should be considered. The first is aimed at improving emulsification, demulsification and phase separation steps by improvement of devices, e.g. mixing and centrifugation, and process configuration, e.g. continuous or batch processes. The second approach is to optimize formulations, improvement of feed preparation in the upstream processes and modifying the surface properties of minerals by using appropriate surfactants. A static mixer might be used for an industrial scale up to process a huge amount of ore; however, it has to be investigated further due to its influences on selectivity. The phase separation process should be also subject to further investigation including demulsification by centrifugation as well as oil separation and recycling which are important parts of the process to overcome the environmental constrains.

4.5 Conclusion

REE's mineral beneficiation through SSE was feasible at laboratory scale without using any kind of surfactants. SSE is able to selectively capture REE bearing minerals based on their wettability differences. The feed of Niobec ore were used in the process at their natural surface without applying any pH and surface modifications. The results for one stage emulsification and not under optimal conditions illustrate that the separation performance is acceptable around 50% recovery and 2.9 enrichment ratio. This application of SSE proposes a novel alternative or supplement prior to conventional froth flotation in a physical beneficiation process of the REE bearing minerals. The grade and size distribution (i.e. liberation size) of the feed has a significant effect on selectivity or the grade of the products. The performance of separation or selectivity can be enhanced by grinding the feed to a size class lower than -20μm followed by a wet sieving prior to emulsification.

4.6 Acknowledgment

The authors gratefully acknowledge financial support from the Natural Sciences and Engineering

Research Council of Canada and the supporting received from NIOBEC inc. The authors are also very thankful to Cornelia Chilian, Maryam A.Neysani and Darren Hall (NAA laboratory in Polytechnique Montreal) for the analysis and discussion of the assay evaluation.

4.7 Appendix

4.7.1 Mass balance

The mass balance is calculated in each stream feed (F), overflow (O) and underflow (U) using numerical particle size distribution data (PSD). We used PSD which are going to each one of these streams:

$$(q_F)_i = \frac{n_{Fi}}{\sum n_{Fi}} \ , \ (q_O)_i = \frac{n_{Oi}}{\sum n_{Oi}} \ , \ (q_U)_i = \frac{n_{Ui}}{\sum n_{Ui}} \tag{4.13}$$

$$\sum n_{Ui} + \sum n_{Oi} = \sum n_{Fi} \tag{4.14}$$

$$m_F = \rho_p \sum n_{Fi}(k_3)_i {x_i}^3 \tag{4.15}$$

$$m_O = \rho_p \sum n_{Oi}(k_3)_i {x_i}^3 = \rho_p k_3 \sum n_{Oi} \sum q_{Oi} {x_i}^3$$

$$m_U = \rho_p \sum n_{Ui}(k_3)_i {x_i}^3 = \rho_p k_3 \sum n_{Ui} \sum q_{Ui} {x_i}^3$$

$$\sum n_{Fi} = \frac{m_O}{\rho_p k_3 \sum q_{Oi} {x_i}^3} + \frac{m_U}{\rho_p k_3 \sum q_{Ui} {x_i}^3} \tag{4.16}$$

Where n_i is number of particles in size interval x_i, , k is a particle shape factor, ρ_p is particle density, m_F mass of particles in the feed stream, m_O mass of particles attached to droplets in overflow, m_U mass of non-emulsified particles in underflow and q_i is a numerical size distribution density in size interval x_i (Wills and Finch 2015) (Bazin and Hodouin 2001, Scientific 2012). By applying a proportional relation in mass continuity equations between each

stream, we are able to calculate the mass fractions. However, we should highlight the assumptions that i.e. density and shape factor remain similar for all particles:

$$\frac{m_O}{m_F} = r\ ,\ \ \frac{m_U}{m_F} = r' = 1 - r \tag{4.17}$$

$$\frac{\rho k_3 \sum n_{Fi}}{m_F} = \frac{1}{\sum q_{Fi}\, {x_i}^3} = \frac{r}{\sum q_{Oi}\, {x_i}^3} + \frac{1-r}{\sum q_{Ui}\, {x_i}^3} \tag{4.18}$$

$$\frac{m_O}{m_F} = r\ = \frac{1 - \frac{\sum q_{Fi}\, {x_i}^3}{\sum q_{Ui}\, {x_i}^3}}{\frac{\sum q_{Fi}\, {x_i}^3}{\sum q_{Oi}\, {x_i}^3} - \frac{\sum q_{Fi}\, {x_i}^3}{\sum q_{Ui}\, {x_i}^3}} = \frac{\frac{1}{\sum q_{Fi}\, {x_i}^3} - \frac{1}{\sum q_{Ui}\, {x_i}^3}}{\frac{1}{\sum q_{Oi}\, {x_i}^3} - \frac{1}{\sum q_{Ui}\, {x_i}^3}} \tag{4.19}$$

$$\frac{m_U}{m_F} = r' = \frac{1 - \frac{\sum q_{Fi}\, {x_i}^3}{\sum q_{Oi}\, {x_i}^3}}{\frac{\sum q_{Fi}\, {x_i}^3}{\sum q_{Ui}\, {x_i}^3} - \frac{\sum q_{Fi}\, {x_i}^3}{\sum q_{Oi}\, {x_i}^3}} = \frac{\frac{1}{\sum q_{Fi}\, {x_i}^3} - \frac{1}{\sum q_{Oi}\, {x_i}^3}}{\frac{1}{\sum q_{Ui}\, {x_i}^3} - \frac{1}{\sum q_{Oi}\, {x_i}^3}} \tag{4.20}$$

$$\frac{m_O}{m_U} = \frac{\sum q_{Oi}\, {x_i}^3}{\sum q_{Ui}\, {x_i}^3} \times \frac{(\sum q_{Fi}\, {x_i}^3 - \sum q_{Ui}\, {x_i}^3)}{(\sum q_{Oi}\, {x_i}^3 - \sum q_{Fi}\, {x_i}^3)} \tag{4.21}$$

4.7.2 Obtaining the grade by image analysis (IMGA)

In fact, samples of interest were put in the vials and once the sediment of minerals stick well to the bottom, photos were taken from the upside down vials in a symmetric arrangement (Figure 4.20). Later on, the photos were analyzed by the ImageJ software.

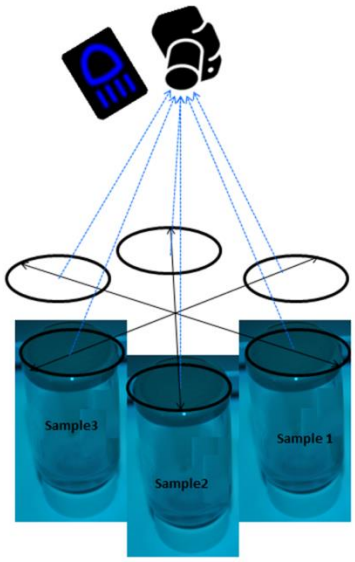

Figure 4.20 Mineral samples with symmetric arrangement in the upside down vials to take the photos

The ImageJ software provides the level of brightness in the RGB standard format which is a value between 0 and 256 for each red, green and blue pixel colors. Since the REE bearing minerals have specific light absorption behavior, i.e. wave length absorbance, the brightness level of samples differs via grade of the rare earth elements(Aneus 1965). In fact, a higher grade or concentration of REE bearing minerals results in a lower RGB brightness level for a given sample. Taking this behavior into account, brightness level of a sample of fresh ore (BFO) and brightness level of a concentrate of ore (BCO) were measured and a parameter called brightness level ratio (BLR) was defined (4.23). The grade of this concentrate was obtained by NAA and in fact considered as a calibrated indicator for extreme of beneficiation. In other words, a BLR value close to 100% indicates that the experimental sample had a low grade close to CSF of fresh ore. Figure 4.21 compares REE grade data of the three feeds with a -37 µm size by NAA versus their estimated BLR values. As expected, BLR varied in opposite to the trend of REE grade. We calibrate the IMGA method for any unknown samples using NAA results. A linear function was observed (Figure 4.22). Thus, the preliminary calibration was performed between F.O and concentrated ore of 7% TREE whereas both come from physical beneficiation and their BLRs show a linier function versus concentration. To justify the approach, the upper and lower concentration points were always indicated by NAA on which the middle point were estimated

by IMGA. This quick and simple approach establishes a quantitative method to estimate the grade in an unknown sample.

$$\frac{(\text{B.F.O.} - \text{B.S.}) \times (\text{E.C.O.} - \text{E.F.O.})}{\text{B.F.O.} - \text{B.C.O.}} + \text{E.F.O.} = \text{E.S.} \qquad 4.22$$

Where B.F.O. is level of brightness emitted from fresh ore, B.S. is level of brightness emitted from the sample, B.C.O. is level of brightness emitted from calibrated sample ore, E.C.O. is elemental assay of calibrated sample ore, E.F.O. is elemental assay of fresh ore and E.S. is elemental assay of the sample:

$$\frac{\text{B.F.O.} - \text{B.S.}}{\text{B.F.O.} - \text{B.C.O.}} = \text{Brightness level ratio "BLR"} \qquad 4.23$$

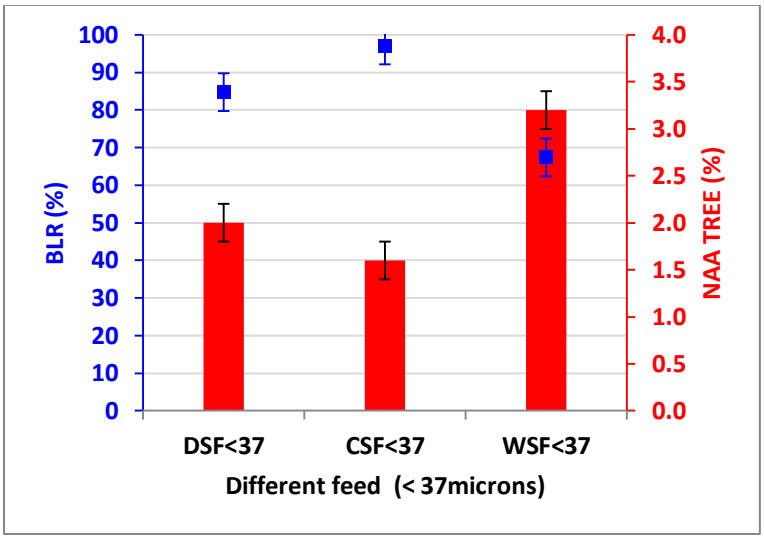

Figure 4.21 Obtaining the grade by IMGA when compared with NAA results

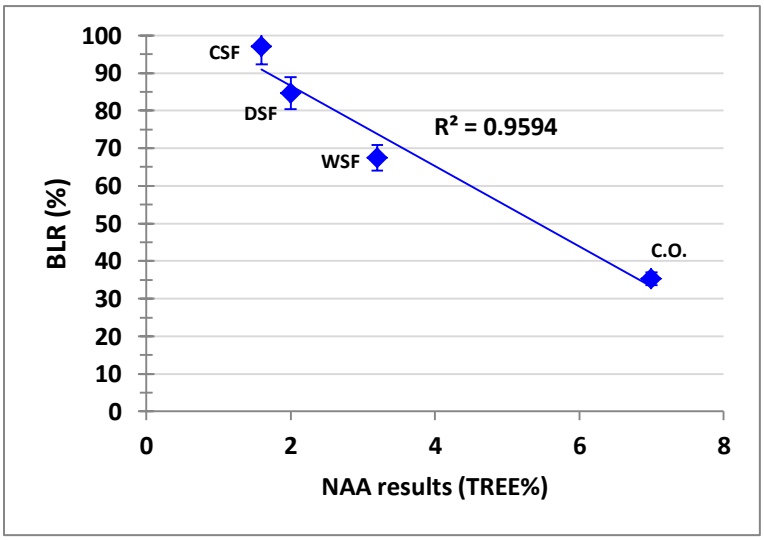

Figure 4.22 Correlation of IMGA results with NAA, the first three points from DSF, CSF and WSF feed samples and 4th point is the concentrated ore from emulsification

4.7.3 Particle size class attachment

Feed size fewer than -63µm was prepared to investigate the mass fractions of each particle size class attached into the interface. The all size classes belong to feed -63µm and the mass fractions of each size intervals were calculated based on the mass distribution balance (4.15). The mass of particles of cut size interval (i) in the overflow (particles attached to the droplets) over the mass of the same size interval (i) in the feed is shown as function of each cut size. Figure 4.23 clearly indicates that lower size has tendency to attach more into the oil droplet interface. The trend for DSF and CSF at -37µm is interesting when compared with WSF. There are fine particles accumulated in WSF under -37µm while the fine particles which are remained attached to coarse particles makes the differences for DSF and CSF at bigger cut sizes.

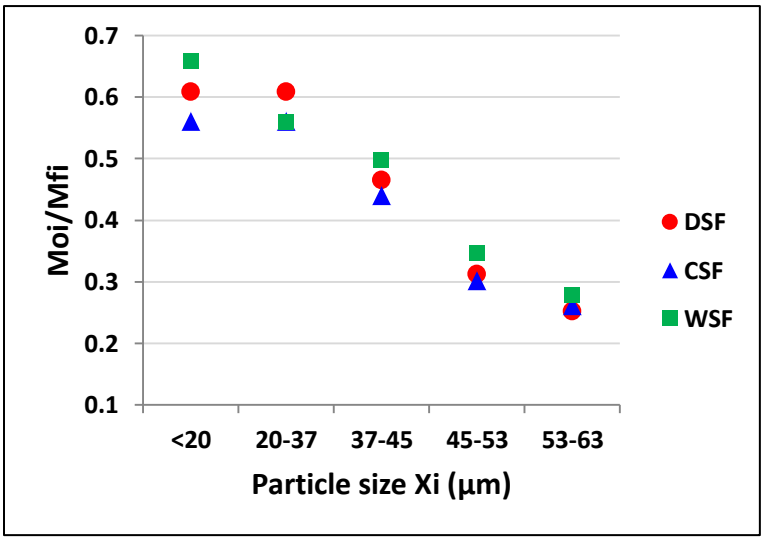

Figure 4.23 Overflow particle size attachment, ($Feeds\ are - 63\ \mu m, \Phi_d$=9%, PDMS oil 50 cSt, Ms=5%, 15minPBT@1000 rpm)

CHAPTER 5 ARTICLE 2: CONCENTRATED MONAZITE AND BASTNAESITE THROUGH PICKERING EMULSIFICATION: THE EFFECT OF PROCESSING CONDITIONS

Rahi Avazpour, Mohamamd Latifi, Louis Fradette, Jamal Chaouki[2]

Department of Chemical Engineering, École Polytechnique de Montréal, c.p. 6079, Succ. Centre-ville, Montréal, Québec, H3C 3A7, Canada

(Journal of CHEMICAL ENGINEERING AND PROCESSING, Date submitted: 15/04/2019)

5.1 Abstract

The rare earth elements have many applications especially in green energy and electronic sectors. Separation of REE bearing minerals from their associated gangues (e.g. dolomite and calcite) is challenging since they have similar physicochemical properties. Froth flotation is an option to produce a concentrate of rare earth elements, but it uses costly and eco-destructive surfactants. The Pickering selective emulsification was introduced as a novel approach for physical beneficiation of rare earth bearing minerals. The effects of mixing intensity (i.e., changing RPM) and shear uniformity (i.e., comparing Maxblend and PBT impellers) on recovery and grade of product were investigated. NIOBEC ore is used on which the most abundant REE bearing minerals are the carbonatite types of bastnäsite ((Ce, La, Nd, Y) FCO_3) and monazite ((Ce,La,YNd,Th) PO_4). Recovery and grade enhance by increasing the impeller speed. Also, the emulsion droplet size distribution tends to be eventually more uniform with Maxblend; hence, we get higher recovery and grade. The recovery of one stage emulsification is improved significantly by adjusting the RPM of Maxblend impeller. A65% recovery is achieved along with an enrichment ratio around 3.85 in the products.

Keywords: Pickering emulsification, Mixing, Rare earth elements, beneficiation

[2] Correspondence concerning this article should be addressed to L. Fradette at Louis.fradette@polymtl.ca

5.2 Introduction

The rare earth elements (REE) are strategic materials with a diverse range of applications in the current high-tech such as renewable energy, catalysts, permanent magnets, motors, power generation, electronics, and medical devices (e.g. MRI) due to their unique physicochemical properties (Jordens, Cheng et al. 2013). The REE are called rare not because of their abundance on the earth crust, which is indeed quite plentiful, but because their extraction from nature is very challenging in terms of economy, yield (i.e., grade and recovery) and environment (Haque, Hughes et al. 2014, Navarro and Zhao 2014). A process of rare earth elements production includes: a physical beneficiation step to produce a concentrate of REE from the raw ore; a thermochemical (i.e., thermal backing and hydrometallurgy) step to crack the REE bearing minerals of the concentrate to produce a high-grade mixture of rare earth oxides; a separation step to produce individual rare earth oxides.

Each of these steps usually includes a complex array of unit operations. This is because, as a characteristic feature of the REE deposits, the REE bearing minerals are in the vicinity of gangue minerals that have very similar physicochemical properties. In addition, a production process of high-grade rare earth oxides from mining through enrichment processing is costly and carries serious environmental problems due to consumption of considerable amounts of energy and reagents, and generation of hazardous tailings. Moreover, the rare earth elements have similar chemical properties due to special electronic configurations of their atoms that make their production in individual forms also cumbersome (Castor and Hedrick 2006). Therefore, it is crucial to develop feasible processes with a high enough yield and the lowest detrimental impacts on the environment.

Froth flotation is the most common process in physical beneficiation step. However, it suffers from consumptions of chemicals as surfactants, pH modifiers, and depressants (Sprecher, Xiao et al. 2014). Also, the water can hardly be recycled inside the process, because of the numerous additives input, thus, a large tailings ponds are being created at the process site (Bulatovic 2007, Bulatovic 2010, Sprecher, Xiao et al. 2014). As an alternative process to froth flotation, authors have developed a new physical beneficiation process to concentrate rare earth bearing minerals [Chapter 4]. The new process is based on Pickering–Ramsden or solid stabilized emulsification (SSE) that has been practised for more than one century in other industries (Ramsden 1903,

Binks and Whitby 2004). The SSE process takes advantage of wettability of solid fine particles that can play the role of an emulsifier so that there is no need to a surfactant to generate an emulsion. This process is environmental friendly as it only employs oil and water, and no other chemicals. More specifically, the ore particles emulsify oil droplets as the dispersed phase in water that is the continuous phase. Figure 5.1 illustrates an oil droplet surrounded by the ore particles that was formed in a solid stabilized emulsion.

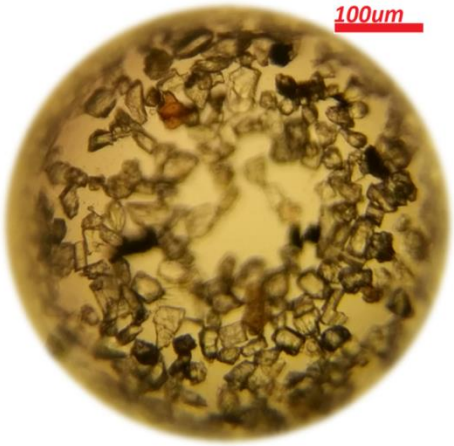

Figure 5.1 Solid stabilized droplets covered with minerals particles taken by Microscopic NIKON ALPHAPHOT2-YS2 zoom 50x

The authors applied the SSE process to the Niobec ore that contains bastnäsite and monazite, (i.e., two REE bearing minerals for a viable REE extraction). Monazite and bastnäsite are more hydrophobic when compared with the associated gangues (Bulatovic 2007), thus, they have more affinity to the oil phase and competitively attached more into the oil-water interface. Hence, the gangues tend to remain more in the aqueous phase and sediment afterward. Authors' earlier work proved the SSE process could selectively separate the REE bearing minerals and produces a REE concentrate with an enrichment ratio of more than 300% [Chapter 4]. The process is yet to be optimized in favor of minimum cost and maximum yield of REE. As part of the process optimization, this article is to do with the impact of mixing conditions on the selectivity of the SSE process towards bastnäsite and monazite. To do so, the physicochemical properties of ore minerals in the feed, the oil type, and parameters such as setup scale, pH, solid mass fraction, and oil to water ratio were kept constant for the entire experiments. More specifically, impacts of mixing intensity (i.e., the variation of rotation speed) and shear uniformity (i.e., Maxblend impeller versus PBT impeller) were investigated. Maxblend impeller can generate much more

uniform shear rate in the entire emulsification system compared to PBT impeller; that is, the difference between the maximum and minimum shear rate in the system equipped with Maxblend is much lower (Leng and Calabrese 2004, Paul, Atiemo-Obeng et al. 2004).

5.3 Materials and methodology

5.3.1 Experimental setup

A full SSE experimental apparatus procedure includes an emulsification followed by a demulsification for phase separation, and centrifugation for oil recovery and recycling. A schematic of the experimental setup is presented elsewhere [Chapter 4]. Figure 5.2 illustrates the agitation tank inside which a controllable pitched blade turbine (PBT) and a Maxblend impeller were employed for emulsification tests. Table 5.1 presents the pertinent dimensions.

The PBT was installed off-centered to avoid vortex formation and to generate turbulence in a flow field with the standard configuration (i.e., H=T). This setup is equivalent to a centered impeller with baffles (Karcz, Cudak et al. 2005, Gingras, Tanguy et al. 2012).

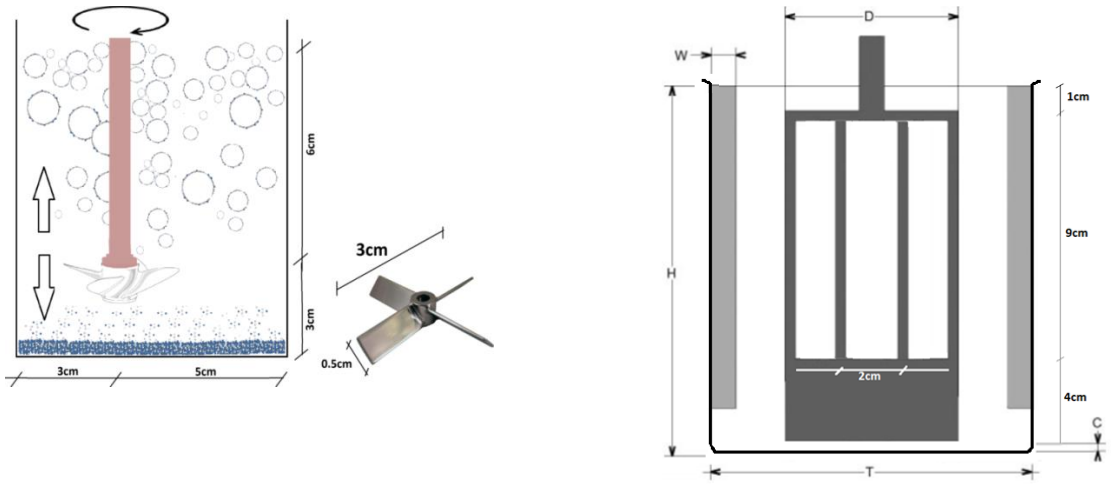

a b

Figure 5.2 Stirrer tank installation configuration and dimensions- a) PBT b)Maxblend

Table 5.1 Setup specific dimensions for both PBT and Maxblend

Dimensions (cm)	PBT	Maxblend
D	3	7.5
T	8	13
H	8	14
4×W	-	1.1
C	0.5	0.5

The oil-to-water volume ratio was adjusted at 10 (% v/v) or $\Phi_d = 9\%$ to make a dilute emulsion. Φ_d is adjusted for an appropriate interface generation always more than coverage potential of available REE bearing minerals in the system (Tsabet and Fradette 2015). Also, the particle-to-liquid mass fraction was set at 5% wt. This value is less than solid mass ratio into froth flotation process which is usually above 20% wt, but this amount of solid mass fraction takes place in cascade stages of thickening, cleaning and scavenger with multiple series of cells. Thus, for a single stage emulsification, 5% wt of solid mass can be comparable with single stage of a micro flotation cell. After each experiment, the size distribution and the Sauter mean diameter (i.e., D_{32}) of the particles and of the droplets were estimated by a Mastersizer 3000 (Malvern Inc.) instrument.

An image analysis method was employed for a quick screening of the product samples [Chapter 4]. Subsequently, the concentration of the REE measured by the k0-Neutron activation analysis (NAA) (M. Abdollahi Neisiania 2017) was utilized to calculate the enrichment ratio (i.e., grade of product/grade of the feed) and recovery of the REE. Since the feed grade can influence the grade and recovery in the product, the PSD and the head grade of the bulk feed were kept constant in all tests.

5.3.2 Materials

The Niobec supplied the raw ore from its mine located in the municipality of Saint-Honore in Saguenay-Lac-Saint-Jean in Québec province of Canada.

Table 5.2 Group of the consistent gangues in Niobec ore and weight percentages (Lafleur, Eng et al. 2012)

Name	association (%wt)	Calculated grain Size (µm)	Category
Bastnaesite/Synchisite	1.96	14.34	Fluorocarbonate
Monazite/Th-Monazite	1.43	12.63	Phosphate
Other REE minerals	0.14	_	Phosphate
Fe-Oxides	5.85	21.43	Oxide
Chlorite	4.43	18.37	Silicate
Dolomite	50.00	27.23	Carbonate
Calcite	13.16	20.21	Carbonate
Ankerite	13.72	21.96	Carbonate
Other Gangues	9.31	_	-
Total	**100.00**		**-**

Table 5.2 presents available minerals of the ore along with their respective composition and the calculated grain size that were detected by QEMSCAN. Carbonate minerals of calcite, dolomite, and ankerite were the main gangues of the ore (i.e., more than 77 wt%). Other abundant gangues were oxides such as iron oxide (about 6 wt%), silicates such as chlorite (about 4.5 wt%), and other gangues including sulfides and sulfate respectively such as pyrite, barite and etc. (above 9 wt%). However, it is noteworthy that the concentration of the REE bearing minerals was considerably lower, i.e., bastnäsite and monazite with concentrations of 1.96 wt% and 1.43 wt%, respectively. Theoretically, with respect to the estimated grain size of the main gangue minerals in Table 5.2, the REE bearing minerals would be ideally liberated from the ore if it were ground to a maximum size less than 20 µm. In an industrial scale, the techno-economic analysis of overall process will obtain on which particle size should be used.

5.3.3 Experimental feed

Solid stabilized emulsification separates minerals based on their wettability that is usually measured by their contact angle in an oil/water interface. Author's previous work showed that the contact angle of the REE bearing minerals (slightly above 50 °) was higher than the main gangue minerals of the ore; in other words, the REE bearing minerals were relatively more hydrophobic and tended competitively to immerse or attach to the oil droplets [Author's article].

The study on the yield of SSE versus the ore size cut revealed the highest grade would be obtained after a wet sieving with the size cuts of -20 and -37 µm was applied to the fresh ore (i.e., the grades were measured around 4.3 and 3.3 %TREO respectively) [Author's article]. This observation confirmed that the emulsification process could provide a very promising selectivity for separation of the REE bearing minerals due to their wettability difference. Our previous work also showed the superior advantage of the wet sieving over the dry sieving as the fine particles would be washed away from the surface of the larger particles with the former sieving method. Therefore, the fresh ore following wet sieving with size cuts of -20 and -37 µm (D_{32} 10 and 14 µm respectively) was selected for this investigation. The total concentration of REE (TREE) of the ore size cuts of -20 and -37 µm was 3.3 wt% and 3.1 wt%, respectively.

5.3.4 Liquid phases

The continuous phase of the experiments was distilled water with the surface tension of 72.6 mN/m at 22ºC. The dispersed phase was a typical silicone oil of polydimethylsiloxane (PDMS) from CLEARCO Inc. Physical properties of two PDMS oil employed in this research is presented in Table 5.3.

Table 5.3 Silicon oil properties

Silicone oils	Density (kg/m3)	Dynamic viscosity (mPa.s)	Surface tension (mN/m)
S50	**960**	**48.0**	**20.8**
S200	**968**	**193.6**	**21.0**

5.3.5 Experimental procedure

An experimental test started off by mixing the distilled water and the feed at 1000 rpm for 3min to homogenize particle dispersion, and to break down probable aggregates. Once a reasonable dispersion of the solids was reached, mixing was stopped. Subsequently, a PDMS oil was added, and subsequently the mixing restarted. While mass ratio between feed, water, and oil was fixed at the all tests, the mass of each phase was different depending on the impeller type (Table 5.4).

Table 5.4 The amount of materials in each setup

PBT	15	300	30
Maxblend	80	1600	160

Then mixing continued for a certain time at a specified rpm to reach the emulsion equilibrium. The emulsion equilibrium is defined here as minimum droplets mean size and span, along with maximum possible selectivity. Three different mixing durations (MD) of 5 and 15 min as well as 24 h were investigated to find an optimal duration for mixing to reach the emulsion equilibrium.

The emulsion was then left for 1 h to be stabilized before collecting the fraction of creamed droplets through a separation funnel. Later, centrifugation was employed to break down the stabilized oil droplets by applying force acceleration as much as 900 times the gravity acceleration for 15 min (Hirajima, Sasaki et al. 2005).

Apart from the standard emulsification procedure, impact of the order of adding the materials (i.e., the feed and the liquids) on the yield of SSE was investigated:

1. In the standard emulsification, particles of the feed ore were added to distilled water. The oil was added in the next step and the slurry mixed to achieve a full dispersion and emulsification of oil droplets.
2. In the mixing order 1, the pre-wetted particles were added to the water mixture and mixing continued for 3 min to be well dispersed. Then the oil portion was added suddenly to the mixture while the mixing was continued for 15 min to achieve a full dispersion and emulsification of oil droplets..

3. In the mixing order 2, a procedure similar to the latter one, but oil is added first and the pre-wetted particles were added suddenly after an initial 3 min of oil and water mixing. In this order, the oil droplets firstly formed and reach to the equilibrium size before adding the feed ore.

5.3.6 Mixing parameters

5.3.6.1 The just suspended agitation speed

The "just suspended" speed (Njs) is the minimum agitation speed at which all particles reach a complete suspension. The rotational speed should be always above Njs to ensure there is an effective particle-droplet interaction of all the particles during emulsification. Applying the Zwietering correlation (Paul, Atiemo-Obeng et al. 2004), a Njs of around 700 rpm was estimated for the setup equipped with PTB impeller at a very low clearance (C/T=0.06). There is no correlation for Njs in the stirred tank equipped with Maxblend; thus Njs should be defined visually (Jafari 2010, Hashem 2012, Jafari, Chaouki et al. 2012). Accordingly, the speed on which no mineral particle remained at the bottom corner of the tank was taken for this impeller (around 180 rpm).

5.3.6.2 The average turbulent energy dissipation rate

The power inlet from an impeller to the system can be expressed in term of power number $N_p = \frac{P}{\rho * {N_i}^3 {D_i}^5}$ where the inlet power on the shaft is equal to $P = 2\pi N_i \tau$. Thus, $N_p = \frac{2\pi\tau}{\rho * {N_i}^2 {D_i}^5}$ where τ is the torque on the impeller shaft, ρ* is the density of slurry, N_i is the impeller speed in rotation per second, and D_i is the impeller diameter size.

The average turbulent energy dissipation rate can be calculated by $\varepsilon_{ave} = \frac{P}{M_t}$ where M_t is the total theoretical mass of the system including solids and liquids (Paul, Atiemo-Obeng et al. 2004).

5.3.7 The performance of separation

Since there are excess particles in the system, the mass of particles is more than the amount needed to fully cover the generated interface. In other words, the selectivity of Pickering

emulsion can be dedicated to a competitive attachment between targeted particles and undesired particles in the system. Hence, we investigated the global attachment efficiency of monazite and bastnäsite with respect to their associated gangues.

The wettability for bastnäsite and monazite was characterized, respectively, by a mean contact angle of 54±5º and 60±5º. The contact angle between water and pure monazite is reported above 49° (Abaka-Wood, Addai-Mensah et al.) that is consistent with our data. The contact angle of calcite and dolomite that exist significantly in Niobec's ore are less than 50° (Zhang 2014).

The competitive attachment of minerals is controlled by their wettability in conjunction with the oil and water interface. Due to their wettability difference with the gangues, once the Pickering emulsion is generated, monazite and bastnäsite particles are expected to be attached to oil droplets. The stabilized droplets have low density than particles, thus they cream on the top and can be collected after phase separation.

The experimental performance of separation is evaluated quantitatively by means of recovery and grade. The grade of REE in the product is defined by 5.1:

$$\text{Grade TREO\%(wt)} = \sum \frac{\%Elemental\ assay}{2 \times REE's\ Atomic\ weight} \times (\ Molar\ mass\ of\ ((REE)_2O_3) \qquad 5.1$$

However, we use enrichment ratio which is a common method to indicate the performance of separation:

$$\text{ER\%(enrichment ratio)} = \frac{\text{Overflow or products (TREO\%)}}{\text{Feed garde or head grade (TREO\%)}} \qquad 5.2$$

The recovery of REE minerals was estimated by 5.3:

$$\%Recovery\ = \frac{Grade\ in\ product\ (Overflow) \times mass\ flow\ of\ product\ stream}{Grade\ in\ feed \times mass\ flow\ of\ feed\ stream} = \frac{G_O \times\ M_O}{G_F \times M_F} \qquad 5.3$$

A theoretical approach of the "overall probability of attachment" is employed to make a meaningful correlation between the experimental performance data and the force and energy balance behind the selective attachment of specific particles in the system (5.4).

$$\textit{Overall Probabilities of attachment} = \frac{Total\ number\ of\ the\ attached\ particles\ into\ the\ interface}{Total\ number\ of\ the\ particles\ in\ the\ system} \qquad 5.4$$

This probability is a function of different parameters and can be written for REE minerals and the gangues separately:

$$P_{Att}(REE) = f(N_i, \varepsilon_{ave}, \dots) = \frac{N.total_{attached-REE}}{N.total_{REE}} \quad 5.5$$

$$P_{Att}(Gangues) = f(N_i, \varepsilon_{ave}, \dots) = \frac{N.total_{attached-Gangue}}{N.total_{Gangue}} \quad 5.6$$

The probability of attachment for REE's and the gangues can be linked by a factor of a magnitude of selectivity (n_s) which is always more than unity (i.e. >1) because of the higher affinity of REE minerals (i.e., more hydrophobicity) to be attached to the oil droplets. In other words:

$$P_{Att}(REE) = n_s \times P_{Att}(Gangues) \quad 5.7$$

Also, the ideal recovery of monazite and bastnaesite is equal to the theoretical probability of attachment:

$$Ideal\ recovery\ R = P_{Att}(REE) \quad 5.8$$

The grade in the product can be also deduced from selectivity factor:

$$G_O = \frac{P_{Att}(REE) \times M_F G_F}{P_{Att}(REE) \times M_F G_F + P_{Att}(Gangues) \times M_F(1 - G_F))} \quad 5.9$$

$$G_O = \frac{P_{Att}(REE) \times G_F}{P_{Att}(REE) \times G_F + P_{Att}(Gangues) \times (1 - G_F)}$$

$$G_O = \frac{n_s G_F}{1 + G_F \times (n_s - 1)}$$

The recovery can be also driven from the grades in each stream without using the proportional mass directly:

$$R = \frac{G_O}{G_F} \times \left(\frac{G_F - G_U}{G_O - G_U}\right) \quad 5.10$$

G_F, G_O, G_U are respectively the grade in the feed, overflow (products) and underflow (tailings). In 5.9 and 5.10, recovery and the grade of the products can be increased along with augmenting

of the magnitude of selectivity (n_s). This factor is not measured but can be calculated to show the effect of different parameters of operational conditions on the selectivity of REE minerals (a function of various parameters of the emulsification system including operational mixing and formulation).

$$n_s = f(\varepsilon_{ave}, N_i, \mathrm{D32_d}, \dots) \quad 5.11$$

Among them, the $\varepsilon_{\mathrm{ave}}$, $\mathrm{N_i}$, and the final droplet size $\mathrm{D32_d}$ are the most important parameters which can be controlled by the mixing conditions.

Since, the generated interface of the Pickering emulsion can be calculated by $\mathrm{D32_d}$, the amount of theoretical available interface area $\mathrm{A_{Theo}}$ on which the mineral particles can be attached is a fraction of the coverage potential $\mathrm{A_{cov}}$ which is much bigger than the generated interface $\mathrm{A_{gen}}$ because we have always excess particles in the system (available particles > required particles to cover interface), thus we can write (Tsabet 2014):

$$\mathrm{A_{Theo}} = \mathrm{Min}(\mathrm{A_{gen}}, \mathrm{A_{cov}}) \rightarrow \mathrm{A_{Theo}} = \mathrm{A_{gen}} \quad 5.12$$

According to the literature and the fundamentals behind the stabilization phenomenon, the particle adsorption and stabilization at the interface has four main steps including particle-droplet collision, three phases contact line (TPCL) development, particle-droplet attachment, and droplets coverage rate whereas the network of particles formed around droplet interface. There are also four efficiencies regarding these steps end up to the effective covered and stabilized droplets. These efficiencies can be assessed by free energy or force analysis equations (Tsabet 2014).

The effectively covered interface (A_{eff}) is a term of global efficiency of attachment multiple to the theoretical available interface (5.13) whereas the global efficiency of attachment is produced from four steps efficiencies:

$$E_{glob} = \frac{A_{eff}}{A_{gen}} \quad 5.13$$

$$E_{global} = E_{Col} \times E_{TPCL} \times E_{Att} \times E_{Cov}$$

Whereas E_{Col}, E_{TPCL}, E_{Att}, E_{Cov} are respectively the efficiencies of collision, three-phase contact line, attachment, and coverage. These efficiencies can be calculated based on the fundamental

formulas by putting appropriate assumptions and correction factors for the effect of non-spherical particles or sphericity (k_1), the effect of non-liberated or capsulated or conjoint minerals (k_2).

Table 5.5 The four main steps efficiencies for particle adsorption and stabilization at interface

$E_{Col} = exp(-C_1 \frac{t_d}{t_c})$	C.A. Coulaloglou (1975)
$E_{TPCL} = 1 - exp(-\frac{t_c}{t_{TPC_{cir}}})$	H.J. Schulze et al., 1993
$E_{Att} = 1 - exp(1 - C_{Att} \frac{F_{Att}}{F_{Det}})$	H.J. Schulze et al., 1993
$E_{Cov} = exp(-\frac{Freq_{collision\ d/d} \times E_{Coalescence}}{Freq_{collision\ p/d}})$	A.K.Chesters (1991)
Where E_{Col},E_{TPCL},E_{Att}, $E_{Cov}$and $E_{Coalescence}$ are efficiencies of collision, three phase contact line formation, attachment, droplet interface coverage and coalescence respectively, t_c is the contact time, t_d is the drainage time, $t_{TPC_{cir}}$is TPC line expansion time, C_1 and C_{Att} are the constants, F_{Att} is the attachment force, F_{Det} is the detachment force, $Freq_{collision\ p/d}$ and $Freq_{collision\ p/d}$ are the particle/droplet and droplet/droplet collision frequencies (Coulaloglou and Tavlarides 1977, Tsouris and Tavlarides 1994). To see details: (Tsabet 2014)	

The global efficiency of attachment for all attached particles can be divided into two separate categories for REE bearing minerals and the rest of the gangues. So we can also rewrite these efficiencies for the gangues and REE minerals separately (equations 5.145.15):

$$E_{REE} = k_1 \times k_2 \times (E_{Col} \times E_{TPCL} \times E_{Att} \times E_{Cov})_{REE}$$
$$E_{Gangue} = k'_1 \times k'_2 \times (E_{Col} \times E_{TPCL} \times E_{Att} \times E_{Cov})_{Gangue} \quad 5.14$$

The best fit values for correction factors for REE bearing particles and gangues ($k_1, k_2, k'_1\ and\ k'_2$) should be obtained experimentally for our emulsification system.

$$E_{glob} = \frac{A_{eff}}{A_{gen}} = \frac{A_{eff-REE} + A_{eff-Gangue}}{A_{gen}} = E_{REE} + E_{Gangue} \quad 5.15$$

In another side, if the total number of attached particles is taken into account we have:

$$\frac{\boldsymbol{E_{REE}}}{\boldsymbol{E_{Gangue}}} = \frac{A_{eff-REE}}{A_{eff-Gangue}} = \frac{\pi D32^2{}_p \times N.total_{att-REE}}{\pi D32^2{}_p \times N.total_{att-Gangue}} = \frac{N.total_{att-REE}}{N.total_{att-Gangue}} \quad 5.16$$

And the total number of attached REE bearing minerals including monazite and bastnaesite and the gangues can be dedicated to the grade of the overflow (products) in the equation bellow:

$$\frac{N.total_{att-REE}}{N.total_{att-Gangue}} = \frac{\frac{N.total_{att-REE}}{N.total_{att}}}{\frac{N.total_{att-Gangue}}{N.total_{att}}} = \frac{G_O}{1-G_O} \quad 5.17$$

Thus, it is also true:

$$\frac{\boldsymbol{G_O}}{\boldsymbol{1-G_O}} = \frac{\boldsymbol{E_{REE}}}{\boldsymbol{E_{Gangue}}} = \boldsymbol{K} \times \frac{(E_{Col} \times E_{TPCL} \times E_{Att} \times E_{Cov})_{REE}}{(E_{Col} \times E_{TPCL} \times E_{Att} \times E_{Cov})_{Gangue}} = I_{Att} \quad 5.18$$

$$\boldsymbol{K} = \frac{k_1}{k'_1} \times \frac{k_2}{k'_2}$$

Where I_{Att} is the attachment efficiency index [Chapter 4]. Regarding the shape factors, $k_1 and\ k'_1$ are similar. *The best fit values for the K were found near to 0.83 in our experiments.* However, it very depends on the specification of the feed ore and the liberation size. From above mentioned, the particle selective attachment can be modeled to predict the performance of separation based on the operational conditions and the emulsion properties (i.e., droplets size distribution) and compare it with the recovery and the grade calculated based on the experimental results. Figure 5.3 shows the flowchart of data acquisition from the experimental results and the model.

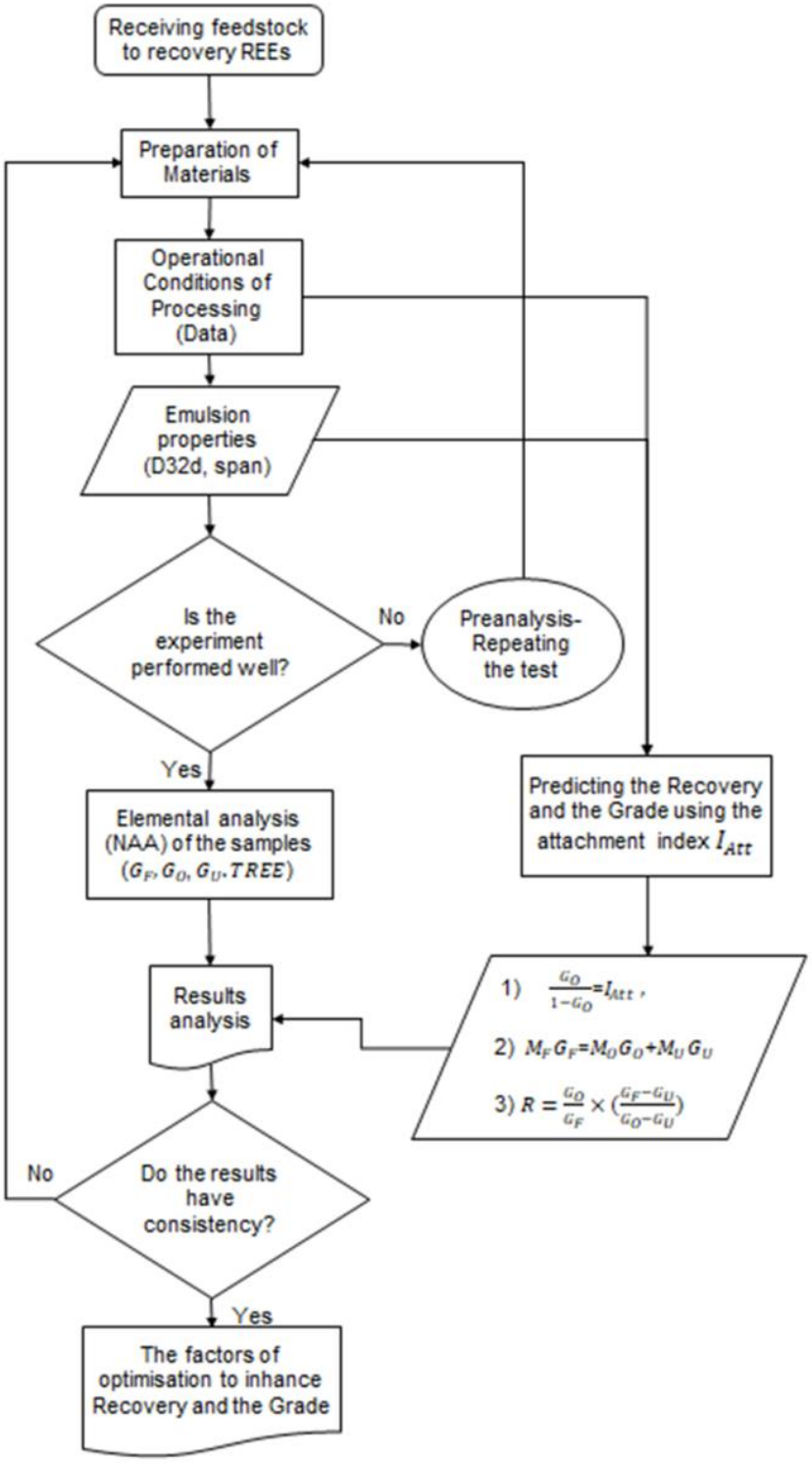

Figure 5.3 Model vs. experimental data in an acquisition flowchart diagram

5.4 Results and discussion

5.4.1 Alignment of operating conditions

Characterization of mixing setups

The power number of the impellers, the inlet power and the average turbulent energy dissipation rate were obtained. The estimated average power numbers were, consequently, around 2.35 for Maxblend and around 1.25 for PBT in a turbulent regime where the Re number was more than 10^4 (Figure 5.4). The density of the slurry was calculated based on an apparent density $\rho_{Slurry} = \frac{\rho_L}{[1-M_s\left(1-\frac{\rho_L}{\rho_S}\right)]}$ where ρ_L is liquid phase apparent density, ρ_S is solid phase bulk density and M_s is the solid mass fraction.

The apparent viscosity of the slurry could not be obtained experimentally mostly due to the fact of sedimentation of minerals. The results in other literatures and experiments shows that the viscosity at turbulent regime is very near to the viscosity of continuous phase for a dilute emulsion. Hence, the apparent viscosity of the emulsified slurry is expected to be very close to the water viscosity. Nonetheless, to determine the power number in a turbulent regime based on the power curve, Np is curved as a function of Re number multiplied by viscosity. The uncertainties are assigned to the device's error and three times repeated tests.

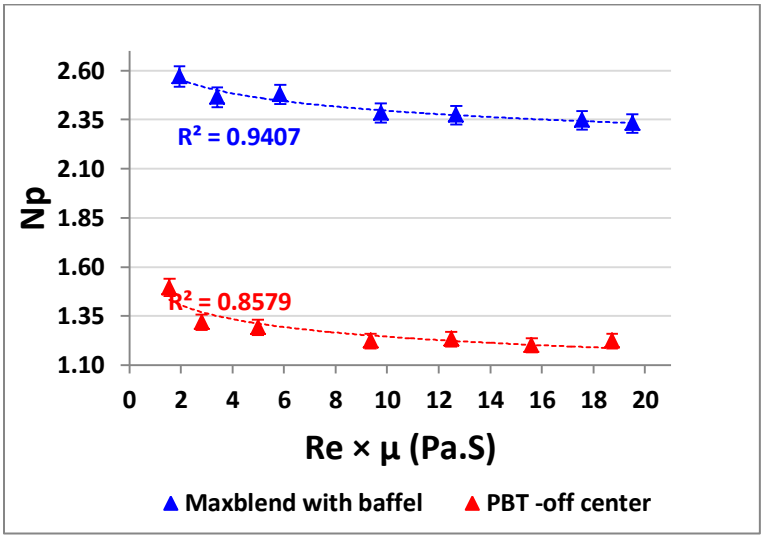

Figure 5.4 Experimental points of power curve, Maxblend with baffle vs. PBT off centered- Feed WSF<20 microns , oil PDMS 200 cSt, Φ_d 9%, Ms= 5%

One of the most important dimensionless numbers to explain emulsification behavior is Webber number (We) on which we can explain emulsion properties (i.e., droplet mean size D32d), and use it in the model. By keeping the same We number in two setups with different impellers, it is expected to have similar as possible emulsification behavior, and thus a similar final equilibrium emulsion size at which the coalescence and breakage of droplets reach an equilibrium rate. Figure 5.5 indicates the average turbulent energy dissipation rate for both Maxblend and PBT setups with the same Weber number and different impeller speed. The RPM for the impellers were adjusted delicately to hold a similar Weber number.

The average turbulent energy dissipation rate is different in two systems, and as expected, its values are much lower for Maxblend at the same Weber number. In other words, under given operating conditions such as the feed particles, physicochemical properties, O/W/solid ratio, oil type, and viscosity, the Maxblend with bigger setup scale consumes significantly less energy per unit volume of slurry to generate the emulsion interface (Figure 5.5). It should be also noted that there is a longer circulation time for the bigger scale (i.e., Maxblend). The circulation time is a time when a particle or droplet passes through and returns to the impeller zone. We assume that the effect of circulation time is negligible where the emulsion size is almost similar (Paul, Atiemo-Obeng et al. 2004, Tsabet and Fradette 2015).

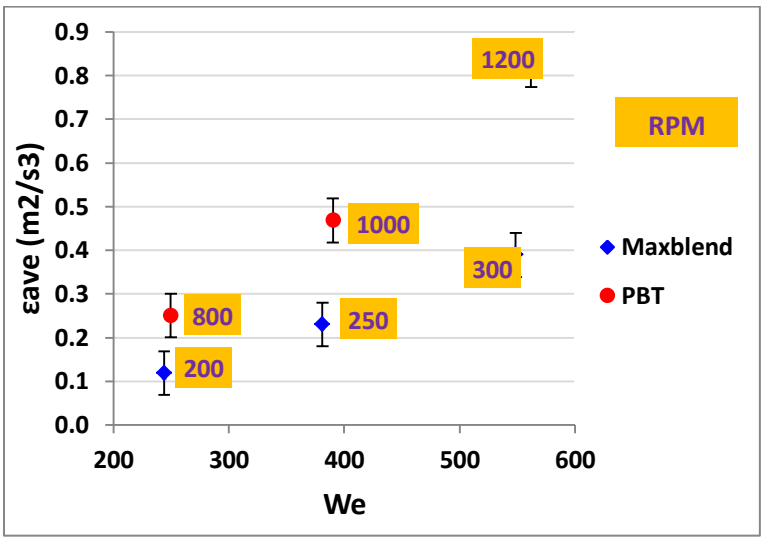

Figure 5.5 Average turbulent energy dissipation rate vs. We number and RPM for both impeller types PBT and Maxblend -Feed WSF<20 microns , oil PDMS 200 cSt, Φ_d 9%, Ms= 5%

It should be mentioned that there is no kinetic modeling for the effect of temperature on the phenomenon in this article. Nonetheless, we know that a higher temperature make the emulsion unstable and hence a lower recovery will be achieved.

5.4.2 Effect of mixing duration

A longer mixing duration can enhance the selectivity by increasing particle-droplet interactions and the probability of attachment in the system. To find out the minimum time required to reach a maximum performance, three mixing durations were investigated. The results indicate that a mixing duration of 15 min was enough to reach a maximum grade and recovery of the rare earth elements while the emulsion size reaches an equilibrium at which the coalescence and breakage of droplets reach an equilibrium rate (Figure 5.6). The droplet size associated with the mixing duration of 24 h was slightly less than the one at 15 min that could explain equilibrium was a bit stable due to higher rate of droplets coverage after such a long time even though it did not have an observable impact on separation of rare earth elements. Three different mixing durations were performed and adjusted at optimum 15 min. This is a shortest time to reach the equilibrium and thus an optimum recovery.

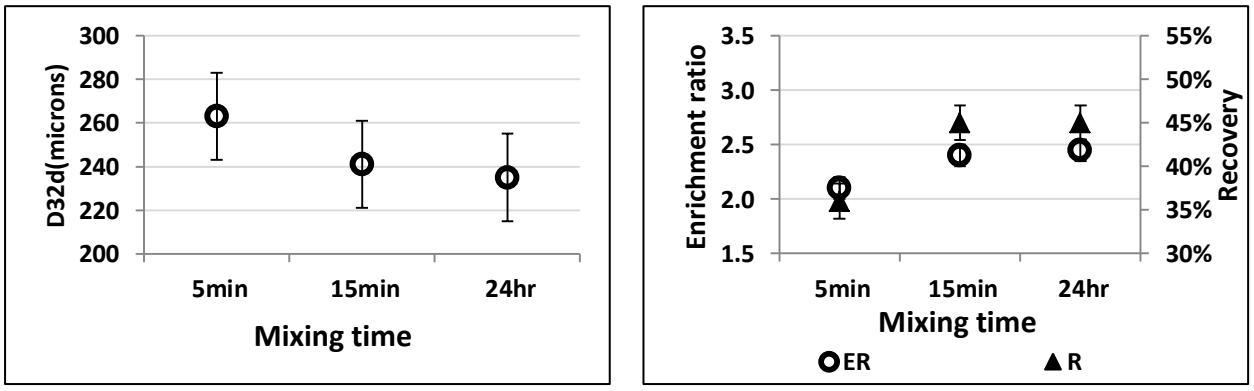

a b

Figure 5.6. Effect of mixing duration on (a) emulsion mean droplet size; (b) recovery and enrichment ratio of rare earth bearing minerals in overflow. Feed: WSF<37, Φ_d=9%, PDMS oil 50 cSt, Ms=5%, PBT@1000 rpm

5.4.3 Order of mixing

The best selectivity was achieved when the oil was well dispersed in the system and the pre-wetted mineral particles were added by a deferment of 3min after starting the agitation (mixing order 2 or M.O2). In the standard mixing (S.M) for emulsification, the oil and mineral particles were present respectively top at bottom of the tank and the interface was being generated by the time. It hinders to achieve the required interface at the beginning of the emulsification and reduces the chance of capturing the targeted minerals. In M.O2, we increased the probability of selective attachment, a consequence of increasing the chance of monazite and bastnäsite to be captured by a larger interface. This offset before adding oil is not enough for mixing order1 (M.O1) to reach the equilibrium size of the droplets or maximum available interface.

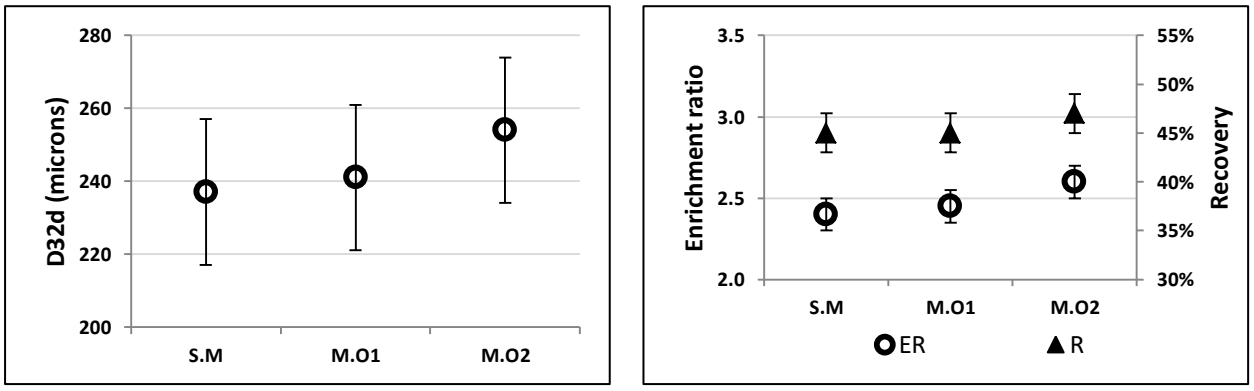

a b

Figure 5.7 a) Mean droplet size for different order of mixing, b) Recovery and enrichment ratio of monazite and bastnaesite in the overflow for different order of mixing, (Feed WSF<37, Φ_d=9%, PDMS oil 50 cSt, Ms=5%, 15minPBT@1000 rpm)

5.4.4 Effect of the mixing RPM

Figure 5.8 shows the emulsion size evolution as a function of impeller speed in the PBT setup. The increasing of the mixing RPM will lead to higher Weber number, thus smaller droplet size. In fact, since there are excess particles in the system, a faster RPM enhances the breakage rate while the coalescence rate doesn't change a lot, and consequently, we have smaller droplet size (Tsabet and Fradette 2015). It is noteworthy that the droplet size reaches equilibrium at a RPM around 1200. The bigger droplet sizes at lower RPM values are also dedicated to a lower

average turbulent energy dissipation rate and even the effect of Njs where the mineral particles are not well suspended and dispersed in the system. Thus, the coalescence rate might increase.

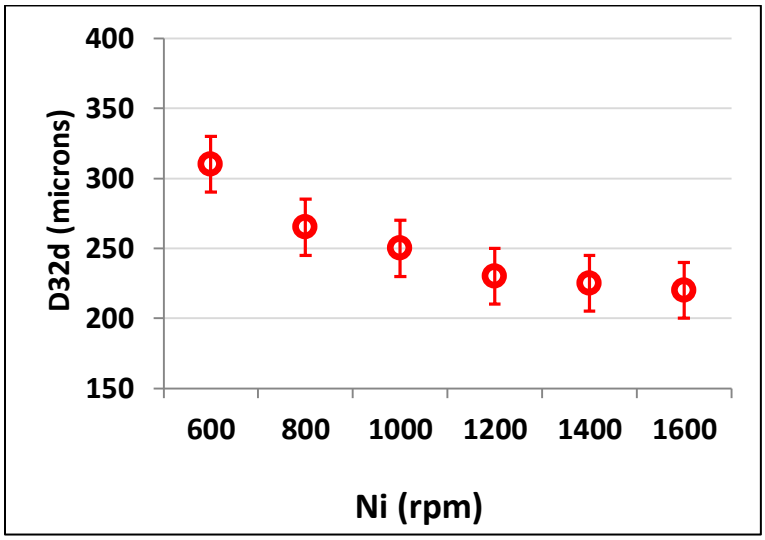

Figure 5.8 Mean droplet size (emulsion size) at different impeller speed, (Feed WSF<37, Φ_d=9%, PDMS oil 50 cSt, Ms=5%, 15minPBT@1000 rpm)

A higher inlet energy will lead to higher selectivity towards REE bearing minerals due to the effect of higher average turbulent energy dissipation rate and smaller droplet size (Figure 5.8). An maximum in REE recovery and enrichment ratio was also observed at a RPM of 1200; this explains that a higher dissipation energy reduces the global attachment efficiency but we have much reduction for those particles which has a lower contact angle or less hydrophobicity (i.e., the gangues). So the system reached globally a separation equilibrium.

Among the four stages of stabilization, the efficiencies of particle attachment and TPCL are always higher for those particles with more hydrophobicity, and this is why we see a less global efficiency of attachment for those gangues particles which have higher affinity to the water phase. Thus, the global efficiency of attachment for monazite and bastnaesite to cover interface will enhance by increasing the mixing RPM when compared with the gangues (Figure 5.9). Two different feed sizes were used whereas the head grade and liberation of the grains was a bit different and thus their ER was not similar (a better ER for WSF<-20 μm). Nonetheless, the related recoveries did vary a lot mostly due to the fact of higher mass of minerals recovered with WSF<-37 μm. Smaller particle size has bigger coverage potential, hence the generated interface will covered with fewer amount of mass particles.

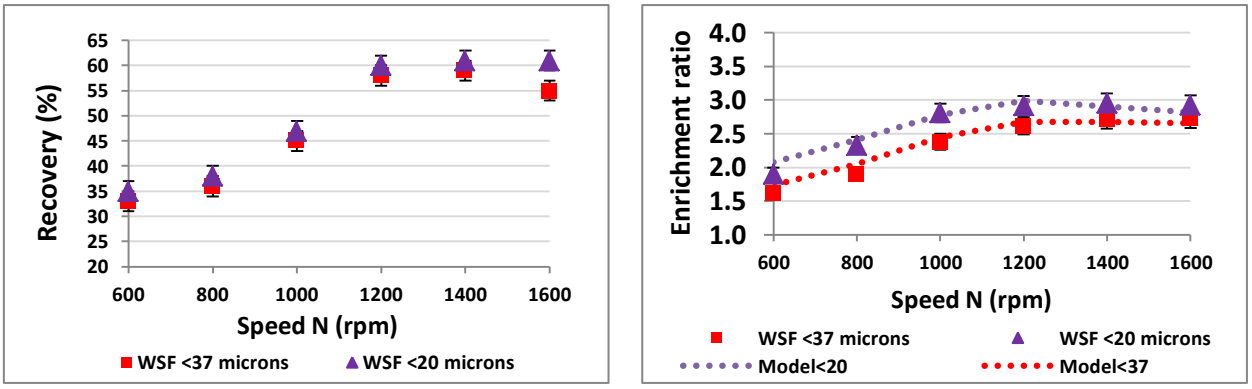

a b

Figure 5.9 a) Recovery of monazite and bastnaesite in overflow at different impeller speed,b) Enrichment ratio of monazite and bastnaesite in overflow at different impeller speed, (Feed WSF, Φ_d=9%, PDMS oil 50 cSt, Ms=5%, 15minPBT@1000 rpm)

The theoretical model (5.18) predicts interestingly the trend of enrichment ratio in the product (Figure 5.9). However, the values are quite higher than the experimental data. Furthermore, the higher mixing RPM cannot achieve higher performance due to the effect of high shear rate. It makes very small droplets which have lower selectivity along with less ability to cream at the top. The settled small droplets cannot be recovered easily and normally go to the tailings, the main reason for the lost. Also, a high shear rate can hinder the selective attachment and increase the probability of detachment which in turn decline the performance of separation. In fact, Pickering selective emulsification is a sensitive process that should be optimized between several parameters with opposite effects.

5.4.5 Effect of the shear uniformity

The impeller transfers the energy of mixing into the emulsification system by making turbulent fluid flow and shear profile. The results illustrate that the higher average turbulent energy dissipation rate, up to certain values, enhances particle attachment and has a positive effect on the selectivity (Tsabet and Fradette 2015). However, the selective attachment efficiencies which are linked to the overall probability of particle attachment can be hindered by increasing the shear rate in the system. The shear rate reaches a maximum value right in the vicinity of the impeller or at impeller zone and it is not constant everywhere in the tank. The shear rate also makes breakage or disperses oil phase. The Maxblend setup provides lower

average turbulent energy dissipation rate (Figure 5.5) in addition to a uniform and a lower shear rate compared to PBT at a similar We number (Paul, Atiemo-Obeng et al. 2004). Figure 5.10 presents emulsion size and the span, i.e. $\frac{D_{90}-D_{10}}{D_{50}}$, associated with both the Maxblend and the PBT setups at similar We numbers. The lower span values were obtained in the Maxblend setup that explains a lower average turbulent energy dissipation rate and a higher shear rate uniformity in the system. From another point of view, smaller droplets were formed in the PBT setup that was expected because a higher average turbulent energy dissipation rate was consumed to break the droplets.

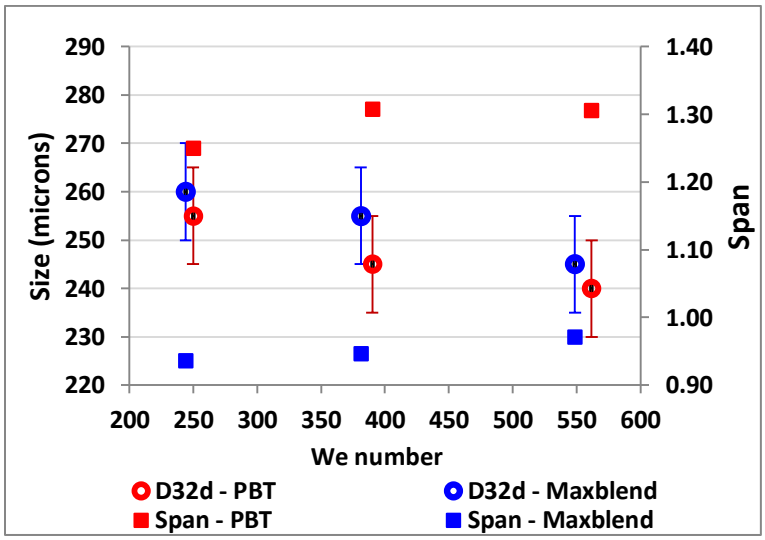

Figure 5.10 Mean droplet size (emulsion size) vs. different Weber number for both impeller types PBT and Maxblend, (Feed WSF<20, Φ_d=9%, PDMS oil 200 cSt, Ms=5%, 15min@1000 rpm)

In terms of recovery of rare earth elements, the Maxblend setup resulted a recovery almost 1.2 times more than in PBT setup at similar We numbers. With respect to observations in Figure 5.11 one may conclude that the PBT generates more small droplets that does cause less overall attachment efficiency. On the other hand, the Maxblend setup generated uniform droplet size in favor of higher REE recovery. It is evident that the enrichment ratio grows slowly by increasing RPM in Maxblend setup while it rises up faster in PBT setup. However, the enrichment ratio obtained the Maxblend setup was almost 1.3 times more than in PBT setup at similar We numbers and it achieved much more creamed droplets while the solid mass fraction and O/W ratio were the same in both setups. The results clearly indicate that while there is a same available interface versus the coverage potential in both setup (i.e., the same D32p/D32d and O/W ratio

versus mass solid), but the shear uniformity with Maxblend makes higher droplet size uniformity (lower span) and eventually provides better recovery and the grade. In other words, a high enrichment ratio is attainable at low energy consumption with Maxblend that is beneficial in term of process economy. It is noteworthy that our developed model was very consistent with experimental data, and it could favorably predict the REE recovery and enrichment ratio under different We number, feed and mixing setup. Therefore, this model is a reliable tool to predict the process performance in further investigations as well as in process scale up.

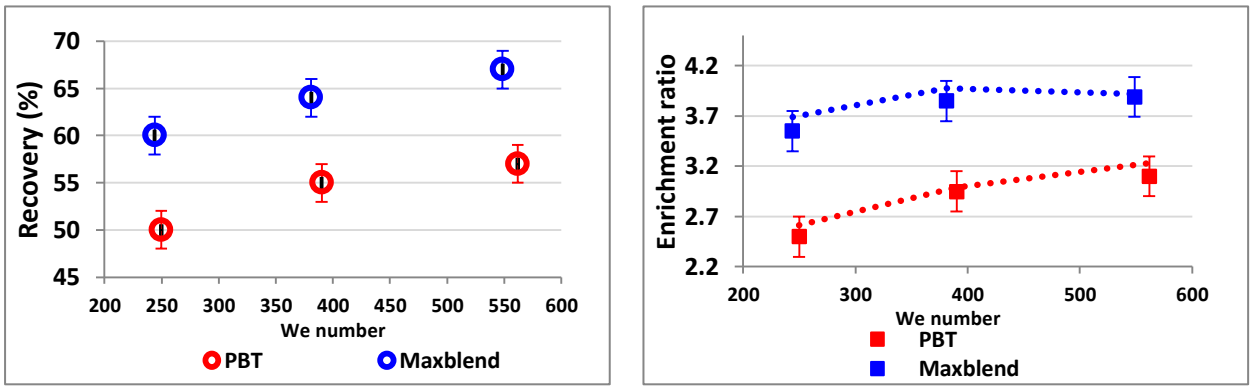

a b

Figure 5.11 a) Recovery of monazite and bastnaesite in overflow at different Weber number for both PBT and Maxblend impellers, b) Enrichment ratio of monazite and bastnaesite in overflow vs. Weber number for both PBT and Maxblend impellers, (Feed WSF<20, Φ_d=9%, PDMS oil 200 cSt, Ms=5%, 15min@1000 rpm)

5.5 Conclusion

A semi-empirical approach was used to investigate the significant effects of mixing conditions on monazite and bastnaesite beneficiation through Pickering emulsification. An existing model has been developed for REE bearing minerals to consider the global selective attachment of targeted particles into the interface. The experimental results were completely accord with trends in the model. The grade and recovery are enhanced by increasing impeller speed. Also, the setup equipped with Maxblend impeller has a higher grade and recovery when compared with PBT while we have the same Weber numbers and droplet size, a consequence of higher shear rate uniformity with Maxblend. The selectively of SSE to capture monazite and bastnaesite is improved in Maxblend setup. Recovery of monazite and bastnaesite from one stage

emulsification under the best conditions was around 65% while the grade in the products enriched up to 3.85. Hence, we propose SSE as an alternative or supplement process prior to conventional froth flotation; especially it works very well with the feed of the fresh ore without applying surfactants and pH modifications. The MD enhanced the recovery however an optimal MD of 15min was obtained. Sequential mixing orders have been tested. The oil well dispersed for a while before adding pre-wetted mineral particles and the selectivity was improved.

5.6 Acknowledgments

The authors gratefully acknowledge financial support from the Natural Sciences and Engineering Research Council of Canada and the supporting received from NIOBEC inc. The authors are also very thankful to NAA laboratory in Polytechnique Montreal for the analysis and discussion of the TREE assay evaluation.

CHAPTER 6 ARTICLE 3: PHYSICAL BENEFICIATION OF RARE EARTH BEARING MINERALS WITH PICKERING EMULSIFICATION: EFFECT OF OIL PROPERTIES, INTERFACIAL PARAMETERS AND FORMULATION

Rahi Avazpour, Mohamamd Latifi, Louis Fradette, Jamal Chaouki[3]

Department of Chemical Engineering, École Polytechnique de Montréal, c.p. 6079, Succ. Centre-ville, Montréal, Québec, H3C 3A7, Canada

(Journal of GREEN CHEMISTRY, Date submitted : 17/04/2019)

6.1 Abstract

The ability of Pickering emulsion to selectively separate and concentrate rare earth bearing minerals from their associated gangues (e.g. dolomite and calcite) in physical beneficiation is being studied versus the effect of physical properties of the phases. The results can be used to improve the performance of selective separation of the process. The reasonable recovery and grade is achieved through an improvement of the emulsion formulation and selecting appropriate oil versus water. The study investigates the effect of interfacial tension (IFT), oil polarity, mass fractions and formulation. The alternative oils with different viscosities (i.e., PDMS, oleic acid, paraffin and kerosene) plus additives (i.e., 1-hexanol 1%) to modify IFT and also another continuous phase than water (i.e. ethylene glycol) were examined. A viscosity of 200 cSt, oil to water ratio 10% and solid fine particle concentration of 5% can reach to the best selectivity results. Since PDMS oil is not economically feasible in large-scale, paraffin oil 100 cSt which is less expensive oil were tested and illustrated a better selectivity. The wet sieved feed from NIOBEC mine Quebec original ore with an abundant of bastnäsite and monazite around TREE 3.3% were used. The recovery of one stage emulsification is improved significantly by choosing paraffin oil up to 60% along with an enrichment ratio around 2.7 in the products.

[3] Correspondence concerning this article should be addressed to L. Fradette at Louis.fradette@polymtl.ca

Keywords: solid stabilized emulsification, Picketing emulsion, Rare earth elements, physical beneficiation,

6.2 Introduction

The utilization of rare earth components in numerous fields has been examined as of late in kinds of literature including the green power, strong permanent magnets, medical gadgets, and the recent innovative industries. Since REE minerals have very similar physicochemical properties comparing to their associated gangues such as dolomite and calcite, separation, and recovery of them would be difficult, costly and generally comes with unavoidable environmental impacts during conventional purification stages (Jordens, Cheng et al. 2013, Haque, Hughes et al. 2014). In the first decade of 19th century Pickering–Ramsden developed the notion of solid stabilized emulsion (SSE) by the fact of using fine solid particles to stabilize dispersed oil droplets in water. Solid particles act in many manners such as an emulsifier surfactant and more importantly are captured selectively (i.e., based on their wettability) right around the interface of droplets and make a steric barrier of particles around the oil drops to prevent unwanted coalescence (Binks 2002). Our previous works centered on the recovery of bastnaesite and monazite through Pickering selective emulsification and demonstrated the feasibility of the approach as a novel alternative method to froth flotation in physical beneficiation stage. Indeed, Pickering selective emulsification, like many other processes, it is subject to optimization and improvement. Thus we investigated the effects of feed composition, wettability, particle size distribution and mixing conditions on recovery and the grade of final products. As an important complementary, this research will be focused more particularly to improve the procedure through adjustment of oil properties, interfacial parameters and formulation (i.e., solid mass fraction, O/W ratio). Based on the former results, monazite and bastnaesite particles are more hydrophobic (Table 6.1) or have more affinity to be captured by the oil droplets when compared to the gangues (Abaka-Wood, Addai-Mensah et al. , Bulatovic 2007). Subsequently, they have competitively attached more into the oil-water interface, and the gangues remain more in the aqueous phase and will sediment after a while so that concentrates can be easily recovered with oil droplets through a transfer phase separation (Figure 6.1).

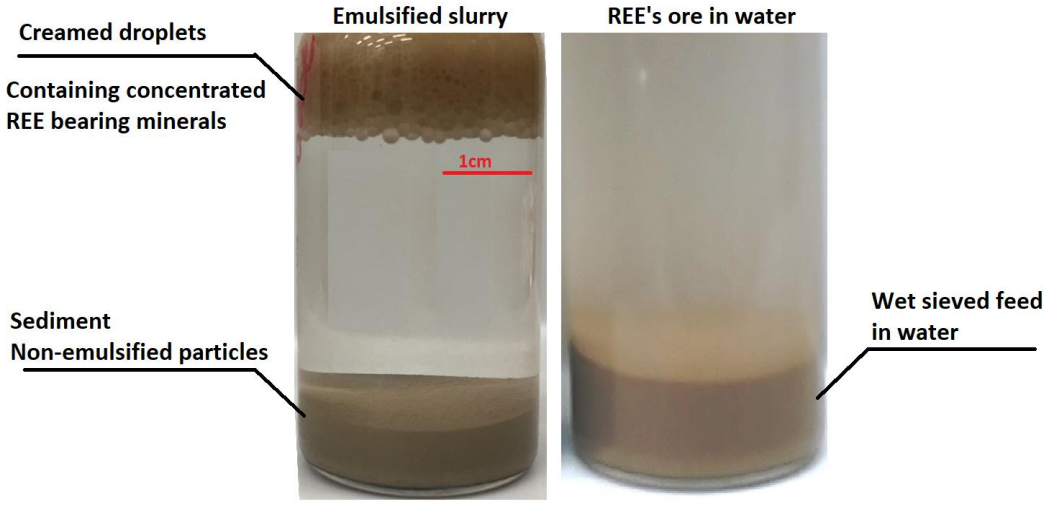

Figure 6.1 Fresh ore in water-oil slurry before and after emulsification (Ms=5%, PDMS oil Φd 9%, , PBT@1000rpm)

6.3 Materials and Methodology

6.3.1 Rare earth elements bearing ore

Niobec Inc. located in the province of Quebec in Canada provided the rare earth elements bearing ore (RBO) for this research. Bastnäsite and monazite are the rare earth elements bearing minerals (RBM) of the RBO. Bastnäsite is a carbonatite mineral of the REE whereas monazite is a phosphate mineral of REE. The RBO is associated with gangues minerals majority of which are calcite, dolomite and ankerite. It has been reported that the abundance of RBO minerals varies from one drill spot or a deposit to another.(Lafleur, Eng et al. 2012) Niobec supplied several batches of the RBO, so we mixed them all, and started the project off with the new sample. Table 6.1 presents mass fraction of the minerals of the RBO that was determined by QEMSCAN at SGS Inc. Our previous research showed that the Pickering Emulsification is more selective in favor of separation of monazite and bastnäsite when particle size distribution of the feed is close to their liberation size (i.e. less than 20 µm). In addition, we observed that applying a wet sieving process would help capture the fine particles in the lower size cut at the end of the sieving operation. Therefore, we used a feedstock with a particle size distribution of less than -37 µm after wet sieving herein after called WSF. Concentration of TREE of the WSF is about 3.3%.

6.3.2 Characterization

In this paper, we will discuss the effect of liquid phase's properties including dispersed phase (oil), continuous phase (water, ethylene glycol) and solid particles on the emulsion properties and selectivity to enhance recovery and enrichment ratio of the products (Figure 6.2)

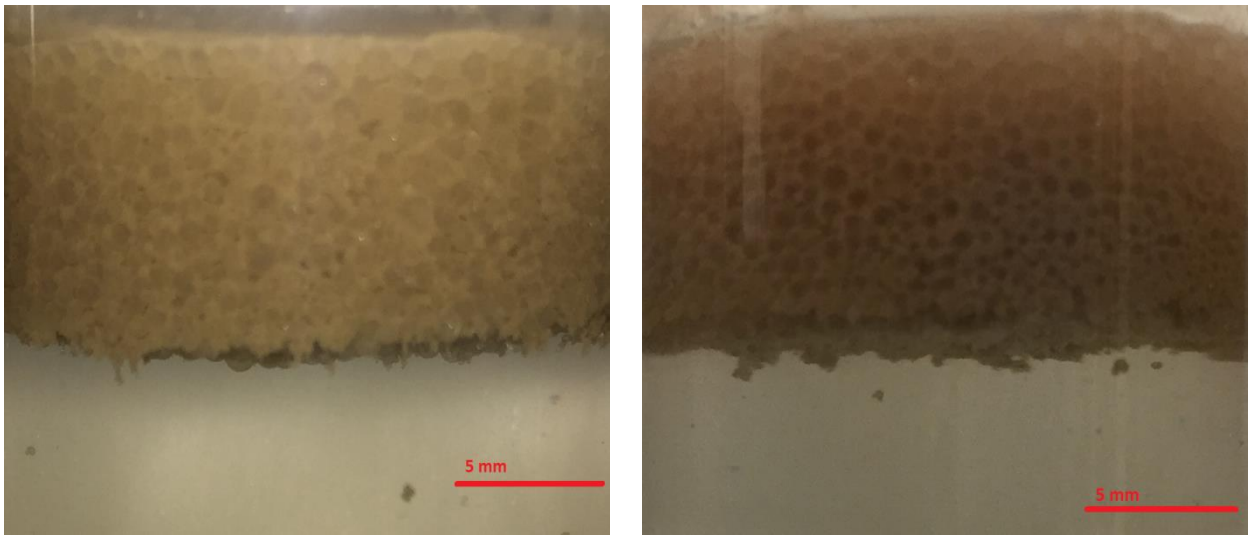

a b

Figure 6.2 The slurry of creamed droplets after emulsification of REE ore in water (Ms=5%, Φd 9%, , PBT@1000rpm) (a) PDMS 100cSt (b) paraffin oil as dispersed phases

The mineral particles that can be competitively adsorbed and stabilized into the interface should commonly be described regarding particle wettability or contact angle. However, the water or oil affinity of a surfactant is being quantified as Hydrophilic–Lipophilic Balance (HLB) number regarding their two hydrophilic-lipophilic heads. From our previous work, the Table 6.1 dedicate the higher contact angles to the REE-bearing minerals on which they are more hydrophobic and attached more into interface comparing to the most abundant gangues.

Table 6.1 The measured contact angle of bastnaesite, monazite and majority of gangue types

	Average contact angle ±4°	
	Solid-water	**Solid-oil-water**
Bastnaesite	58	60
Monazite	55	55
Dolomite	52	49
Pyrite	53	51
Calcite	51	48
Aaragonite	42	30
Mica	40	25
Hematite	37	15
Barite	41	27

Even though, the recovery and enrichment ratio of the products were interestingly declared in previous work while we applied neither pH modifications nor surfactants in the natural slurry. The preliminary results have shown that monazite and bastnäsite were captured in only one stage emulsification, while flotation involves many more stages along with various surfactants and pH adjustment agents which make the processing, more costly and detrimental to the environment (Bulatovic 2007) (Bulatovic 2010, Sprecher, Xiao et al. 2014). Nevertheless, Pickering selective emulsification under specific conditions (i.e., To be defined objective in this work) can circumvent most of the difficulties of conventional flotation (Castor and Hedrick 2006, Jordens, Cheng et al. 2013). The oil properties, interfacial tension, and formulation of emulsification including mass ratios, and particle concentration have a significant effect on the final recovery or performance of separation. Therefore, selection of an appropriate oil type along with the adjusted formulation of emulsion will be discussed hereafter to enhance the beneficiation. We will show that the oil properties significantly affect the selectivity of the process to capture targeted mineral particles during emulsification, eventually recovery and the grade. In other words, separation of monazite and bastnäsite can be improved by choosing proper oil and appropriate formulation of emulsion. The physicochemical properties of the oil, particle concentration, interfacial tension, and formulation (oil to water volume ratio) are taken into consideration.

6.3.2.1 Elemental assay analysis

The Slowpoke reactor is used to measure elemental assay of the WSF and product streams by the Neutron Activation Analysis (NAA)(M. Abdollahi Neisiania 2017). Since our samples were in solid state, the NAA was preferred over other methods such as induced couple plasma and microwave plasma that require the solid sample to undergo an upstream digestion step. The NAA was also preferred to X-ray florescence (XRF) because the latter required more than eight grams of a sample that was beyond the mass generated in our tests.

6.3.3 Dispersed phases

The dispersed phase of a solid stabilized emulsion is usually a liquid with a density lower than density of continuous phase, which is usually the water. The dynamic viscosity and the IFT are the two key parameters that impact the size and the number of the droplets in the emulsion, and consequently, performance of the separation. On the other hand, price of the dispersed phase may be a limited factor for process scale up.

Hence, several liquids such as silicone oil (i.e. polydimethylsiloxane or PDMS) from CLEARCO Inc is opted. with some different viscosities, Oleic acid oil 18:1 cis-9 from SigmaAldrich with a purity higher than 98%, light kerosene jet-A from SigmaAldrich, and heavy white paraffin oil from A&C American Chemicals Ltd. Table 5.3 provides the physical property of the oils. In two case studies, the 1-hexanol 98% from SigmaAldrich was added once to kerosene, and once to paraffin oil, each with a mass ratio of 99:1, in order to reduce IFT and investigate the significance of its effect.

6.3.4 Continuous phases

Continuous phases could be one of these liquids: Distilled water and ethylene glycol 90% (SigmaAldrich) which were used as continuous phases to investigate the effect of lower IFT and higher specific density. The surface tension of water is 72 mN/m at 25ºC. The IFTs of PDMS S100 and paraffin vs. ethylene glycol are in Table 6.3.

Table 6.2 Physical properties of liquid phases opted as dispersed or continuous phase for solid stabilized emulsification of REE bearing ore

Oil type at 25˚C	**Density (kg/m^3)**	**Viscosity (cSt)**	**Surface tension (mN/m)***	**Interfacial tension-water (mN/m)***
PDMS S1	818	1	17	39
PDMS S10	935	10	20	40
PDMS S50	960	50	21	40
PDMS S100	966	100	21	40
PDMS S200	968	200	21	40
PDMS S500	971	500	21	41
Paraffin	885	100	36	53
Paraffin+1-Hexanol 1%	885	95	33	35
Kerosene	810	1	31	50
Kerosene+1-Hexanol 1%	810	1	27	42
Oleic acid 18:1 cis-9	890	31	32	17
Ethylene Glycol 90%	1113	16	47	_

* Uncertainty ± 2%

Table 6.3 IFT of the oils versus ethylene glycol

Oil type at 25˚C	**Interfacial tension Oil- EG90 (mN/m)**
PDMS S100	33
Paraffin	23

* Uncertainty ± 2%

A tensiometer (Data Physics OCA with SCA20 software) was employed with the sessile drop technique to obtain the intermediate equilibrium water-solid contact angle of some available

gangue minerals directly on their clean and polished flat surface. The oil-water-solid contact angle of pure monazite and bastnäsite which were provided in powder form with a D_{32} size of about 20μm, was estimated from the Blake–Kozeny equation and based on a capillary rise in a capillary tube filled with the powder (Table 6.1) (Fournier, Fradette et al. 2009).

The interfacial tension at liquid-liquid interfaces was also conducted with the tensiometers (Data Physic OCA, SCA20 software) based on the pendant drop shape fast analysis (immediately after the preparation); this technique is appropriate for the liquids with significant density differences (Berry, Neeson et al. 2015). Either ionized pure water or ethylene glycol (where applicable) was initially filled in a 500 μL Hamilton syringe that had a special needle with a diameter of about 1.7 mm. The droplet of water was pendent into an oil phase in a quartz cube (40 x 40 x 30 mm) at the temperature of 25 ˚C. The measured interfacial tension at the oil and water interface or at the oil and ethylene glycol interface was within 10% of the literature data (Table 5.3) (Spelt and Neumann 1987, Hoke, Segars et al. 1990).

6.3.5 Enrichment ratio and recovery of TREE

We define the enrichment ratio as the grade of TREE of an overflow product divided by the grade of TREE of the WSF. Whereas, recovery of TREE is the fraction of TREE mass of the WSF that was recovered in the overflow product.

6.3.6 Modeling of separation efficiency

A correlation was developed based on particle attachment efficiencies approach to predict selectivity of the process (i.e. enrichment ratio). Having said that, the important parameters including oil viscosity, particle concentration (i.e. Φ_d), oil type (i.e. polarity vs. non-polarity), and interfacial tension (e.g., oil-water and oil-ethylene glycol) were taken into the consideration. Since there are excess particles in the system versus the available interface (i.e., a coverage potential larger than the generated interface) the Pickering emulsion creates a competitive attachment between the RBM and gangue particles in the system which is led to a selective separation. To investigate the selectivity, a global attachment efficiency of the RBM was compared to that of the gangues taking the wettability differences (Table 6.1) (Abaka-Wood, Addai-Mensah et al. , Zhang 2014). The global efficiency is a function of the generated interface or the final size of the oil droplet; i.e. $D32_d$. There are four main steps of particle-droplet

interaction in course of solid stabilized emulsification: 1) collision; 2) three phases contact line (TPCL) development; 3) attachment; and 4) coverage of the interface, which consists of network formation during the phenomenon of particle adsorption, and stabilization at the interface. To effectively cover droplets with the particles and end up to the stabilization, the efficiencies of each step should be applied which can be assessed by the free energy or force analysis (Tsabet 2014). The model which was developed in our latest work using the correlations can thus predict the overall selectivity. Equation 6.1 defines the global efficiency of attachment:

$$E_{global} = \frac{A_{eff}}{A_{gen}} \tag{6.1}$$

Where A_{gen} and A_{eff} are, respectively, the generated and effectively covered interfaces. The global efficiency of attachment can be written as Eq. 6.2 and 6.3 for RBM and the gangues:

$$E_{REE} = k_1 \times k_2 \times (E_{Col} \times E_{TPCL} \times E_{Att} \times E_{Cov})_{REE} \tag{6.2}$$

$$E_{Gangue} = k'_1 \times k'_2 \times (E_{Col} \times E_{TPCL} \times E_{Att} \times E_{Cov})_{Gangue} \tag{6.3}$$

Where E_{Col}, E_{TPCL}, E_{Att}, E_{Cov} are the efficiencies of, respectively, collision, three-phase contact line, attachment, and coverage. These efficiencies are calculated based on the fundamental formulas with appropriate assumptions and correction factors including the effect of sphericity (k_1), and the effect of non-liberated minerals (k_2).

In the compatible model, the selectivity is deduced based on global efficiency of attachment. The global efficiency of attachment for all attached particles can be divided into two categories for RBM and the rest of the gangues. Thus, we could write:

$$\frac{A_{eff-REE}}{A_{eff-Gangue}} = \frac{E_{glob-REE}}{E_{glob-Gangue}} = \boldsymbol{K} \times \frac{(E_{TPCL} \times E_{Att} \times E_{Cov})_{REE}}{(E_{TPCL} \times E_{Att} \times E_{Cov})_{Gangue}} = \frac{G_O}{1 - G_O} = I_{Att} \tag{6.4}$$

$$\boldsymbol{K} = \frac{k_1}{k\prime_1} \times \frac{k_2}{k\prime_2} \qquad 6.5$$

Where I_{Att} is the attachment efficiency index [Chapter 5]. It is also true that $(E_{Col})_{REE} = (E_{Col})_{Gangue}$ on which the collision efficiencies for both categories of particles were assumed similar. The shape factors, k_1, and k'_1 are the same. The best fit values for the K were found near to 0.83 in our latest experiments. However, K very depends on the specification of the feed ore such as size distribution, head grade, composition, and, etc. The values which are calculated through attachment efficiencies were compared to predict the grade of products by the model and the performance of separation measured experimentally. Thus, a semi-empirical approach would be used to predict the effect of physical properties of phases. Table 6.4 summarized the effect of main parameters on the related efficiencies.

Table 6.4 The theoretically expectation of the effect of physical properties of phases on selectivity based on the efficiencies of three stages of particle stabilization at interface

Physical properties of phases	Optimal values	Effect on efficiencies	I_{Att}	Selectivity (ER-R)
Oil viscosity (η_d) ↑	200cSt	$\downarrow E_{TPCL}, \uparrow E_{Att}, \downarrow E_{Cov}$	↑	↑-↑
O/W (Φ_d) ↑	10%	$\uparrow E_{TPCL}, \uparrow E_{Att}, \downarrow E_{Cov}$	↓	↓-↑
Particle concentration (Φ_s)↑	5%	$\downarrow E_{TPCL}, \downarrow E_{Att}, \uparrow E_{Cov}$	↑	↑-↓
IFT (γ_{ow}) ↑	50 mN/m	$\uparrow E_{TPCL}, \downarrow E_{Att}, \uparrow E_{Cov}$	↑	↑-↑

Among the physical properties of phases that affect significantly the final selectivity, the main affected property is the emulsion size or the final stabilized droplet size ($D32_d$). Based on the prediction, an increasing in droplet size will enhance the selectivity. Hereafter, a graph of attachment efficiency index as a function of droplet mean size can be deduced from the model which is, in turn, coming from wettability differences for both REE and gangues particles (Figure 6.3 is at the same operational conditions i.e. WSF<37, PDMS 100cSt-W, Φ= 9%v , PBT-1000 rpm):

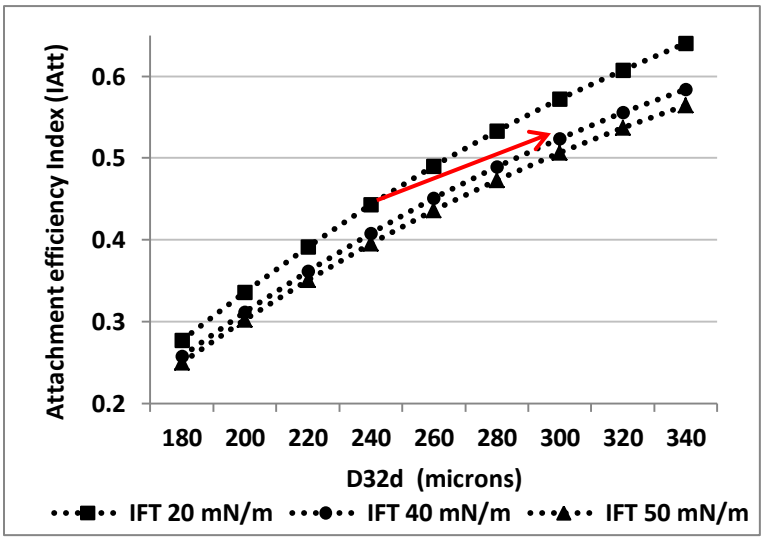

Figure 6.3 Attachment efficiency index as function of droplet mean size (Feed WSF<37 microns, Ms=5%, oil Φd 9%, PDMS (γ=20mN/m), Paraffin (γ=40mN/m) and Kerosene (γ=50mN/m), PBT@1000rpm)

It might seem that the lower IFT has a higher attachment efficiency index or selectivity. However, we should consider the effect of emulsion size at the same time which might be larger and much more uniform with higher oil-water IFT (Thus, we may see a shift like as the red arrow on Figure 6.3).

6.3.7 Experimental methods

The standard emulsification procedure is described in chapter 5 where water, oil and the WSF are mixed at 1000 rpm for 15 minutes. The other operating conditions such as setup configuration, scale, the order of mixing, resting time, sample collection and phase separation are also kept the same. We obtained the size distributions of the particles, and of the droplets as well their Sauter mean diameter (i.e. D32d) with the Mastersizer 3000 instrument.

6.4 Results and discussion

6.4.1 Surface tension and contact angle

Surface tension of each of continuous phase and dispersed phase govern oi-water contact angle and thus emulsification process.

The Young's equation (6.6) explains that the water-oil-solid contact angle (i.e. particle contact angle) is a function of the surface tensions, solid-water contact angle (assuming water is the continuous phase), and solid-oil contact angle. In Eq. 6.7, $Cos\theta_{aw} = \frac{\gamma_{sa}-\gamma_{sw}}{\gamma_{wa}}$ and $Cos\theta_{ao} = \frac{\gamma_{sa}-\gamma_{so}}{\gamma_{oa}}$; in other words, the contact angle that a solid particle forms with in the interface of two phases depends on the surface tension of the phases.

$$Cos\theta_{OW} = \frac{\gamma_{aw}Cos\theta_{aw} - \gamma_{ao}Cos\theta_{ao}}{\gamma_{wo}} \qquad 6.6$$

Our measured data of the oil-solid-air contact angle (i.e. θ_{ao}) were close to zero degree for all the oils we used in this research, so we assumed that $Cos\theta_{ao}$ was unity. Thus, we re-wrote the Young's equation in the form of 6.7 where $A = \frac{\gamma_{aw}}{\gamma_{wo}}$ and $B = \frac{-\gamma_{ao}}{\gamma_{wo}}$.

$$Cos\theta_{OW} = A.Cos\theta_{aw} + B \qquad 6.7$$

The higher θ_{aw} values will lead to a higher θ_{OW} contact angle, which is thus a higher oil-solid affinity, and reverse versa. The final contact angle has a high impact on the stability of Pickering emulsions and thus on the selectivity of the process. The higher in wettability difference will lead to higher selectivity. The effect of the limits on the upper and lower oil-water contact angle versus air-water contact angle (Eq. 6.7) is being discussed in Figure 6.4 (Binks and Clint 2002). Since all the measurement was performed at natural pH, we should notice about the effect of pH on the IFT. The basic pH of slurry is around 9 which has a reducing impact on surface energy (Danielli 1937). Since the surface tension of water does not change at basic pH, we expect that the interfacial energy of oil-water interface declined with higher pH around 9 and thus all graphs shift down a bit in the Figure 6.4 (Beattie, Djerdjev et al. 2014). In order to simplify the justification of the data on the graph with experimental results we neglect the effect of the pH on the IFT.

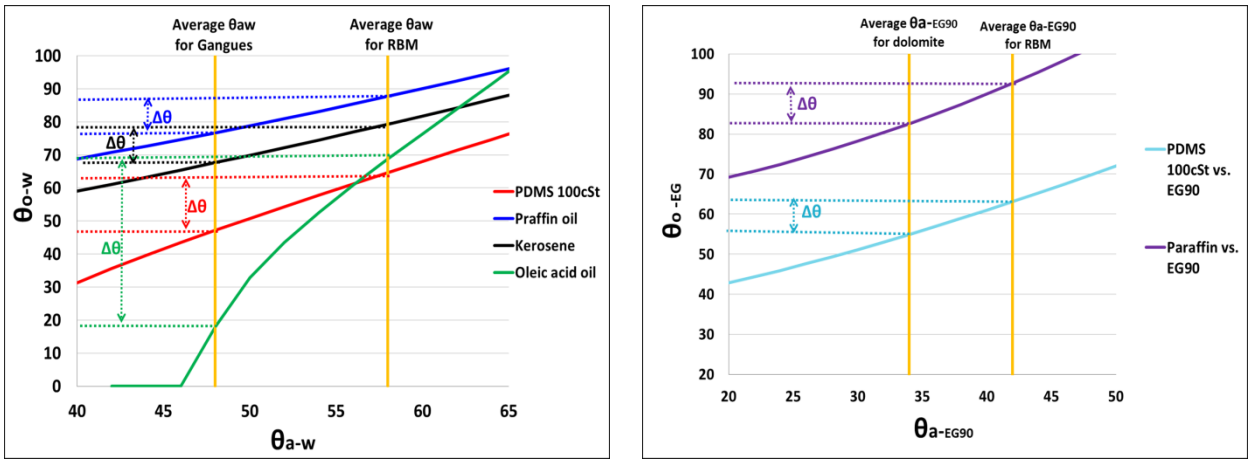

a b

Figure 6.4 The oil-water contact angle as function of air-water contact angle, the wettability differences of REE minerals and the gangues is indicated for different oils versus water at natural pH of slurry around 9 (a) and ethylene glycol EG90 (b)

Table 6.5 summarized the comparison oil-water contact angle of RBM and of the gangues that we measured for several configurations of continuous phase/dispersed phase (i.e., the wettability difference $\Delta\theta_{OW}$). The largest difference was observed in the Oleic acid/water configuration and the smallest in the PDMS 100 cSt/ethylene glycol configuration; consequently, it is expected that the highest enrichment ratio of TREO in the former, and the lowest in the latter. In other words, the greater wettability difference between $\theta_{ow,RBM}$ and $\theta_{ow,gang}$ would lead to higher selectivity of TREE. However, a larger contact angle (i.e. θ_{ow}) could provide a negative impact on the global attachment efficiency (6.7), and thus on the final TREO selectivity because of a higher level of interfacial energy needed for stabilized attachment. In other words, there should be an optimum contact angle in terms of selectivity and the global attachment efficiency.

Table 6.5 The average of contact angles and wettability differences for the systems with different oils and continuous phases.

	θ ow (RBM)	θ ow (Gangues)	Δ θ ow
PDMS 100cSt Vs. Water	65	47	17
Praffin oil Vs. Water	88	77	11
Kerosene Vs. Water	82	70	12
Oleic acid oil Vs. Water	69	18	51
PDMS 100cSt Vs. Ethylene glycol	63	55	8
Paraffin Vs. Ethylene glycol	93	83	10

In the case of EG the contact angle should be considered as θo-EG90 as it mentioned in the Figure 6.4.

6.4.2 The effect of oil viscosity

The viscosity of the oil is an extremely important parameter in all Pickering emulsification processes such as the case of RBM beneficiation. We employed PDMS oil with different viscosities (Table 5.3) to investigate the impact of viscosity on recovery of RBM and enrichment ratio of TREE. We assumed that the minor differences of density and surface tension do not affect the separation performance. The RBM recovery and the TREE enrichment ratio increased with a rise viscosity of the PDMS oil (Figure 6.7a). The TREE enrichment ratio spiked higher than the RBM recovery though in the logarithmic scale. This should imply that ER is more sensitive to the viscosity changing. It is wroth noting that our model based on the global attachment efficiency index was quite in a good agreement with the experimental data (Table 6.4, Figure 6.3 and Figure 6.7b). That is, the beneficiation process follows the governing stabilization phenomena involved in the course of Pickering emulsification. The minor differences in R^2 values could be due to either error of measurements of NAA, heterogeneity of the RBO, or the inherent assumptions in the attachment efficiency correlations (Eq. 6.4). It is also evident from Figure 6.4b that the selectivity will be enhanced by increasing the oil viscosity mostly due to the fact that the emulsion size enlarge with the higher capillary number or number of viscosity (Tsabet and Fradette 2015). The bigger droplets have more tendencies to capture particles whereas the attachment efficiency index will be improved by using viscose oils. Taking to account that the higher viscosity itself has a negative impact on the effective attachment of a single particle, however, it provides a positive effect on the competitive attachment of RBM when compared with their associated gangues in the emulsification system. Neglecting the impact

of the lowest viscosity, our separation index model was also in good agreement with the experimental data of average size of droplets $(\text{i.e. } D_{32} = \frac{6V_d}{A_{gen}})$ and the size span of the oil droplet (i.e. $\frac{D_{90}-D_{10}}{D_{50}}$) . However, a wider span itself cannot improve selectivity due to the less uniformity, but the larger droplet to about 25% with viscose oils significantly enhances selectivity.

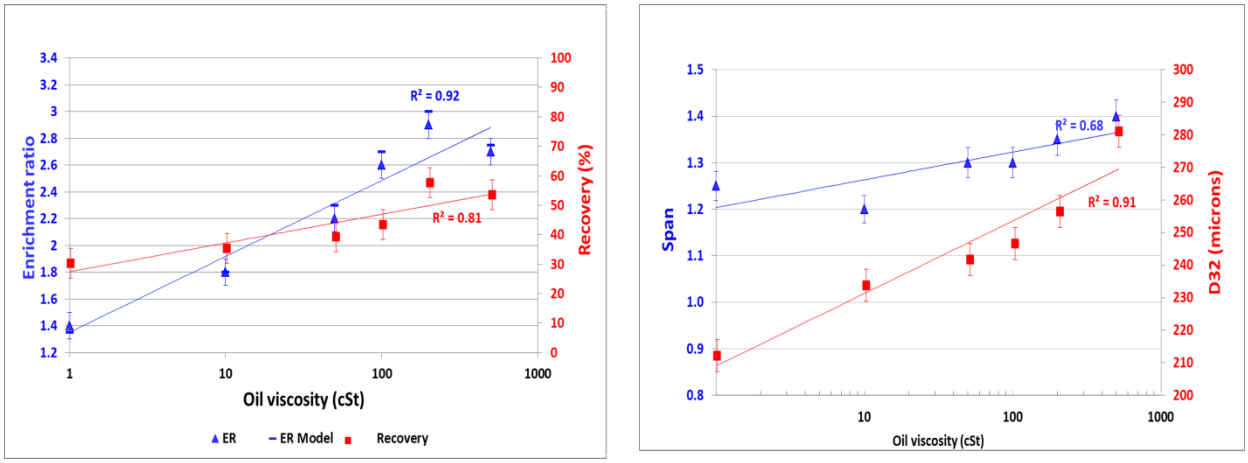

a b

Figure 6.5 (a) The recovery and the grade of products (i.e. overflow) and (b) the emulsion droplet size and span as a function of oil viscosity (Ms=5%, PDMS oil $\Phi_d = 9\%$, PBT@1000rpm)

6.4.3 The effect of oil/water ratio

The amount of available oil-water interface is an important physical property of phase on which the targeted particles will compete with the unwanted particles to attach at the stabilized position. If oil to water ratio increases, in fact, we will lose the selectivity by increasing the generated interface and opening extra space at the interface for both RBM and the gangues. Also, we observed that an adequately low amount of oil makes smaller emulsion size (Binks and Whitby 2004) which is, in turn, has a negative impact on the attachment efficiency index, thus leading to a decrease in the ultimate recovery. Having said that, the amount of oil-water ratio should be adjusted and optimized well to make a competitive attachment of particles and improve selectivity (i.e., both recovery and grade). The optimal amount of o/w was found by both the

model and the experiment data something around 10% for $\Phi_d = \frac{V_d}{V_c+V_d}$ right near the intersection point on the graph (Figure 6.6).

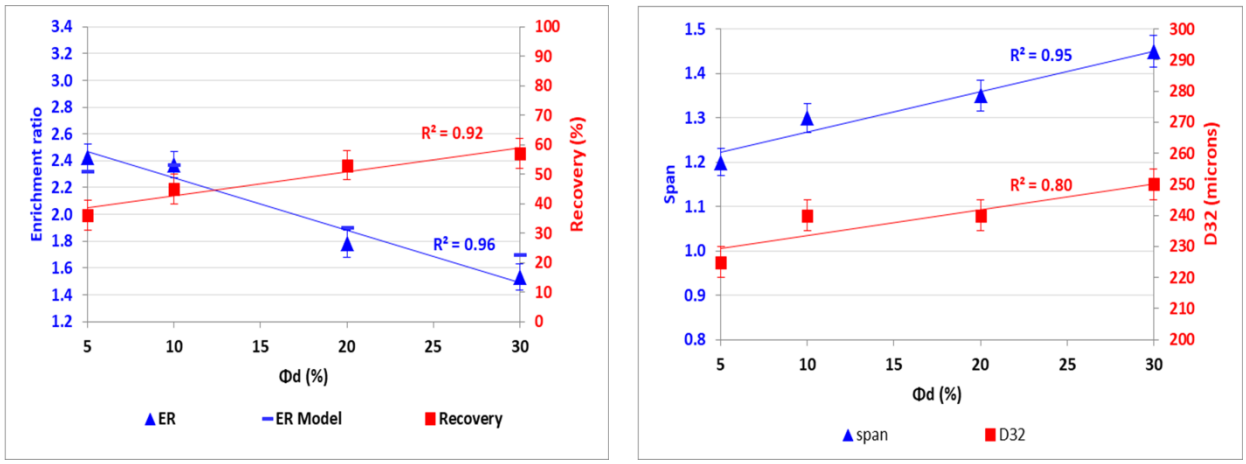

a b

Figure 6.6 (a) The effect of oil to water ratio on selectivity and (b) the emulsion droplet size or generated interface (Ms=5%, PDMS oil 50 cSt , PBT@1000 rpm)

6.4.4 The effect of particles concentration

The number of particles in the suspension also has a significant effect on the final recovery. It is obvious and observed that adding more feed mass ratio in the system will improve the grade of the product mostly due to the fact that the extra particles lead to higher coverage efficiency. In other word, the interaction frequency of particle-droplet significantly increases in the system. However, the emulsion droplet size will be decreased slightly, mostly due to reducing the coalescence rate and a faster reaching to the equilibrium covered and stabilized interface in the system which in turn has a positive effect on the attachment efficiency index (i.e., selectivity) and a negative effect on the final mass recovery. Thus, increasing the particle concentration or feed mass ratio would not be a good idea to improve the process beneficiation (Binks 2002).

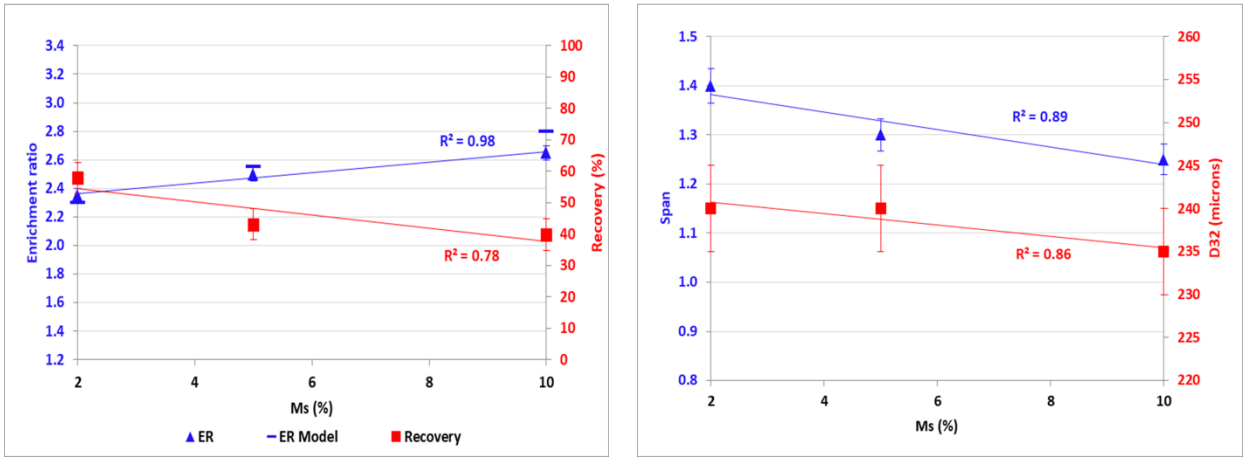

a b

Figure 6.7 (a) The effect of particle concentration on selectivity and (b) the emulsion droplet size (WSF<37, PDMS 50cSt-W, Φ_d = 9% , PBT@1000 rpm)

6.4.5 The effect of interfacial tension and oil polarity

Interfacial tension and polarity of the oil are two sides of the same coin. A polar oil contains heteroatoms in one side with differential electronegativity between the two bonded atoms (e.g., oxygen) vs. single bonded atoms (e.g., hydrogen) which results from a dipole molecular structure as we have in common polar oils such as fatty alcohols, esters, and triglycerides. To consider the effect of polarity, oleic acid oil was compared with PDMS at similar viscosity range and operating conditions. Regarding Table 6.5, oleic acid oil has a better wettability difference, but a lower IFT (Table 5.3). We should also consider the polarity effect versus surface charges of the minerals in the aqueous system. The results show that the polar oil like as oleic acid has achieved much lower recovery and grade. Thus, polar oils might not be a good option to do selective emulsification toward recovery of RBM (Table 6.6).

Table 6.6 The rare earth minerals recovery and grade of products after emulsification with polar oil vs. non-polar oil and size of the emulsion

	Enrichment ratio		**Recovery**	**D32**	**Span**
WSF<37, Φ= 9%v , PBT-1000 rpm, Ms=5%	Model	NAA ±5%	±5%	μm± 3%	±0.1
PDMS 50cSt-Water	2.3	2.2	42	240	1.4
Oleic acid oil-Water	1.45	1.3	29	200	1.5

The polar oils have much lower IFT versus water compared to the non-polar oils (El-Mahrab-Robert, Rosilio et al. 2008). In general, stabilization of the Pickering emulsification with polar oils requires more emulsifying particles mostly due to the smaller droplet size. Indeed, the polar oils result in a larger generated interface compared to non-polar oils at the similar operating conditions. There are interfered interactions with the polar oils and the surface charges (double layer) of the mineral particles in aqueous-ionic phase compared to the nonpolar oils such as mineral oils (Danov and Kralchevsky 2006). This last rises up the effect of electrostatic forces vs. van der Waals forces or capillary forces to be more pronounced. Thus, the selectivity of the emulsification process of minerals slurry might be affected more by their surface charges than wettability, a high tendency to capture surface charged of minerals including gangues which has a negative impact on the final selectivity, a disadvantage of polar oils. Also, a lower IFT would lead to higher attachment efficiency, and a lower coverage and contact line expansion efficiencies. In the other side, the lower IFT of polar oils makes smaller emulsion droplet size and larger available interface on which we lose the selectivity.

6.4.6 PDMS 100cSt vs. paraffin

The non-polar oils (i.e., Paraffin-PDMS and kerosene-PDMS) also compared with different IFT at respectively two viscosity ranges (i.e., 100 cSt and 1 cSt). The emulsion made with paraffin oil which has lower IFT versus water shows a better selectivity compared to PDMS oil 100 cSt. We also added 1% 1-hexanol to paraffin oil in order to reduce IFT (Table 5.3). As a benefit of 1-hexanol, it works as a polar agent with high solubility in both paraffin and kerosene, and act as oil surfactant or IFT modifier. The experimental results prove the negative impact of lower IFT on the performance of separation at the same operational conditions (Table 6.7).

Table 6.7 The recovery and grade of rare earth minerals in the overflow (products) and the size of droplets after emulsification with paraffin and PDMS oil 100cSt

	Enrichment ratio		**Recovery**	**D32**	**Span**
WSF<37, Φ= 9%v , PBT-1000 rpm, Ms=5%	Model	NAA ±5%	±5%	μm± 3%	±0.1
PDMS 100cSt-Water	2.7	2.6	45	245	1.3
Paraffin-Water	2.8	2.7	56	240	1.2
Paraffin-1-Hexanol 1%-Water	2.45	2.4	50	225	1.2

6.4.7 PDMS 1cSt vs. Kerosene

The same orientation was achieved with the emulsion used kerosene as dispersed phase whereas it has higher IFT and in the same manner a better selectivity than the emulsion used PDMS oil 1cSt (Figure 6.8 and Table 6.8). Again, the modified kerosene with 1-hexanol to a lower IFT, does not show any improvement in recovery and grade, a consequent of smaller droplet mean size.

Table 6.8 The recovery and grade of rare earth minerals in the overflow (products) and the size of droplets after emulsification with kerosene and PDMS oil 1cSt

	Enrichment ratio		**Recovery**	**D32**	**Span**
WSF<37, Φ= 9%v , PBT-1000 rpm, Ms=5%	Model	NAA ±5%	±5%	μm± 3%	±0.1
PDMS 1cSt-Water	1.35	1.4	32	210	1.3
Kerosene-Water	1.55	1.5	31	215	1.2
Kerosene-1-Hexanol 1%-Water	1.35	1.4	29	210	1.3

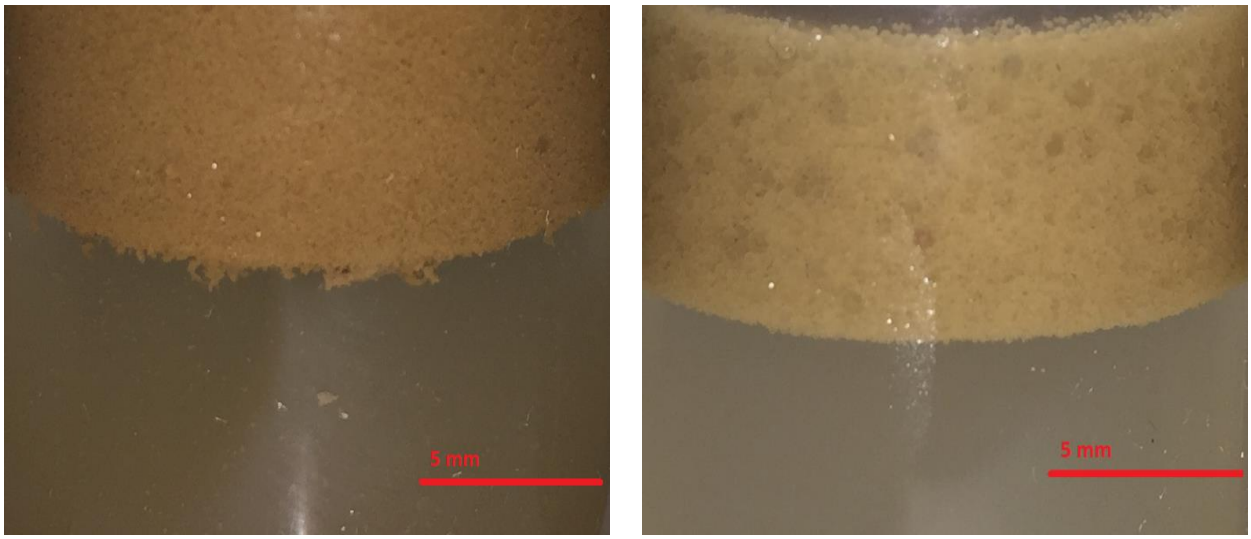

a b

Figure 6.8 Droplets shape cluster uniformity and aggregation after emulsification with different dispersed phases (Ms=5%, Φd 9%, , PBT@1000rpm) (a) kerosene and (b) PDMS 1cSt

6.4.8 Water vs. EG90 as continuous phase

The mechanisms of particle attachment into the interface are mostly related to the oil–water interfacial tension and the contact angle at the particles stabilized position. Then, both parameters should be taken into consideration together to demonstrate their effects on the competitive attachment of the REE minerals vs. gangue particles at the interface (Pichot, Spyropoulos et al. 2012). We performed some experiments with ethylene glycol 90% as the continuous phase. By using EG90 instead of water, the contact angles vary to higher values, although, the wettability differences and oil-EG90 IFT reduce significantly (Table 6.3 and Figure 6.4). In another side, it should be noted that there are many parameters particularly affect the contact angle and IFT such as temperature, aging, salinity (the effect of double layer formation of free ions in the bulk aqueous system around the particle), but we assumed that they were not varied in this research. (Pichot, Spyropoulos et al. 2012). The results indicate that the higher IFT along with lower contact angles but higher wettability differences (Table 6.5 and Figure 6.4) can make a better selective separation of REE minerals from the ore mostly due to their effect on final droplet size and improvement of global attachment efficiency of REE minerals vs. the gangues. On the other

hand, water as a continuous phase is still working better than EG90 (Table 6.9) for both paraffin and PDMS 100cSt as dispersed phases.

Table 6.9 The recovery and grade of rare earth minerals in the overflow (products) and the size of droplets after emulsification with paraffin and PDMS oil 100cSt as dispersed phase versus water or ethylene glycol as continuous phase

	Enrichment ratio		**Recovery**	**D32**	**Span**
WSF<37, Φ= 9%v , PBT-1000 rpm, Ms=5%	Model	NAA ±5%	±5%	μm± 3%	±0.1
PDMS 100cSt-Water	2.70	2.6	45	245	1.3
PDMS 100cSt-Ethylene glycol	2.05	2.1	39	190	1.2
Paraffin-Water	2.8	2.7	56	240	1.1
Paraffin-Ethylene glycol	1.95	2.0	38	180	1.3
Oleic acid oil-Water	1.45	1.3	29	200	1.4
Oleic acid oil-Ethylene glycol	1.35	1.2	34	170	1.4

By applying various physical properties of the phases under similar operating conditions for a given feedstock, different grade of products or enrichment ratio were achieved. Figure 6.9 depicts variety of colors in the products (overflow) after emulsification with different dispersed phases.

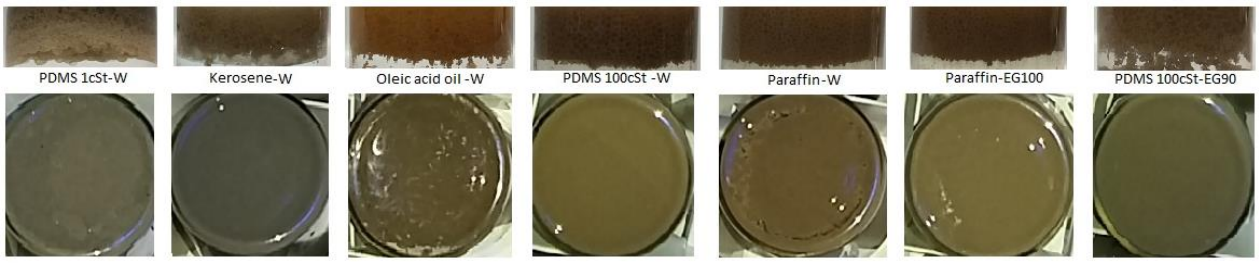

Figure 6.9 Variety of colors in the products (overflow) after emulsification with different liquid phases which consists of concentrated REE bearing minerals

This work, in turn, indicates the effects of IFT, oil properties and formulation of emulsification on the final selective particle attachment. The best recovery and the grade were obtained with paraffin oil and water.

6.5 Conclusion

The competitive attachment of REE-bearing minerals and gangues at the oil/water interface was investigated at same process conditions and different physical properties of the phases. The effects of physical properties of the phases on the improvement of selective separation of REE minerals were investigated. The selectivity of the process was shown to depend on oil viscosity, oil to water ratio, particle concentration, and interfacial tension. Viscose oils have better selectivity due to the larger droplet sizes and better attachment efficiency. The probability of REE minerals attachment at the interface increases with the larger droplets which results in a selective interface coverage and restrain space for the gangue particles to be attached. In opposite, by decreasing the available interface generated, the competition between the REE-bearing particles and the rest of the gangues to attach at the interface becomes much more meaningful. Thus, a lower O/W ratio makes a better competitive attachment, coverage efficiency and so a better final enrichment ratio of products. By increasing particle solid mass ratio, we can have better enrichment ratio; however, it is evident that the ultimate recovery would be lower. The polarity of oil can be represented as its very low IFT in the system. The final selectivity with the polar oil is also dictated by the surface properties of particles affected by ionic exchange in the aqueous phase. Pure oleic acid oil shows lower selectivity due to both smaller emulsion size and effect of polarity. The lower interfacial tension makes a better attachment efficiency which also seems to be the reason for applying IFT modification during the flotation process (e.g., surfactants, frothers). However, it shows reverse results on the selectivity of SSE mostly due to the effect of emulsion size. The higher IFT makes a larger and much more uniform droplet size which might seriously enhance the final recovery of REE-bearing mineral particles. 1-hexanol 1% was added into paraffin oil and kerosene which tends to keep the interfacial tension lower when compared to the pure oil systems. The results also indicate that selectivity is then restrained with the modified IFT. Same results induced by the use of ethylene glycol as a continuous phase instead of water due to the effect of lower IFT. However, there were contrary results regarding the contact angle and wettability differences of REE minerals and the gangues (i.e., the difference between contact

angles). Regardless of the contact angle, the final recovery and the grade was proved to be dictated to both IFT and wettability differences. More specifically, the selectivity of the process can be strongly improved by using the appropriate amount of solid particle mass ratio behind viscose oil which has higher IFT versus aqueous system. ACKNOWLEDGMENTS

The authors gratefully acknowledge financial support from the Natural Sciences and Engineering

Research Council of Canada and the supporting received from NIOBEC inc. The authors are also very thankful to NAA laboratory in Polytechnique Montreal for the analysis and discussion of the TREE assay evaluation.

6.6 Acknowledgments

The authors gratefully acknowledge financial support from the Natural Sciences and Engineering Research Council of Canada and the supporting received from NIOBEC inc. The authors are also very thankful to NAA laboratory in Polytechnique Montreal for the analysis and discussion of the TREE assay evaluation.

CHAPTER 7 TECHNO-ECONOMIC EVALUATION OF THE RECOVERY OF RARE EARTH BEARING MINERALS BY PICKERING SELECTIVE EMULSIFICATION VS. FROTH FLOTATION

The potential substitutes for less expensive crucial REE metals are highly unlikely or almost not exist either now or in the future. Beneficiation of REE is a crucial field in the new world, unexpectedly given the fact that we saw uncertainties of supply originally from China, and the world's economies are growing increasingly, related to the green, efficient, and high-tech applications. Whether or not, REE will get a remarkable price which should not be shoved wisely only by China. Whereas, the industry has an enormous irreversible environmental impact that would not easily be compensated. China's share of the light and heavy REE global market is about 87% and 99% respectively. The rest, initially comprising LREE, is produced in the U.S. and Australia. In another side, recycling of REE is less than 1%; hence, the majority of continuing supply in the midterm must exploit from mining. Regarding the recent environmental challenges, we should find the ways that the beneficiation of REE would be efficient, cost-effective, and environmentally friendly or in one-word sustainable as much as possible. Regrettably, in the real case, all stages from mining to beneficiation, and purification of REE which are carried out in China, generates tremendous tonnes of waste and tailing ponds whereas environmental restrictions either are not legislated or are weakly heeded (Izatt, McKenzie et al. 2016).

Notwithstanding, the other countries, fortunately, Canada is recently attempting to find or develop new resources of REE, the industry requires innovative and sustainable approaches to produce high quality of REE; inexpensive processes with reasonable outcomes with the minimum water/energy consumption, tailing disposal including effluents of surfactants, and acidic-basic chemical reagents. Our previous researchs centered on the recovery of bastnaesite and monazite through Pickering emulsification process and more particularly to improve the procedure regarding to mineral properties and formulations. We introduced and demonstrated the feasibility of the approach as a novel alternative method to froth flotation (FF) in physical beneficiation

stage while we investigated the effects of feed composition, particle size distribution and mixing conditions on recovery and the grade of final products. Since REE minerals have very similar physicochemical properties comparing to their associated gangues such as dolomite and calcite, separation, and recovery of them would be difficult, costly and generally comes with unavoidable environmental impacts during conventional purification stages. This fact is mostly the reason that Lanthanides are named as rare and not because of their abundant (Jordens, Cheng et al. 2013, Haque, Hughes et al. 2014). In first decade of 19th century Pickering–Ramsden developed the notion of solid stabilized emulsion (SSE) by the fact of using solid fine particles to stabilize dispersed oil droplets in water. Solid particles act in many manners like as emulsifier or surfactants right around interface of droplets and make a steric particles barrier around the oil drops to prevent unwanted coalescence (Binks 2002). Based on the former results, monazite and bastnaesite particles are more hydrophobic or have more affinity to be captured by the oil droplets when compared to the gangues (Abaka-Wood, Addai-Mensah et al. , Bulatovic 2007). Subsequently, they have competitively attached more into the oil-water interface and the gangues remain more in aqueous phase and will sediment after a while, so concentrates can be easily recover with oil droplets through a transfer phase separation.

In our latest works, we introduced the employment of Pickering emulsification or SSE for physical beneficiation of REE-bearing minerals. The demonstration of the feasibility of deployment of this new technic at a pilot or an industrial scale very depends on an authentic techno-economic analysis. However, the final cost of each individual element per kg REO should be normalized for the processes which are right before thermo-chemical treatments (i.e., form extraction to physical beneficiation) on which the TREO go to the upstream process. In another side, the final cost should be compared with the legal production price despite illegal market on which minimum standards will not be taken into the consideration, especially regarding environmental challenges and obviously does not come as a hidden cost into the final cost. Addressing that, the chapter focuses on the ease and economics of scale-up to the commercial implementation of this newly applied technology comparing to the conventional physical beneficiation (i.e., froth flotation “FF”) with the same size. However, we reserve the advantages of SSE when compared with magnetic, gravitational, and electrostatic physical separation methods which are out of the scope of this work only to the applicable feeding tonnage which is much higher for both SSE and FF. Our intention is to separate rare earth bearing minerals mostly

including monazite and bastnaesite at the enrichment ratio (ER) level of 3 to 4 times higher than the feed (i.e., the ratio of TREE%). The recovery (R) is accomplished with a mass ratio of products over the feed multiple by ER. Surpassing purities is achievable by applying additional stages. However, in this paper, the objective is just to get the enrichment ratio near to the one that practices FF with the same feed rate (tonnage) and specification. We take entire the process and subprocesses from feed to the final outlet at the same ER&R to evaluate the techno-economic aspects for the approach. Our previous works represent quantitatively the ER up to 3.5 and R around 60% for both SEE and FF with the same feeding conditions. In comparing OPEX and CAPEX for an alternative technology, such as SSE, with conventional technology, such as FF, many factors must be taken into consideration. For sure, some of these factors are not possible to be evaluated simply in generally quoted OPEX assessments (e.g., the cost of the required environmental treatment proceeding with the pollutants and effluents associated with the conventional process, long-term energy, and water consumption). About apply a process, an LCA can also help to assess the additional cost of the true and complex impacts and normalized over a unit mass of TREE in products. Nevertheless, that these costs are sometimes very crucial and can overwhelm the costs associated with the new alternative technique comparing to the conventional physical beneficiation of the REE (i.e., SSE vs.FF), but such this investigation is out of our scope for now. To elucidate the point, we need to focus on the main possible contributors to the expenses of both alternative SSE and FF that are comprehensive and not wholly, accounted in standard assessments of OPEX –regardless of evaluating the environmental extra huge costs. In the SSE, as opposed to FF, waste generation is minimal, so the environmental costs from this processing stage are also much lower. In FF, wastewater, effluent generation contaminated with surfactants and chemical reagents are enormous when compared with SSE which has water and oil recycling circuit without using a drop of pH conditioner and/or surfactants, however, these substantial externality costs with extensive destructive consequences to the environment and human health, is not included in the cost inventory in this work. These costs are not simple to be determined with enough accuracy, but they are socially crucial and real. E.g., from the literature (Yang, Lin et al. 2013), the REE mining in the South China Ganzhou's region has disposed 191 million tons of tailings and destroyed forests areas increasingly from 23 km^2 in the year 2000 to 153 km^2 in 2010 based on an available satellite image while the reclamation for sites was evaluated at the approximately U.S. $ 5.8 billion regardless of other environmental detriments

and human health factors. It is obvious that these costs of using conventional FF are mainly not incorporated in the common asserted OPEX of producing a unit mass of concentrated REE ore and it is remarkably smaller in this regard by applying alternative SSE. Having said that, we have only considered the sectors of preliminary materials, energy consumption in OPEX, and the required equipment in CAPEX.

The output of the physical beneficiation process is priceless due to the required further purification process and separation of individual metals, and we assume an average up to date price per kg ore of the final grade (i.e., TREE%) based on the NIOBEC fresh ore specification and the feed inlet tonnage. By doing so, we can evaluate the CAPEX and its amortization period considering the overall recovery rate of the process. The overhead expenses including buildings, site development, and auxiliaries are not taken into account, because we assume respectively the same portion of CAPEX and OPEX for both processes. The other surcharge costs such as inherent risks, metal inventory, the variation of the feed and impurities, and the labor cost (i.e., expertise working hours cost) have been delicately estimated the same for in the final cost per kg concentrated ore TREO%. However, we should mention that one of the principles of sustainable chemical processing is to avoid as possible the use of chemical reagents. The use of pH conditioner and surfactants not only requires higher of CAPEX and OPEX but it intrinsically ends up to an additional cost of the risks of the environment, human health, and exposes workers. These expenditures increase again when, in addition to the use of chemical reagents, the FF process is not perfectly selective. As a result, dealing with these chemical agents in subsequent steps, where the waste and tailing are being treated to disposal, can have a significant impact on OPEX and CAPEX. Furthermore, if these are not separated from the effluent in the initial beneficiation stage, they are finally discharged downstream into the environment which makes severe environmental and human health issues.

On the other hand, FF is an inefficient process with low performance and selectivity while we did not consider all these surcharges to compare conventional FF with its new alternative. However, SSE attains comparable performance of separation with fewer stages (i.e., two stages) without using any chemical reagents. As we have pointed out, SSE recovers monazite and bastnaesite with faster throughput and much fainter environmental footprints along with minimum tailing and waste generation (Yang, Lin et al. 2013, Van Gosen, Verplanck et al. 2014).

Towards elegant REE minerals beneficiation breakthrough

In the case of SSE, the performance of separation (selectivity) and recycling of carrier mediums (i.e., oil and water) are both crucial advantages. The key point is to separate the entire set of REE-bearing minerals (i.e., monazite and bastnaesite) from their associated gangues as fast and simply as possible while the oil and water is being recycled into the process. In the novel method, the concentrated ore is produced from the fresh ore by improvement of TREE% (comparable to the conventional FF). By the gangues removal at the early stage of beneficiation, the remaining concentrated ore is then getting ready for the further selective separation of each individual REE metals into the downstream process. Through the SSE process, it successfully generates a high grade of REE-bearing concentrates, early in the processing circuit and absolutely free of chemical reagents and surfactants. Excellent ER of 3.5 was achieved by separating the rest of gangues. This performance highlighted a prominent advantage of SSE over traditional FF; the ability to remove the majority of nuisance gangues at two stages of emulsification, while recovering basically most of the monazite and bastnaesite at an overall recovery of 65%. The economics advantages benchmark from this fulfillment can be clarified when compared with the relatively same R&ER rates of conventional FF. Using this critical techno-economic analysis, we will show the advantages of SSE within the metallurgy community that had spread proven difficulties with FF: The recovery of the REE-bearing minerals without the aid of surfactants and chemical reagents potentially expensive and destructive to the environment. Successful completion of the project was stated in our release of the previous papers. The chapter represented the separation of monazite and bastnaesite through Pickering selective emulsification. By rising attention to the production of REE in the investment sector in recent years, numerous techniques have been suggested for the physical beneficiation of the individual minerals. Notably, farther of the separations latterly achieved by SSE, to our consciousness, there has been no indication that any of these approaches have perfectly recovered the REE-bearing minerals at their natural surface in the aqueous phase. Particularly, we should mention that a single stage of FF generally operates at low selectivity. Hence, it has constitutionally required of multiple separation stages and conditioning stages to produce high performance.

Beyond the apparent gains of selectivity, SSE is outstanding for a plainness of its process structure and easiness of application which comes with a remarkable discount in CAPEX, OPEX, processing rate, and environmental footprint. This increased performance follows from the high REE-bearing minerals selectivity to reduced environmental hidden costs comparable to conventional FF. Since fewer separation stages are required and effluent generation is minimized and no surfactants and chemical reagents are employed.

Hence, we do not need reclamation and eventually disposal of hazardous tailing processes. Moreover, the capacity of the SSE process to concentrate monazite and bastnaesite at the desired level of separation significantly humbles Th and its radioactivity issues. Notwithstanding, our mid-term goal is to clear the pathway for the design of a pilot plant to further proof of the application of SSE at process scale.

In the recovery of the rare earth elements, further downstream processing would be affected by upstream process as with many purifying processes. In another word, the downstream production of rare earth elements can be substantially more or less expensive depends on upstream process such as communion processes (i.e., size reduction and classification) and physical beneficiation (e.g., SEE or FF). Thus, we take most commercially relevant and uniform (e.g., particle size, head grade, tonnage of feed ore) options into consideration to compare the economic advantages of SSE vs. FF in a case study. Physical beneficiation of bastnaesite and monazite through SSE requires solid–liquid separation stages. Solid mineral particles can be separated from the liquid phases (i.e., oil and water) firstly by gravity sedimentation followed by centrifugation process accompanied with recycling circuits. A rotary mixer and agitation tank is suitable for batch processing, but for a massive amount of mineral in a continuous stream, we could design a circuit equipped with static mixer. In the economic cases study in pilot scale, the wet sieved feed of ore with constant grade about 3.3% TREO is used in both FF and SSE processing and it is about 7% TREO in the products, an acceptable enrichment ratio of 4 in a single stage recovery. The overall SSE processing consists of one stage emulsification and centrifugation vs. the overall FF processing consists of one stage conditioning (i.e., pH modification) and cleaning. Demulsification performed by centrifugal force around 2000g. The oil and water are separated after the demulsification process and can be recycled around 99% with less than 1% overall lost. The processes flow for SSE and FF are illustrated in the Figure 7.1 and Figure 7.2 respectively. The amount of recovery which is determined as separation

efficiency or separation performance is also above 75% for both approaches. These values for SSE have been examined and validated by an analytical protocol using Neutron activation elemental analysis (NAA) at laboratory scale and for FF have been deducted from literatures (Bulatovic 2010, Jordens, Cheng et al. 2013, Xia, Hart et al. 2014, Liu, Wang et al. 2016). The OPEX, CAPEX and total energy consumption of overall SSE processes including emulsification and demulsification at pilot scale is calculated based on laboratory scale results and for overall FF processes including conditioning and cleaning is based on available information and the related industrial documents.

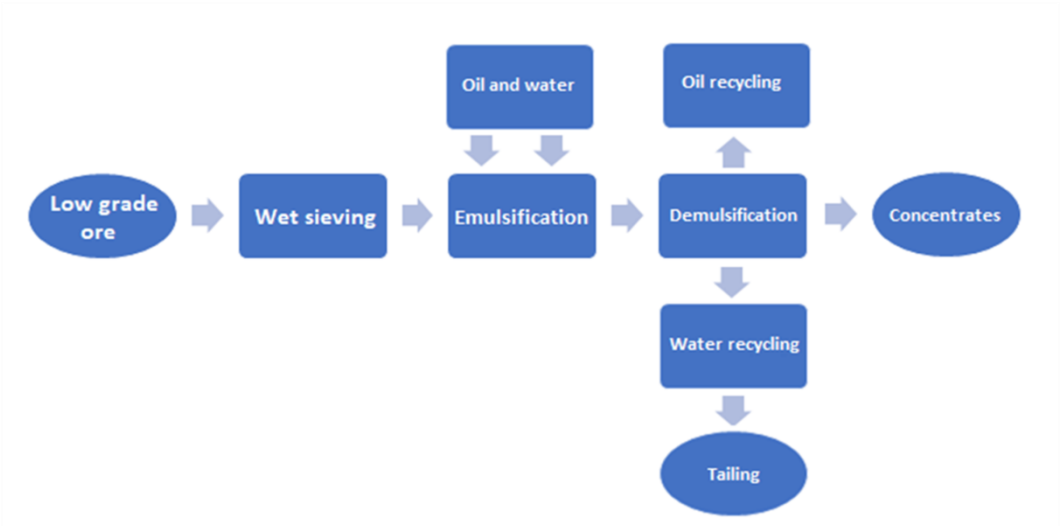

Figure 7.1 Process flow diagram of Pickering emulsification of fine rare earth bearing mineral particles followed by phase separation steps from low grade ground ore to recovery of concentrates

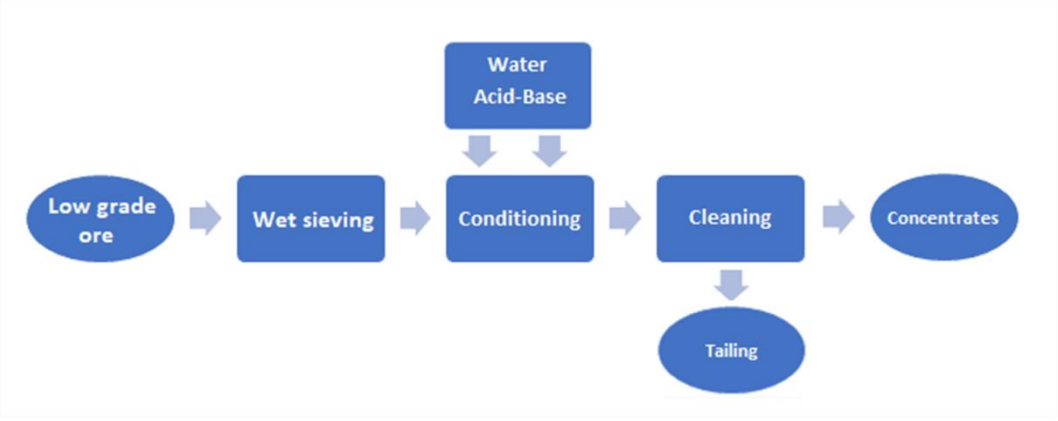

Figure 7.2 Process flow diagram of froth flotation of fine rare earth bearing mineral particles followed by phase separation steps from low grade ground ore to recovery of concentrates

Techno-economic analysis provides data to optimise the pilot or even industrial scale configuration plan. Conventionally, physical beneficiations circuits are sized empirically to reach a maximum performance of separation. The mathematical models somewhat can offer optimisation procedures for alternative network configurations using simulator software. However, hitherto few algorithms for optimisation of complex circuit have been proposed. Preliminary economic evaluation for pilot plan can help to reach optimum plant design and minimize the associated risks. For example, plant with larger scale cost less due to eliminate duplication of processing lines and etc., and thus lower OPEX. In another word, techno-economic evaluation for a pilot scale clearly consequents a better decision making enabling to find alternative process configuration for a larger industrial scale and answering the questions about size and combination, such as: Is the extra CAPEX/OPEX due to reducing the size and increasing the number of stages could be compensated by higher performance of separation (restrain short-circuiting effect)? How should the complex circuit network be designed to reach the maximum beneficiation while the other techno-economic variables change?

In this chapter somehow guide lines are set out for a scaling-up from laboratory to pilot that allows to compare FF vs. SSE in a single stage. The proposed configuration is not neither economically the optimal nor with the best performance of separation. In practice, all the processing constraints should be obtained and weighed for the both aspects (i.e., cost and performance). Indeed, a complete procedure leads to the best financial efficiency. The block diagram flowchart depicts the tasks and information circuit for design optimization (Figure 7.3). The flowchart can help to analyse complex processing configuration looking for cost effectiveness. Using accurate data in software, we can make a faster decision due to assess alternative network interconnections, size and configuration in less time and effort toward maximize the margin (Schena, Villeneuve et al. 1996).

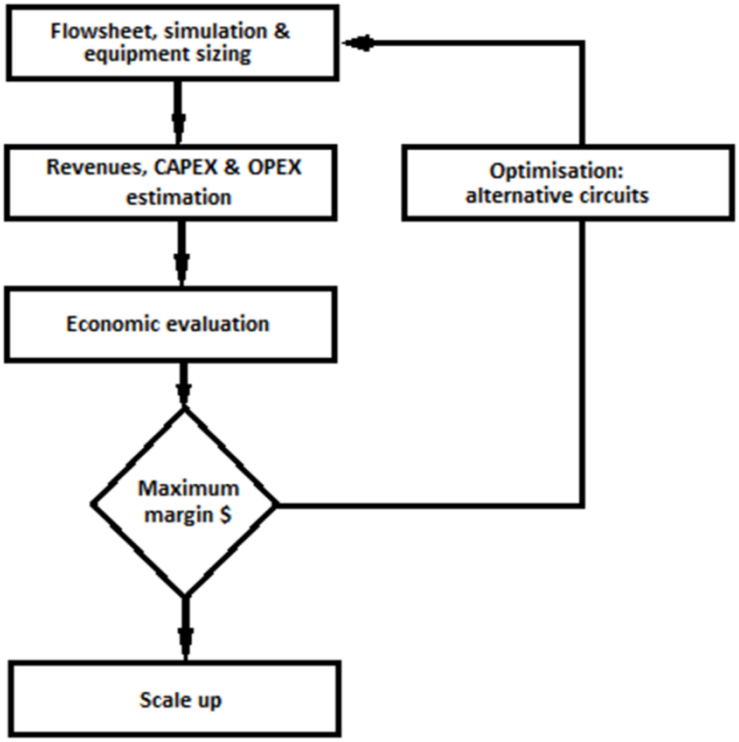

Figure 7.3 Economic evaluation flowchart to optimize the alternative process configuration

7.1 Material and method

Monazite and bastnaesite as the most abundant REE bearing minerals in Niobec mine fresh ore is being recovered through FF and SSE processing. Also, the typical ore consists gangue minerals such as dolomite and calcite. The results of QEMSCAN method made by SGS, is used to obtain ore composition (Lafleur, Eng et al. 2012). We performed wet sieving under 37 microns (near to preferred liberation size) to prepare the feeds for laboratory scale processing (SSE) and the results from previous works and literatures is being used for evaluation. Heavy white paraffin oil (A&C American Chemicals Ltd.) and light kerosene jet-A (SigmaAldrich) were used as they received for dispersed phase of emulsion. Water pH around 7 was used as continuous phase.

The enrichment ratio (ER) and recovery are obtained in products based on a quantitative elemental k0-Neutron activation analysis (NAA) on the product samples(M. Abdollahi Neisiania 2017). To identify the grade of TREE in the samples, NAA was performed on the bulk of concentrated ore. The head grade is about 3.3% TREE. The standard emulsification is followed according to the previous work. The other operational conditions such as setup configuration,

scale, order of mixing, resting time, sample collection and phase separation are also kept the same. Figure *7.4* illustrates also the process flow circuit for both FF and SSE in an industrial scale. Emulsification is being performed by two static mixers in cascade stages while flotation needs conditioning prior to three stages of roughing, cleaning and scavenging for each with five series of cells. In this research, we investigate the heart of the processes in a single stage (Figure 7.4) at pilot scale to simplify the techno-economic analysis and to give comparable guide lines for SSE as an alternative to FF.

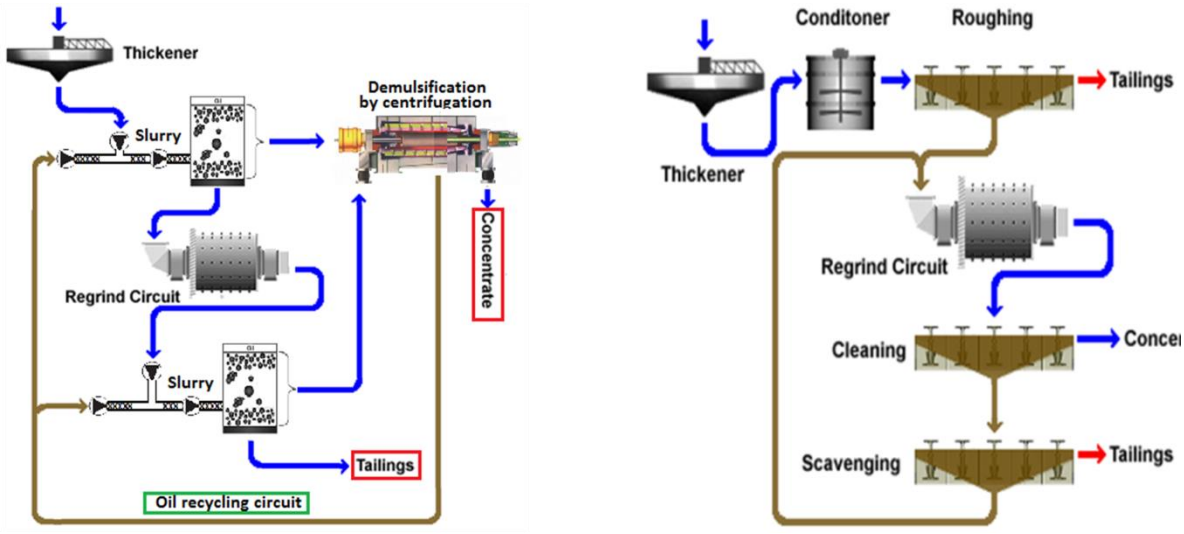

a b

Figure 7.4 Process flow circuit of physical beneficiation of REE-bearing minerals from low grade ground ore (a) with two cascade stages of emulsification, and phase separation by centrifugation (b) with three stages of froth flotation (5 cells of roughing, cleaning, and scavenging)

In SSE, separation of mineral particles by centrifugation may be the most satisfactory and feasible method because it can process large volumes relatively fast and less energy consumer. For a high tonnage of feed, other method of demulsification such as magnetic field, chemical and thermal treatment and even gravity sedimentation, possibly enhanced by adding oil, may be the other options. A further and important sub-process is a suitable oil-water recycling circuit which has a minimum level of oil and moisture in the product and tailing pond. A thermochemical treatment supplement to centrifugation could be enough for a maximum recycling efficiency. A high volume of oil and water lost (in the products and tailings) can substantially influence the process economics further downstream and thus the final price of products recovery. However,

thermal treatment is expensive and should be done on the mount of products after centrifugation whereas the heating value of oil can be added to the thermal treatment process.

In FF, surfactants are employed to create froth with controlled properties, i.e. size of bubbles, stability, lifespan, and etc. They are also used to modify the surface of minerals of interest and most often in combination with pH control of the aqueous phase. The employed surfactants molecules are in overall expensive and as said very hard to be recycled and hence detrimental to the environment. Moreover, there are normally various sorts of surfactants in a FF processing cells for mentioned purposes such as frothers, collectors and depressants to reach a desired recovery and grade (Table 4.1 and Table 7.1) (Mittal and Shah 2013) (Anderson, Taylor et al. 2016).

Table 7.1 Some chemicals in FF processing with comparison prices (CAD$ 2018) (Xuefang 1985)

Chemicals	Oleic acid	$C_{5\text{-}9}$alkyl hydroxamic acid	Naphthenic hydroxamic acid	Benzohydroxamic acid	Sodium carbonate	Lignin sulfonate
CAD$/kg (Ave.~)	1.1	1.8	4.2	8.1	0.65	1

Environmental problems associated with the flotation surfactants are doubled felt due to the lack of promising surfactants for a desired recovery and grade. Beside surfactants, numerous pH tuners, either acidic or basic, should be used.

7.2 CAPEX

The labour cost and maintenance is supposed to be the same for both FF and SSE. The cost of water and water treatment is completely different whereas the water is fully recycled in SSE while it is almost impossible in FF. However, we do not aim the calculation of environmental cost in this research. Since the processing tonnage is the same for both SSE and FF, the CAPEX for land, properties and infrastructure are supposed to be the same, hence the comparison CAPEX data is for pilot scale equipment only.

The sizes are proposed based on the tonnage for a small pilot batch of 4 tons per hour (Table 7.2) for 345 (8300 hr.) operation days per year.

Table 7.2 Estimation for sizing based on 4ton/hour dry ore with head grade 3.3% TREO (the product with 7% TREO of grade, Recovery=75%, total residence time **15 minutes overall operation per batch** of mass solid=20% wt of slurry)

SSE equipment	**Sizes index**	
Emulsification tank	Effective volume 5 [m3]	D=2m, H=2m, C=0.05H
	Mixer (Maxblend)	Power 5.5 kW
Centrifuge decanter FLOTTWEG Z3E Capacity 10 (m^3/h)	4500g force 2 minutes 4times/hr	3.3 kW

FF **equipment**	**Sizes index**	
Conditioner	Mixer	2.5 kW
	Tank	D=2m, H=2m
***Cleaner cell Outotec TC5**	Effective volume 5 [m3]	Power 15.5 kW

* Float cell, mixer, heater, sparger

We calculate CAPEX based on CAD$ 2018 for equipment and installation (Table 7.3). The Annual cash flow Diagram, capital cost, net present value (NPV), internal rate of return (IRR) and Payback Period are calculated later by applying 8% fixed annual discount rate for investment (Ulrich 1984).

Table 7.3 Total CAPEX for pilot scale processing

FF	**Equipment**	***Installation**	**CAPEX**
Conditioning	46000	87400	133400
Cleaning	35000	66500	101500
Total Physical Plant Cost			234500
+ construction and risk 45%			105500
Total Fixed CAPEX (Rounded)			**340000**

SSE	**Equipment**	**Installation**	**CAPEX**
Emulsification	50000	95000	145000
Centrifugation	18000	34000	52000
Total Physical Plant Cost			197000
+ construction and risk 45%			88600
Total Fixed CAPEX (Rounded)			**285000**

*installation including instrumentation and process piping is equal to 190% of equipment cost (CAD$) [CostMine2014] (Schena, Villeneuve et al. 1996, Gorain, Franzidis et al. 2000, Rinne and Peltola 2008)

7.3 OPEX

To estimate the portion of OPEX for chemicals, an approximate quantity fed of reagents or oil with an average price per kg were considered (Table 7.1, Table 7.4 and Table 7.5)

Table 7.4 Approximate OPEX regarding chemicals for FF at mining tonnage flow of 4 tons dry ore per hour R=75%, (Schena, Villeneuve et al. 1996, Yang, Satur et al. 2015)

	Approx. quantity fed of reagents (kg/dry ton ore 3.3% TREO)	**Average price CAD$ per kg**	**Total average cost CAD$ per kg REO (OPEX)**
surfactants	8	0.9	0.3
reagents	10	0.45	0.18
Total chemicals cost			**0.48**

Table 7.5 Approximate OPEX regarding oil consumption for SSE at mining capacity rate of 4 tons dry ore per hour, R=75%, $\Phi_d = 9\%$

	Approx. quantity loss* of oil (kg/dry ton ore 3.3% TREO)	**Average price CAD$ per kg**	**Average cost CAD$ per kg REO (OPEX)**
Oil	5	0.9	**0.18**

*The amount of loss is being selected based on the laboratory results

The portion of energy in OPEX is in average cost per ton REO and average domestic price of electricity in Canada is 0.15 CAD$ per KWh (Table 7.6).

Table 7.6 Approximate OPEX regarding energy consumption for FF and SSE at mining capacity rate of 4 tons dry ore per hour R=75% (Safari, Harris et al. 2016, Tabosa, Runge et al. 2016)

Overall Process	**Sub-process**	**Approx. quantity energy (KWh/dry ton ore 3.3% TREO)**	**Average cost CAD$ per ton REO (OPEX)**

FF	Conditioning& Cleaning (Heating 80˚C)	4.5	26.7
SSE	Emulsification Centrifugation	2.2	13.3*

*the total energy consumption for SSE is 50% less than FF (Ityokumbul, Bulani et al. 1987, Schena, Villeneuve et al. 1996, Mankosa, Kohmuench et al. 2018, Zhang and Zhang 2019)

Figure 7.5 depicts a comparison for annual expenses for 345 working days or 8300 operational hours per year, supposing that maintenance cost is 10% of total CAPEX. The average total annual labor cost including an engineer, a control room operator, a maintenance technician and two general laborer **is** calculated based on average salary 2018 and 40 working hours per week, equal to **270000 CAD$** for the pilot size (Ityokumbul, Bulani et al. 1987, Fraser, Walton et al. 1991, Rinne and Peltola 2008).

$$NPV = \sum_{t=0}^{n} \frac{R_t}{(1+i)^n}$$

Where: Rt is a net cash inflow-outflows during a single period of time (e.g., annual, or season), i is a discount rate (e.g., annual 8%) , n= number of time periods over life span (e.g., 5 years).

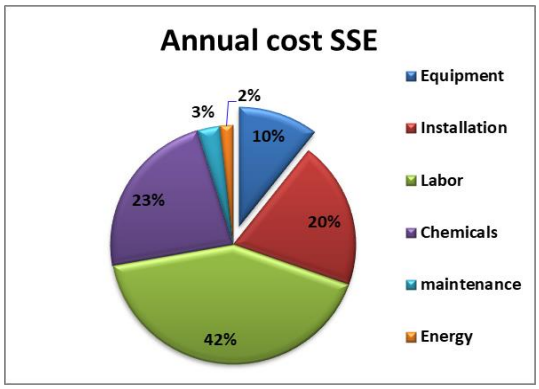

a

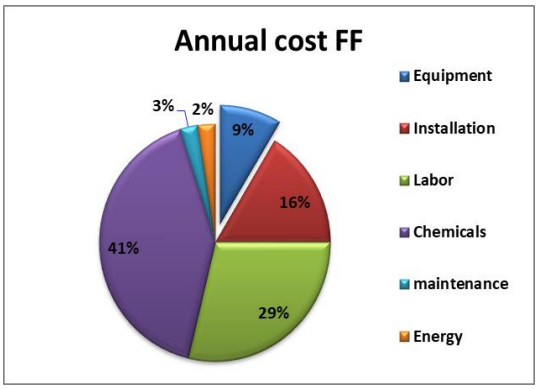

b

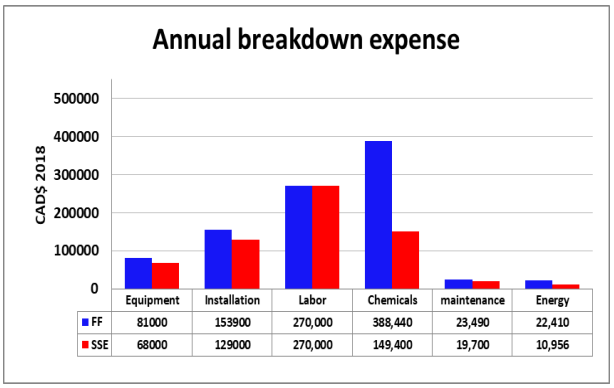

c

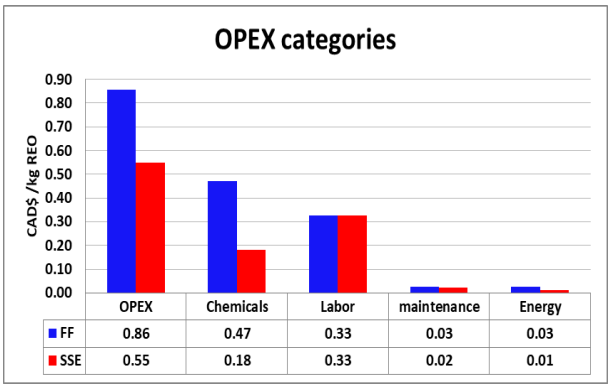

d

Figure 7.5 Breakdown of annual cost for overall processes a) SSE b) FF c) Annual expenses d) detailed comparison for OPEX categories

The outlet of physical beneficiation process does not have commercial values as raw product. However, in order to find a break-even point over cumulative cash flow, capital cost, NPV, IRR and payback period for both processes, we try to estimate an average price of major REE's abundant in bastnaesite and monazite. There are for sure sorts of HREE and LREE in the feed ore (i.e., Niobec ore) with big difference in prices per kg REO (Table 7.7). In , we used a common model for economic evaluation (Peters, Timmerhaus et al. 1968, Ulrich 1984) while considered a time span of typical total ownership over 1 year and a fixed annual banking interest rate for investment 4.5% (value of CAD$ 2018).

The average price for 1kg REO in the product is calculated based on our assumptions (CAD$ 2018 www.statista.com):

$$Price\ 1\ kg\ REO\ = (Purity\ factor = 0.07) \times \sum (P_{REO} \times Average\ wt\%\ in\ the\ ore) \quad 7.1$$

Table 7.7 The abundant of selected rare earth oxides in the ore feed and their global price as of January 2018 and average price for 1 kg REO

Rare earth elements	Symbol	REE's Name	Bastnäsite/ Monazite/ Parisite Average (wt %)	Average price CAD$ per kg REO (2018)	Price× wt%
LREE	Ce2O3	Cerium	50.9	7	3.41

	La2O3	Lanthanum	22	9	2.08
	Sm2O3	Samarium	2	8	0.17
	Nd2O3	Neodymium	17.9	139	24.79
	Pr2O3	Praseodymium	5	154	7.72
HREE	Eu2O3	Europium	1.1	190	2.09
	Gd2O3	Gadolinium	1.1	33	0.37
			100		**1.34**

The typical cumulative gain revenue and payback period or BEP of cash flow is estimated over the 5 years life cycle of the pilot plant (Figure 7.6):

$$\text{Cumulative gain}_{revenue} = Annual\ production \times (Price - OPEX)_{/1kg\ REO} - CAPEX \quad 7.2$$

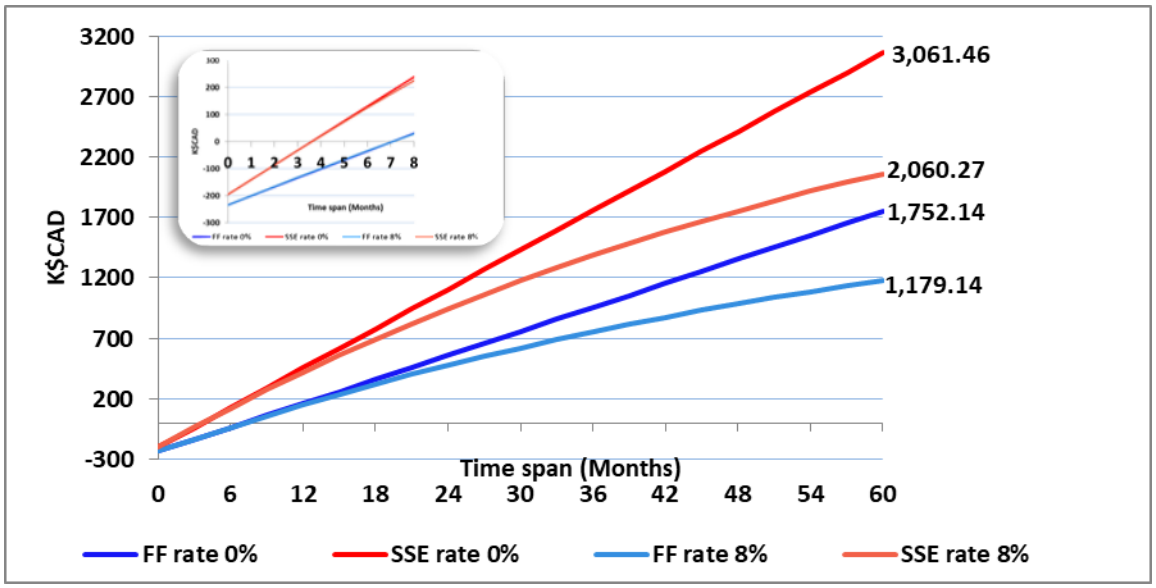

Figure 7.6 Cumulative cash flow, payback period and NPV over 60 months life span of the pilot plant. BEP is less than 2 months for SSE and it is above 6 months for FF

The internal rate of return can be calculated as follow:

$$IRR = \frac{NPV - R_{t0}}{R_{t0}} = \sum_{t=0}^{n} \frac{R_t/R_{t0}}{(1+i)^n} - 1 \quad (7.3)$$

Table 7.8 Internal rate of return for SSE and FF

IRR SSE	IRR FF
14.5	6.5

7.4 Economic evaluation

Regarding to Table 7.8 we should mention that IRR is much more sensitive to the price values (quality values e.g., effect of impurities or the grade) and overall recovery than CAPEX or OPEX. In another word, if we could be able to improve recovery or the grade on the products even by a reasonable increasing on CAPEX or OPEX, the IRR can be even augment. Table 7.9 tabulates a summary of economic evaluation for both processes.

Table 7.9 Economic evaluation comparison of pilot scale physical beneficiation by FF or SSE capacity 4 ton/day feed of dry ore of 3.3%TREO

	FF	SSE	%
Total CAPEX (K$CAD)	234	197	-15.8
Annual OPEX (K$CAD)	704	450	-36.1
Unitary OPEX ($CAD/kg REO)	0.86	0.55	-36

7.5 The sustainability of the process

To compare the sustainability of the processes both economic and environmental evaluation are essential. For analysing life cycle impacts, we considered the main 7 categories of impacts. P.S.Arshi et al performed an overall evaluation of impacts for producing 1kg REO and give a percentage contribution of normalized impacts for physical beneficiation (Arshi, Vahidi et al. 2018). We use the same approach to give a comparison for FF vs. SSE. The impacts of

acidification, eutrophication, ozone depletion potential (OZP) and smog are almost equal zero for SSE. The human health and human carcinogen are calculated based on two different oil scenarios (i.e., paraffin and kerosene) comparing available datasheets (Navarro and Zhao 2014, Sprecher, Xiao et al. 2014, Jin, Park et al. 2017). The energy consumption is the basis for calculation CO2eq (Table 7.10). The normalized environmental impacts depict a very significant reduction for SSE vs. FF (Figure 7.7).

Table 7.10 Life Cycle Impacts of physical beneficiation by FF vs. SSE for producing 1 kg REO

	Acidification	Entrophication	GHG	HH Particulate air	HT carcinogen	OZP	Smog Air
	kg SO2-eq	kg N2-eq	kg CO2-eq	kg PM2.5-eq	CTUh	kg CFC11-eq	kg O3-eq
FF	3.18E-02	7.47E-03	3.85E+00	1.62E-02	1.01E-06	1.13E-07	2.86E-01
SSE - Paraffin oil	0.00E+00	0.00E+00	2.01E+00	6.96E-04	1.08E-07	0.00E+00	0.00E+00
SSE - Kerosene	0.00E+00	0.00E+00	2.01E+00	1.62E-03	1.30E-07	0.00E+00	0.00E+00

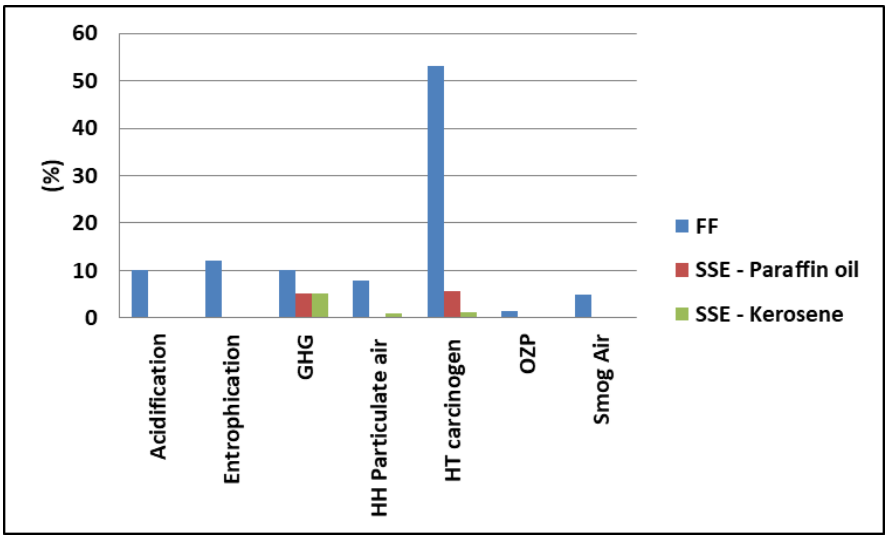

Figure 7.7 Percentage contribution of normalized impacts for producing 1kg REO by FF vs. SSE

The cost breakdown shows a huge reduction for CAPEX and OPEX categories in SSE around -16% and -36% respectively, mostly due to the expenses of chemicals, reagents and surfactants in FF while SSE just uses oil and has significantly less energy consumption. The study shows that SSE beneficiation of monazite and bastnaesite from Niobec wet-sieved ore

3.3% TREO in a pilot scale of 4 tons dry feed ore per hour has huge economic benefits and much less environmental impacts than conventional FF with the exact same feed rate, recovery and the grade in product (i.e., R=76% and 7% TREO). This preliminary analysis determined that SSE is more economical and sustainably viable. Since SSE has also simpler equipment and fewer stages to reach the favourable enrichment ratio in an industrial scale, hence, there should be much OPEX and CAPEX raise up in FF which needs multiple cascade stages mostly with labor, equipment, installation, etc.

CHAPTER 8 GENERAL DISCUSSION

As it is mentioned in their name, rare earth elements can be recovered hardly regardless of their abundance due to very similar physicochemical properties. Among mining early stages processes, physical beneficiation of rare earth bearing minerals comes with numerous challenges. In the conventional froth flotation, the minerals of interest promote to attach to a water-air bubble interface and bubbles lift the particle of interest to the top of the flotation tank and finally will separate using a scrubber at the top with the foam.

Flotation has to apply numerous different surfactants and pH modification factors in order to modify the surface properties and increase the acceptable performance of separation. In other words, to create froth with controlled properties (size of bubbles, stability, lifespan…), surfactants are used, most often in combination with pH control of the aqueous phase using both acids and bases in succession. The surfactant molecules most generally employed are both expensive, impacting the operating costs, and known to create detrimental conditions for the environment. Finally, the recycling of rejected water cannot be easily performed; a result of the numerous additives input during the processing and thus a huge amount of tailing ponds will be generated at the processing location.

Also, many flotation steps such as thickening, conditioning and scavenging combined with cleaning and reverse flotation must be put in place to reach a typical 60% recovery and a concentrated ore seldom above 200% enrichment ratio for a cleaning stage. The processing of rare earth bearing minerals is hence expensive on the economics side and very detrimental on the environment, a consequence of the surfactants cocktail that must be used in combination with all other additives ((Bulatovic 2007, Ni, Parrent et al. 2012, Anderson, Taylor et al. 2016).

In chapter 4, we stand on that SSE is able to selectively capture REE bearing minerals based on their wettability differences. The feed ore from Niobec mine wet sieved into the desired size cut under -37 microns near to liberation size of monazite and bastnaesite grains, the two major REE bearing minerals. The wet sieving help to wash out very fine particles from the surface of bigger particles and we can perfectly have all liberated grains in underflow. The underflow was used into the process at their natural surface or without any surface modification. The results for one stage emulsification and not under optimal conditions illustrate that the separation performance is acceptable around 50% recovery and 290% enrichment ratio. The effects of head

grade and size distribution of the feed were considered. These parameters have significant effect on selectivity or performance of separation. The recovery and grade of products can be enhanced by grinding the feed to a size class lower than -37μm followed by a wet sieving prior to emulsification. The results were compared single stage flotation processes with two different resources from Bayan Obo China and Nechalacho located at Thor Lake in Canada processing carbonatite and phosphate REE bearing minerals. However, there are differences and similarities in their associated gangues and composition when compared with Niobec's ore. The REE recovery from a multi stage micro-flotation applying Hydroxamate as collector is around 15% and the enrichment ratio is around 8 (Xia, Hart et al. 2014, Xia, Hart et al. 2015). The results of a single step of laboratory micro-flotation by applying three different surfactants indicate a maximum average recovery around 60% along with an average enrichment ratio for all rare earth bearing around 200% (Satur, Calabia et al. 2016, Abaka-Wood, Addai-Mensah et al. 2018).

In chapter 5, a semi-empirical approach was used to investigate the significant effects of mixing conditions on performance of separation. An improved model has been developed to predict the global selective attachment of monazite and bastnaesite into the oil-water interface. The experimental results were completely accord with the model. In general, the selective attachment is enhanced by increasing impeller speed. The setup equipped with Maxblend impeller shows a better performance and selectively when compared with PBT impeller at exacts the same Weber number and as a result same oil droplets mean size, a consequence of more shear rate uniformity with Maxblend. The results clearly indicate that while we have exactly the same amount of covered interface in both setups, the higher shear uniformity in Maxblend setup makes higher droplet size uniformity and lower span and eventually provides a better recovery and the grade. Recovery of monazite and bastnaesite in one stage emulsification reached up to 65% while the products enriched up to %385. Mixing duration can also enhance the recovery. However, an optimal MD of 15 min regarding to energy consumption was obtained. Sequential mixing orders have been also tested. The best scenario to improve selectivity is that oil well dispersed for a while before adding pre-wetted mineral particles.

Chapter 6 investigated different physical properties of the phases at the same process conditions. The competitive attachment of REE-bearing minerals and gangues will change at different oil/water interfacial properties. The selectivity of the process depends on oil viscosity, oil to water ratio, particle concentration, and oil-water interfacial tension. The more viscose oils

provide the larger droplet sizes and hence have a better overall selective attachment toward monazite and bastnaesite due to better attachment efficiency. The probability of attachment into the interface increases around the larger droplets for monazite and bastnaesite which results a selective coverage and restrain space for the gangue particles to be attached. In a same direction with larger droplets, the available generated interface will decrease and a competitive attachment to the interface becomes much more meaningful. With a same argue, a lower O/W ratio leads to a competitive attachment or higher coverage efficiency, hence a better performance of separation. A more solid mass ratio gives also a better enrichment ratio, but obviously the ultimate recovery would be lower. The lower interfacial tension makes a better attachment efficiency which also seems to be the reason for applying IFT modification during the flotation process (e.g., surfactants, frothers). The polar oils represent a lower IFT in the system and it seems they should have a better selectivity. But, the selectivity is also dictated by ionic exchange in the aqueous phase and polarity around the particles. In other side, lower IFT leads to smaller droplet mean size at the same mixing condition. It should be mentioned that reducing mixing intensity has a limit to the minimum of Njs. The IFT modified to lower values while 1-hexanol 1% was added into pure paraffin and kerosene oils. The results also indicate that selectivity is then restrained with the modified IFT. The higher IFT makes larger and much more uniform emulsion size which in turn enhances ultimate performance. Therefore, the non-polar oils in overall make a better selectivity than the polar oils. In another approach, we used ethylene glycol as a continuous phase instead of water to investigate the effect of lower IFT. However, we observed contradictory results (a better performance) mostly due to another sort of contact angle or wettability differences of REE bearing minerals and the gangues versus EG-oil interface. As summary, the performance of selective separation was proved to be affected by both IFT and wettability differences. More specifically, the selectivity of the process can be strongly improved by using the appropriate amount of solid particle mass ratio, applying viscose non-polar oil that can provide a high IFT versus aqueous system.

The results in chapter 7 confirmed that the application of SSE in physical beneficiation of REE bearing minerals is technically and economically much more viable and surprisingly profitable than FF at exact the same product enrichment about 200% and recovery of 75% from low-grade ore. In the other hand, SSE has less environmental impacts and higher productivity revenue vs. FF mostly due to the fact of higher selectivity. The techno-economic comparison for

pilot size with 4 tons dry ore per hour and 345 working days or 8300 operation hours was evaluated for both FF and SSE. The cost breakdown for SSE process shows a huge reduction around -36% with unitary OPEX $CAD/kg vs FF, mostly due to the cost of chemicals, reagents and surfactants whereas SSE has significantly less energy and oil consumption. The IRR values at 8% discount rate are also higher for SSE vs. FF about 9.1 and 3.6 respectively. IRR is much more sensitive to the price values than CAPEX or OPEX (quality and quantity, e.g., effect of impurities or the grade and recovery). In another word, if we could be able to improve recovery or the grade on the products even by a reasonable increasing on CAPEX or OPEX, the IRR can be even augment.

Recovery of REE bearing minerals through Pickering emulsification circumvents most of the difficulties of conventional froth flotation processes which can hardly achieve reasonable performance in the current mining industry. In the provided example related to rare earth extraction, bastnäsite and monazite are recovered from the associated gangue minerals. Since the approach does not use any chemicals like pH and surface modification reagents while oil and water is being recycled inside the process, thus it has huge economic and environmental advantages compared to the other conventional physical beneficiation methods such as froth flotation. Also, the SSE process can be applied to an intensive tonnage feed stream whereas the magnetic and electrostatic separation methods have limits.

The validity of the results was examined by NAA and quick image analysis technique (appendix). the grade of the feed (fresh ore commonly under 37 microns size cut near to the liberation size) is around TREO%=3.3 and Pickering emulsification can separate and concentrate REE’s carrier minerals into overflow up to 385% enrichment ratio in a single one-stage process and a recovery up to 75%. These values are exciting and high enough to compare with current conventional physical beneficiation methods such as froth flotation.

CHAPTER 9 CONCLUSION AND RECOMMENDATIONS

9.1 Conclusion

Our study proposes a method for the recovery of rare earth elements (REE) employing oil in water emulsification process. More specifically, SSE are used to selectively and effectively separate and concentrate valuable REE bearing minerals particles in the early stage of physical beneficiation process. The oil dispersed in the water and the droplet tends to capture selectively the more hydrophobic particles of REE's carriers (i.e., monazite and bastnaesite) in the slurry based on their natural wettability. The concentrated REE bearing minerals attached into the creamed droplets and can be easily separated trough a phase separation step.

The results of laboratory scale processing show that SSE opens a new perspective for physical beneficiation and the approach is successfully feasible without using any surfactants or changing natural pH of the slurry. The products reached to a maximum recovery of 75% and a quality grade enriched up to 400% of TREO with paraffin oil and water emulsification, a comparable performance of separation with the results of a micro-flotation cell. Our work reports paraffin oil with the reasonable price, lost and efficiencies as applicable oil into the SSE processing.

9.2 Recommendations

Regarding the environmental and economic viability, physical beneficiation of REE bearing minerals through SSE has numerous advantages vs. conventional F, but like many others, the laboratory results must be optimized toward the highest feasibility at pilot and industrial scale. So, two approaches should be considered. The first is aimed at improving emulsification, demulsification and phase separation steps by improvement of devices, e.g. mixing and centrifugation, and process configuration, e.g. continuous or batch processes. The second approach is to optimize formulations and to improve the feed preparation protocol in the upstream processes.

If we decide to modify the surface properties of minerals, the point might be highlighted as a shortcoming of the process comparing to FF especially when the oil recycling has some deficits and lost. This last is very depends on the performance of separation and the oil lost while evaluating the process configuration in a detailed techno-economic software. Thus, SSE

empowering with the modification of wettability and pH might have still advantages when compared with FF, whereas the overall process has higher performance and efficent recycling process for oil and water, hence, still less cost and environmental impacts.

For a continuous process configuration in an industrial scale up, a static mixer might be designed to process a huge amount of ore. As recommendation for future works, the design of static mixer has to be investigated further due to its influences on performance of separation. In order to increase the viability and overcome some constrains of the overall process, the phases separation stage should be also subject to further investigation including demulsification by centrifugation as well as oil separation and recycling.

The preliminary analysis at laboratory scale demonstrated that SSE is more economical and sustainably viable than FF. Further works could be dedicated to a larger scale, feedstock variation and the effect of multi-stages to reach an acceptable grade for physical beneficiation.

The emulsification process might be combined with supplementary upstream, downstream and sub-process such as prior wet sieving to desired size cut, crushing, washing, thickening, and etc., in order to enhance the performance of separation (e.g. washing cream droplets to prevent non-emulsified particles get trapped between droplets and come into the overflow, which might downgrade the products).

By properly selecting the oil, adjusting the formulation (oil to water ratio), and providing appropriate operational process conditions, it is possible to selectively capture the ore particles of interest at the oil-water interface (i.e., bastnaesite and monazite attached more into the oil droplets) while the ore without value settle at the bottom of the processing tank.

BIBLIOGRAPHY

"Flotation reagent data, https://www.911metallurgist.com/blog/flotation-reagents."

Abaka-Wood, G., J. Addai-Mensah, W. Skinner, G. Abaka-Wood, J. Addai-Mensah and W. Skinner "Physicochemical Characterisation of Monazite, Hematite and Quartz Minerals for Flotation."

Abaka-Wood, G. B., J. Addai-Mensah and W. Skinner (2018). "A study of selective flotation recovery of rare earth oxides from hematite and quartz using hydroxamic acid as a collector." Advanced Powder Technology **29**(8): 1886-1899.

Anderson, C. D., P. R. Taylor and C. G. Anderson (2016). Rare earth flotation fundamentals: A review. Proceedings of the XXVIII International Mineral Processing Congress.

Aneus, J. (1965). "The visible region absorption spectra of rare earth minerals." Am. Mineral **50**: 356-366.

Arditty, S., C. P. Whitby, B. P. Binks, V. Schmitt and F. Leal-Calderon (2003). "Some general features of limited coalescence in solid-stabilized emulsions." The European Physical Journal E **11**(3): 273-281.

Arshi, P. S., E. Vahidi and F. Zhao (2018). "Behind the Scenes of Clean Energy: The Environmental Footprint of Rare Earth Products." ACS Sustainable Chemistry & Engineering **6**(3): 3311-3320.

Aveyard, R., B. P. Binks and J. H. Clint (2003). "Emulsions stabilised solely by colloidal particles." Advances in Colloid and Interface Science **100**: 503-546.

Azimi, G., R. Dhiman, H.-M. Kwon, A. T. Paxson and K. K. Varanasi (2013). "Hydrophobicity of rare-earth oxide ceramics." Nature materials **12**(4): 315-320.

Bazin, C. and D. Hodouin (2001). "Importance of covariance in mass balancing of particle size distribution data." Minerals Engineering **14**(8): 851-860.

Beattie, J. K., A. M. Djerdjev, A. Gray-Weale, N. Kallay, J. Lützenkirchen, T. Preočanin and A. Selmani (2014). "pH and the surface tension of water." Journal of colloid and interface science **422**: 54-57.

Berry, J. D., M. J. Neeson, R. R. Dagastine, D. Y. Chan and R. F. Tabor (2015). "Measurement of surface and interfacial tension using pendant drop tensiometry." Journal of colloid and interface science **454**: 226-237.

Binks, B. and P. Fletcher (2001). "Particles adsorbed at the oil-water interface: A theoretical comparison between spheres of uniform wettability and “Janus” particles." Langmuir **17**(16): 4708-4710.

Binks, B. and S. Lumsdon (2000). "Influence of particle wettability on the type and stability of surfactant-free emulsions." Langmuir **16**(23): 8622-8631.

Binks, B. and S. Lumsdon (2001). "Pickering emulsions stabilized by monodisperse latex particles: effects of particle size." Langmuir **17**(15): 4540-4547.

Binks, B. P. (2002). "Particles as surfactants—similarities and differences." Current opinion in colloid & interface science **7**(1): 21-41.

Binks, B. P. and J. H. Clint (2002). "Solid wettability from surface energy components: relevance to Pickering emulsions." Langmuir **18**(4): 1270-1273.

Binks, B. P. and T. S. Horozov (2006). Colloidal particles at liquid interfaces, Cambridge University Press.

Binks, B. P. and S. O. Lumsdon (1999). "Stability of oil-in-water emulsions stabilised by silica particles." Physical Chemistry Chemical Physics **1**(12): 3007-3016.

Binks, B. P., R. Murakami, S. P. Armes and S. Fujii (2005). "Temperature-Induced Inversion of Nanoparticle-Stabilized Emulsions." Angewandte Chemie **117**(30): 4873-4876.

Binks, B. P., R. Murakami, S. P. Armes and S. Fujii (2006). "Effects of pH and salt concentration on oil-in-water emulsions stabilized solely by nanocomposite microgel particles." Langmuir **22**(5): 2050-2057.

Binks, B. P., J. Philip and J. A. Rodrigues (2005). "Inversion of silica-stabilized emulsions induced by particle concentration." Langmuir **21**(8): 3296-3302.

Binks, B. P. and C. P. Whitby (2004). "Silica particle-stabilized emulsions of silicone oil and water: aspects of emulsification." Langmuir **20**(4): 1130-1137.

Binks, B. P. and C. P. Whitby (2005). "Nanoparticle silica-stabilised oil-in-water emulsions: improving emulsion stability." Colloids and Surfaces A: Physicochemical and Engineering Aspects **253**(1): 105-115.

Braisch, B., K. Köhler, H. P. Schuchmann and B. Wolf (2009). "Preparation and Flow Behaviour of Oil-In-Water Emulsions Stabilised by Hydrophilic Silica Particles." Chemical engineering & technology **32**(7): 1107-1112.

Bulatovic, S. M. (2007). Handbook of flotation reagents: chemistry, theory and practice: Volume 1: flotation of sulfide ores, Elsevier: 172-312.

Bulatovic, S. M. (2010). 22 - Flotation of Niobium. Handbook of Flotation Reagents: Chemistry, Theory and Practice. S. M. Bulatovic. Amsterdam, Elsevier**:** 111-125.

Bulatovic, S. M. (2010). 24 - Flotation of REO Minerals. Handbook of Flotation Reagents: Chemistry, Theory and Practice. S. M. Bulatovic. Amsterdam, Elsevier**:** 151-173.

Castor, S. B. and J. B. Hedrick (2006). "Rare earth elements." Industrial minerals volume, 7th edition: Society for mining, metallurgy, and exploration, Littleton, Colorado: 769-792.

Cauvin, S., P. J. Colver and S. A. Bon (2005). "Pickering stabilized miniemulsion polymerization: preparation of clay armored latexes." Macromolecules **38**(19): 7887-7889.

CH Li, C. and D. W. Fuerstenau (2015). "Surface Chemical Characterization of Bastnaesite through Electrokinetics." KONA Powder and Particle Journal: 176-183.

Chan, D. Y. and R. G. Horn (1985). "The drainage of thin liquid films between solid surfaces." The Journal of chemical physics **83**(10): 5311-5324.

Cheng, J., Y. Hou and L. Che (2007). "Flotation separation on rare earth minerals and gangues." Journal of Rare Earths **25**: 62-66.

Cheng, T. W. (2000). "The point of zero charge on monazite and xenotime." Minerals Engineering **13**(1): 1-6.

Coulaloglou, C. and L. Tavlarides (1977). "Description of interaction processes in agitated liquid-liquid dispersions." Chemical Engineering Science **32**(11): 1289-1297.

Craig, V. S., C. Neto and D. R. Williams (2001). "Shear-dependent boundary slip in an aqueous Newtonian liquid." Physical review letters **87**(5): 054504.

Danielli, J. F. (1937). "The relations between surface pH, ion concentrations and interfacial tension." Proc. R. Soc. Lond. B **122**(827): 155-174.

Danov, K. D. and P. A. Kralchevsky (2006). "Electric forces induced by a charged colloid particle attached to the water–nonpolar fluid interface." Journal of colloid and interface science **298**(1): 213-231.

Dickinson, E. (2010). "Food emulsions and foams: stabilization by particles." Current Opinion in Colloid & Interface Science **15**(1-2): 40-49.

Dobbins, M., P. Dunn and I. Sherrell (2009). Recent advances in magnetic separator designs and applications. Proceedings 7th International Heavy Minerals Conference,'What next', The Southern African Institute of Mining and Metallurgy, Drakensberg, South Africa: 63-70.

Drelich, J., J. Nalaskowski, A. Gosiewska, E. Beach and J. Miller (2000). "Long-range attractive forces and energy barriers in de-inking flotation: AFM studies of interactions between polyethylene and toner." Journal of adhesion science and technology **14**(14): 1829-1843.

Ducker, W. A., Z. Xu and J. N. Israelachvili (1994). "Measurements of hydrophobic and DLVO forces in bubble-surface interactions in aqueous solutions." Langmuir **10**(9): 3279-3289.

El-Mahrab-Robert, M., V. Rosilio, M.-A. Bolzinger, P. Chaminade and J.-L. Grossiord (2008). "Assessment of oil polarity: Comparison of evaluation methods." International journal of pharmaceutics **348**(1-2): 89-94.

Fielden, M. L., R. A. Hayes and J. Ralston (1996). "Surface and capillary forces affecting air bubble-particle interactions in aqueous electrolyte." Langmuir **12**(15): 3721-3727.

Fournier, C. O., L. Fradette and P. A. Tanguy (2009). "Effect of dispersed phase viscosity on solid-stabilized emulsions." Chemical Engineering Research & Design **87**(4A): 499-506.

Fournier, C. O., L. Fradette and P. A. Tanguy (2009). "Effect of dispersed phase viscosity on solid-stabilized emulsions." Chemical Engineering Research and Design **87**(4): 499-506.

Fradette, L., C.-O. Fournier and P. Tanguy (2008). Oil Viscosity Impact on the Production of Pickering Emulsions. The 2008 Annual Meeting: 499-506.

Fraser, K., R. Walton and J. Wells (1991). "Processing of refractory gold ores." Minerals Engineering **4**(7-11): 1029-1041.

Frelichowska, J., M.-A. Bolzinger, J. Pelletier, J.-P. Valour and Y. Chevalier (2009). "Topical delivery of lipophilic drugs from o/w Pickering emulsions." International journal of pharmaceutics **371**(1-2): 56-63.

Frelichowska, J., M.-A. Bolzinger, J.-P. Valour, H. Mouaziz, J. Pelletier and Y. Chevalier (2009). "Pickering w/o emulsions: drug release and topical delivery." International Journal of Pharmaceutics **368**(1-2): 7-15.

Gillies, G. and C. A. Prestidge (2005). "Colloid probe AFM investigation of the influence of cross-linking on the interaction behavior and nano-rheology of colloidal droplets." Langmuir **21**(26): 12342-12347.

Gingras, J.-P., P. A. Tanguy, L. Fradette and E. Jorda (2012). Method for preparing a calibrated emulsion, Google Patents.

Gorain, B., J. Franzidis and E. Manlapig (2000). "Flotation Cell Design: Application of Fundamental Principles." Julius Kruttschnitt Mineral Research Centre. Indooroopilly. Queensland. Australia.

Grenier, L. and J.-F. Tremblay (2013). NI 43-101 Technical report, Surface diamond drilling exploration program for rare earth elements, 2012, NIOBEC MINE PROPERTY.

Gupta, C. K. and N. Krishnamurthy (1992). "Extractive Metallurgy of Rare Earths." International materials review **37**(5): 197-248.

Gupta, C. K. and N. Krishnamurthy (2004). Extractive Metallurgy of Rare Earths.

Haque, N., A. Hughes, S. Lim and C. Vernon (2014). "Rare earth elements: Overview of mining, mineralogy, uses, sustainability and environmental impact." Resources **3**(4): 614-635.

Hashem, M. (2012). Study on the Homogenization Speed in a Tank Equipped with Maxblend Impeller, École Polytechnique de Montréal: 15-30.

Herrera-Urbina, R. and D. Fuerstenau (2013). "Electrophoretic mobility and computations of solid-aqueous solution equilibria for the bastnaesite-H2O system." Minerals & Metallurgical Processing Journal **30**(1): 18-23.

Hey, M. J. and J. G. Kingston (2006). "Maximum stability of a single spherical particle attached to an emulsion drop." Journal of colloid and interface science **298**(1): 497-499.

Hirajima, T., K. Sasaki, A. Bissombolo, H. Hirai, M. Hamada and M. Tsunekawa (2005). "Feasibility of an efficient recovery of rare earth-activated phosphors from waste fluorescent lamps through dense-medium centrifugation." Separation and purification technology **44**(3): 197-204.

Hoke, L., R. A. Segars and R. McDermott (1990). Methods to evaluate solid surface tension for military fabrics, ARMY NATICK RESEARCH DEVELOPMENT AND ENGINEERING CENTER MA.

Horozov, T. S., R. Aveyard, B. P. Binks and J. H. Clint (2005). "Structure and stability of silica particle monolayers at horizontal and vertical octane-water interfaces." Langmuir **21**(16): 7405-7412.

Horozov, T. S., R. Aveyard, J. H. Clint and B. P. Binks (2003). "Order-disorder transition in monolayers of modified monodisperse silica particles at the octane-water interface." Langmuir **19**(7): 2822-2829.

Horozov, T. S., B. P. Binks and T. Gottschalk-Gaudig (2007). "Effect of electrolyte in silicone oil-in-water emulsions stabilised by fumed silica particles." Physical Chemistry Chemical Physics **9**(48): 6398-6404.

Ityokumbul, M., W. Bulani and N. Kosaric (1987). "Economic and environmental benefits from froth flotation recovery of titanium, zirconium, iron and rare earth minerals from oilsand tailings." Water Science and Technology **19**(3-4): 323-331.

Izatt, S. R., J. S. McKenzie, N. E. Izatt, R. L. Bruening, K. E. Krakowiak and R. M. Izatt (2016). "Molecular recognition technology: a green chemistry process for separation of individual rare earth metals." White Paper on Separation of Rare Earth Elements: 1-13.

Jafari, R. (2010). Solid Suspension and Gas Dispersion in Mechanically Agitated Vessels, École Polytechnique de Montréal.

Jafari, R., J. Chaouki and P. A. Tanguy (2012). "A comprehensive review of just suspended speed in liquid-solid and gas-liquid-solid stirred tank reactors." International Journal of Chemical Reactor Engineering **10**(1): 1-32.

Jin, H., D. M. Park, M. Gupta, A. W. Brewer, L. Ho, S. L. Singer, W. L. Bourcier, S. Woods, D. W. Reed and L. N. Lammers (2017). "Techno-economic Assessment for Integrating Biosorption into Rare Earth Recovery Process." ACS Sustainable Chemistry & Engineering **5**(11): 10148-10155.

Jones, A. P., F. Wall and C. T. Williams (1996). Rare Earth Minerals. Chemistry, origin and deposits

Jordens, A., Y. P. Cheng and K. E. Waters (2013). "A review of the beneficiation of rare earth element bearing minerals." Minerals Engineering **41**: 97-114.

Jordens, A., C. Marion, O. Kuzmina and K. E. Waters (2014). "Surface chemistry considerations in the flotation of bastnäsite." Minerals Engineering **66**: 119-129.

Jordens, A., R. S. Sheridan, N. A. Rowson and K. E. Waters (2014). "Processing a rare earth mineral deposit using gravity and magnetic separation." Minerals Engineering **62**: 9-18.

Kabza, K. G., J. E. Gestwicki and J. L. McGrath (2000). "Contact angle goniometry as a tool for surface tension measurements of solids, using zisman plot method. A physical chemistry experiment." Journal of Chemical Education **77**(1): 63.

Karcz, J., M. Cudak and J. Szoplik (2005). "Stirring of a liquid in a stirred tank with an eccentrically located impeller." Chemical Engineering Science **60**(8): 2369-2380.

Khatri, N. L. (2010). Measurement and Modeling of Emulsion Layer Growth in Continuous Oil-Water Separations, University of Calgary :10-19.

Kvítek, L., P. Pikal, L. Kovarikova and J. Hrbac (2002). "The study of the wettability of powder inorganic pigments based on dynamic contact angle measurement using Wilhelmy method." Chemica **41**: 27-35.

Lafleur, M. P.-J., P. Eng and M. A. B. Ayad (2012). "NI 43-101 Technical Report to present the mineral resources of the rare earth elements zone Niobec Mine-IAMGOLD Corporation." Ste-Therese, QC, CA: 1-145.

Langevin, D., S. Poteau, I. Hénaut and J. Argillier (2004). "Crude oil emulsion properties and their application to heavy oil transportation." Oil & gas science and technology **59**(5): 511-521.

Leng, D. E. and R. V. Calabrese (2004). "Immiscible liquid–liquid systems." Handbook of Industrial Mixing: Science and Practice: 639-753.

Levine, S. and B. Bowen (1991). "Capillary interaction of spherical particles adsorbed on the surface of an oil/water droplet stabilized by the particles. Part I." Colloids and Surfaces **59**: 377-386.

Levine, S., B. D. Bowen and S. J. Partridge (1989). "Stabilization of emulsions by fine particles I. Partitioning of particles between continuous phase and oil/water interface." Colloids and surfaces **38**(2): 325-343.

Levine, S., B. D. Bowen and S. J. Partridge (1989). "Stabilization of emulsions by fine particles II. capillary and van der Waals forces between particles." Colloids and surfaces **38**(2): 345-364.

Li, C. C. and D. W. Fuerstenau (2013). "The synthesis and characterization of rare-earth fluocarbonates." KONA Powder and Particle Journal **30**(0): 193-200.

Liang, Y., N. Hilal, P. Langston and V. Starov (2007). "Interaction forces between colloidal particles in liquid: Theory and experiment." Advances in colloid and interface science **134**: 151-166.

Lifshitz, E. M. and M. Hamermesh (1992). The theory of molecular attractive forces between solids. Perspectives in Theoretical Physics, Elsevier**:** 329-349.

Liu, J., Z. Zhou, Z. Xu and J. Masliyah (2002). "Bitumen–clay interactions in aqueous media studied by zeta potential distribution measurement." Journal of colloid and interface science **252**(2): 409-418.

Liu, W., X. Wang, Z. Wang and J. Miller (2016). "Flotation chemistry features in bastnaesite flotation with potassium lauryl phosphate." Minerals Engineering **85**: 17-22.

Loudet, J.-C., A. G. Yodh and B. Pouligny (2006). "Wetting and contact lines of micrometer-sized ellipsoids." Physical review letters **97**(1): 018304.

M. Abdollahi Neisiania, M. L., J. Chaoukia, C. Chilian (2017). "Novel approach in k0-NAA for highly concentrated REE Samples." Talanta www.elsevier.com/locate/talanta.

Mankosa, M., J. Kohmuench, L. Christodoulou and E. Yan (2018). "Improving fine particle flotation using the StackCell™(raising the tail of the elephant curve)." Minerals Engineering **121**: 83-89.

Midmore, B. (1998). "Preparation of a novel silica-stabilized oil/water emulsion." Colloids and Surfaces A: Physicochemical and Engineering Aspects **132**(2): 257-265.

Mittal, K. L. and D. O. Shah (2013). Surfactants in solution, Springer Science & Business Media.

Navarro, J. and F. Zhao (2014). "Life-Cycle Assessment of the Production of Rare-Earth Elements for Energy Applications: A Review." Frontiers in Energy Research **2**: 45.

Ngai, T., S. H. Behrens and H. Auweter (2005). "Novel emulsions stabilized by pH and temperature sensitive microgels." Chemical communications(3): 331-333.

Nguyen, A., H. Schulze and J. Ralston (1997). "Elementary steps in particle—bubble attachment." International journal of mineral processing **51**(1): 183-195.

Ni, X., M. Parrent, M. Cao, L. Huang, A. Bouajila and Q. Liu (2012). "Developing flotation reagents for niobium oxide recovery from carbonatite Nb ores." Minerals Engineering **36**: 111-118.

Nikolaides, M., A. Bausch, M. Hsu, A. Dinsmore, M. Brenner, C. Gay and D. Weitz (2002). "Electric-field-induced capillary attraction between like-charged particles at liquid interfaces." Nature **420**(6913): 299-301.

Ofir, E., Y. Oren and A. Adin (2007). "Electroflocculation: the effect of zeta-potential on particle size." Desalination **204**(1): 33-38.

Owens, C., G. Nash, K. Hadler, R. Fitzpatrick, C. Anderson and F. Wall (2018). "Zeta potentials of the rare earth element fluorcarbonate minerals focusing on bastnäsite and parisite." Advances in Colloid and Interface Science.

Pashley, R. M. and J. N. Israelachvili (1984). "Molecular layering of water in thin films between mica surfaces and its relation to hydration forces." Journal of colloid and interface science **101**(2): 511-523.

Paul, E. L., V. A. Atiemo-Obeng and S. M. Kresta (2004). Handbook of industrial mixing: science and practice: , John Wiley & Sons :p66,185-186,368-370,560-562,1127.

Peters, M. S., K. D. Timmerhaus, R. E. West, K. Timmerhaus and R. West (1968). Plant design and economics for chemical engineers, McGraw-Hill New York.

Pichot, R., F. Spyropoulos and I. Norton (2009). "Mixed-emulsifier stabilised emulsions: Investigation of the effect of monoolein and hydrophilic silica particle mixtures on the stability against coalescence." Journal of colloid and interface science **329**(2): 284-291.

Pichot, R., F. Spyropoulos and I. Norton (2012). "Competitive adsorption of surfactants and hydrophilic silica particles at the oil–water interface: interfacial tension and contact angle studies." Journal of colloid and interface science **377**(1): 396-405.

Pickering, S. U. (1907). "Cxcvi.—emulsions." Journal of the Chemical Society, Transactions **91**: 2001-2021.

Ramsden, W. (1903). "Separation of Solids in the Surface-Layers of Solutions and'Suspensions'(Observations on Surface-Membranes, Bubbles, Emulsions, and Mechanical Coagulation).--Preliminary Account." Proceedings of the Royal Society of London: 156-164.

Rapacchietta, A. and A. Neumann (1977). "Force and free-energy analyses of small particles at fluid interfaces: II. Spheres." Journal of Colloid and Interface Science **59**(3): 555-567.

Rezvantalab, H. and S. Shojaei-Zadeh (2013). "Capillary interactions between spherical Janus particles at liquid–fluid interfaces." Soft Matter **9**(13): 3640-3650.

Rinne, A. and A. Peltola (2008). "On lifetime costs of flotation operations." Minerals Engineering **21**(12-14): 846-850.

Safari, M., M. Harris, D. Deglon, L. Leal Filho and F. Testa (2016). "The effect of energy input on flotation kinetics." International Journal of Mineral Processing **156**: 108-115.

Salazar, K. and M. K. McNutt (2013). Mineral Commodity Summary 2013, U.S. Geological Survey.

Satur, J. V., B. P. Calabia, M. Hoshino, S. Morita, Y. Seo, Y. Kon, T. Takagi, Y. Watanabe, L. Mutele and S. Foya (2016). "Flotation of rare earth minerals from silicate–hematite ore using tall oil fatty acid collector." Minerals Engineering **89**: 52-62.

Schena, G., J. Villeneuve and Y. Noël (1996). "A method for a financially efficient design of cell-based flotation circuits." International journal of mineral processing **46**(1-2): 1-20.

Scientific, H. (2012). A guidebook to particle size analysis, Irvine, CA: Horiba Instruments, Inc.

Simon, S., S. Theiler, A. Knudsen, G. Øye and J. Sjöblom (2010). "Rheological properties of particle-stabilized emulsions." Journal of Dispersion Science and Technology **31**(5): 632-640.

Spelt, J. and A. Neumann (1987). "Solid surface tension: the equation of state approach and the theory of surface tension components. Theoretical and conceptual considerations." Langmuir **3**(4): 588-591.

Sprecher, B., Y. Xiao, A. Walton, J. Speight, R. Harris, R. Kleijn, G. Visser and G. J. Kramer (2014). "Life cycle inventory of the production of rare earths and the subsequent production of NdFeB rare earth permanent magnets." Environmental science & technology **48**(7): 3951-3958.

Tabosa, E., K. Runge, P. Holtham and K. Duffy (2016). "Improving flotation energy efficiency by optimizing cell hydrodynamics." Minerals Engineering **96**: 194-202.

Tadros, T. F. (2009). Emulsion science and technology: a general introduction, Wiley-VCH Verlag GmbH & Co. KGaA.

Tambe, D. E. and M. M. Sharma (1994). "The effect of colloidal particles on fluid-fluid interfacial properties and emulsion stability." Advances in colloid and interface science **52**: 1-63.

Tarimala, S. and L. L. Dai (2004). "Structure of microparticles in solid-stabilized emulsions." Langmuir **20**(9): 3492-3494.

Thompson, W., A. Lombard, E. Santiago and A. Singh (2012). Mineralogical Studies in Assisting Beneficiation of Rare Earth Element Minerals from Carbonatite Deposits. Proceedings of the 10th International Congress for Applied Mineralogy (ICAM), Springer.

Tsabet, È. (2014). "De la Particule au Procédé: Modélisation de la Production d'Émulsions de Pickering." 18-138.

Tsabet, È. and L. Fradette (2015). "Effect of processing parameters on the production of Pickering emulsions." Industrial & Engineering Chemistry Research **54**(7): 2227-2236.

Tsabet, È. and L. Fradette (2015). "Effect of the properties of oil, particles, and water on the production of Pickering emulsions." Chemical Engineering Research and Design **97**: 9-17.

Tsabet, È. and L. Fradette (2016). "Study of the properties of oil, particles, and water on particle adsorption dynamics at an oil/water interface using the colloidal probe technique." Chemical Engineering Research and Design **109**: 307-316.

Tsouris, C. and L. Tavlarides (1994). "Breakage and coalescence models for drops in turbulent dispersions." AIChE Journal **40**(3): 395-406.

Tuinier, R. and C. De Kruif (1999). "Phase separation, creaming, and network formation of oil-in-water emulsions induced by an exocellular polysaccharide." Journal of Colloid and Interface Science **218**(1): 201-210.

Ulrich, G. D. (1984). A guide to chemical engineering process design and economics, Wiley New York: p295.

Van Gosen, B. S., P. L. Verplanck, K. R. Long, J. Gambogi and R. R. Seal II (2014). The rare-earth elements: vital to modern technologies and lifestyles, US Geological Survey.

Vignati, E., R. Piazza and T. P. Lockhart (2003). "Pickering emulsions: interfacial tension, colloidal layer morphology, and trapped-particle motion." Langmuir **19**(17): 6650-6656.

Wan, B. and L. Fradette (2017). "Phase inversion of a solid-stabilized emulsion: Effect of particle concentration." The Canadian Journal of Chemical Engineering **95**(10): 1925-1933.

Whitby, C. P., D. Fornasiero and J. Ralston (2010). "Structure of oil-in-water emulsions stabilised by silica and hydrophobised titania particles." Journal of colloid and interface science **342**(1): 205-209.

Wills, B. A. and J. Finch (2015). Wills' mineral processing technology: an introduction to the practical aspects of ore treatment and mineral recovery, Butterworth-Heinemann: p4-22, 95-122, 458-462.

Xia, L., B. Hart, S. Chelgani and K. Douglas (2014). Hydroxamate collectors for rare earth minerals flotation, Conference of Metallurgists Proceedings ISBN: 978-1-926872-24-7.

Xia, L., B. Hart and B. Loshusan (2015). "A Tof-SIMS analysis of the effect of lead nitrate on rare earth flotation." Minerals Engineering **70**: 119-129.

Xiong, W., J. Deng, B. Chen, S. Deng and D. Wei (2018). "Flotation-magnetic separation for the beneficiation of rare earth ores." Minerals Engineering **119**: 49-56.

Xuefang, X. (1985). A New Collector for Bastnaesite and a Preliminary Analysis of its Flotation Capabilities. New Frontiers in Rare Earth Science and Applications**:** 75-78.

Yan, N., M. R. Gray and J. H. Masliyah (2001). "On water-in-oil emulsions stabilized by fine solids." Colloids and Surfaces A: Physicochemical and Engineering Aspects **193**(1): 97-107.

Yan, N., C. Kurbis and J. H. Masliyah (1997). "Continuous demulsification of solids-stabilized oil-in-water emulsions by the addition of fresh oil." Industrial & engineering chemistry research **36**(7): 2634-2640.

Yan, N. and J. H. Masliyah (1994). "Adsorption and desorption of clay particles at the oil-water interface." Journal of colloid and interface science **168**(2): 386-392.

Yan, N. and J. H. Masliyah (1995). "Characterization and demulsification of solids-stabilized oil-in-water emulsions Part 1. Partitioning of clay particles and preparation of emulsions." Colloids and Surfaces A: Physicochemical and Engineering Aspects **96**(3): 229-242.

Yan, N. and J. H. Masliyah (1995). "Characterization and demulsification of solids-stabilized oil-in-water emulsions Part 2. Demulsification by the addition of fresh oil." Colloids and Surfaces A: Physicochemical and Engineering Aspects **96**(3): 243-252.

Yan, N. and J. H. Masliyah (1996). "Demulsification of solids-stabilized oil-in-water emulsions." Colloids and Surfaces A: Physicochemical and Engineering Aspects **117**(1): 15-25.

Yan, N. and J. H. Masliyah (1996). "Effect of pH on adsorption and desorption of clay particles at oil–water interface." Journal of colloid and interface science **181**(1): 20-27.

Yan, N. and J. H. Masliyah (1997). "Creaming behavior of solids-stabilized oil-in-water emulsions." Industrial & engineering chemistry research **36**(4): 1122-1129.

Yang, F., S. Liu, J. Xu, Q. Lan, F. Wei and D. Sun (2006). "Pickering emulsions stabilized solely by layered double hydroxides particles: The effect of salt on emulsion formation and stability." Journal of Colloid and Interface Science **302**(1): 159-169.

Yang, X., J. V. Satur, K. Sanematsu, J. Laukkanen and T. Saastamoinen (2015). "Beneficiation studies of a complex REE ore." Minerals Engineering **71**: 55-64.

Yang, X. J., A. Lin, X.-L. Li, Y. Wu, W. Zhou and Z. Chen (2013). "China's ion-adsorption rare earth resources, mining consequences and preservation." Environmental Development **8**: 131-136.

Yuan, Y. and T. R. Lee (2013). Contact angle and wetting properties. Surface science techniques, Springer**:** 3-34.

Zhang, H. and X. Zhang (2019). "Microalgal harvesting using foam flotation: A critical review." Biomass and Bioenergy **120**: 176-188.

Zhang, J. and C. Edwards (2012). A Review of Rare Earth Mineral Processing Technology. 44th Annual Canadian Mineral Processors Operators Conference. Ottawa, Ontario. **79**.

Zhang, X. (2014). Surface chemistry aspects of flourite and bastnaesite flotation systems, The University of Utah: 88-146.

APPENDIX A – MASS BALANCE

The mass balance is calculated in each stream feed (F), overflow (O) and underflow (U) using numerical particle size distribution data (PSD). We used PSD which are going to each one of these streams:

$$(q_F)_i = \frac{n_{Fi}}{\sum n_{Fi}} \ , \ (q_O)_i = \frac{n_{Oi}}{\sum n_{Oi}} \ , \ (q_U)_i = \frac{n_{Ui}}{\sum n_{Ui}} \quad 9.1$$

$$\sum n_{Ui} + \sum n_{Oi} = \sum n_{Fi} \quad 9.2$$

$$m_F = \rho_p \sum n_{Fi}(k_3)_i {x_i}^3 \quad 9.3$$

$$m_O = \rho_p \sum n_{Oi}(k_3)_i {x_i}^3 = \rho_p k_3 \sum n_{Oi} \sum q_{Oi} {x_i}^3$$

$$m_U = \rho_p \sum n_{Ui}(k_3)_i {x_i}^3 = \rho \ k_3 \sum n_{Ui} \sum q_{Ui} {x_i}^3$$

$$\sum n_{Fi} = \frac{m_O}{\rho_p k_3 \sum q_{Oi} {x_i}^3} + \frac{m_U}{\rho_p k_3 \sum q_{Ui} {x_i}^3} \quad 9.4$$

Where n_i is number of particles in size interval x_i, , k is a particle shape factor, ρ_p is particle density, m_F mass of particles in the feed stream, m_O mass of particles attached to droplets in overflow, m_U mass of non-emulsified particles in underflow and q_i is a numerical size distribution density in size interval x_i (Wills and Finch 2015) (Bazin and Hodouin 2001, Scientific 2012). By applying a proportional relation in mass continuity equations between each stream, we are able to calculate the mass fractions. However, we should highlight the assumptions that i.e. density and shape factor remain similar for all particles:

$$\frac{m_O}{m_F} = r \ , \ \frac{m_U}{m_F} = r' = 1 - r \tag{9.5}$$

$$\frac{\rho k_3 \sum n_{Fi}}{m_F} = \frac{1}{\sum q_{Fi} x_i{}^3} = \frac{r}{\sum q_{Oi} x_i{}^3} + \frac{1-r}{\sum q_{Ui} x_i{}^3} \tag{9.6}$$

$$\frac{m_O}{m_F} = r \ = \frac{1 - \frac{\sum q_{Fi} x_i{}^3}{\sum q_{Ui} x_i{}^3}}{\frac{\sum q_{Fi} x_i{}^3}{\sum q_{Oi} x_i{}^3} - \frac{\sum q_{Fi} x_i{}^3}{\sum q_{Ui} x_i{}^3}} = \frac{\frac{1}{\sum q_{Fi} x_i{}^3} - \frac{1}{\sum q_{Ui} x_i{}^3}}{\frac{1}{\sum q_{Oi} x_i{}^3} - \frac{1}{\sum q_{Ui} x_i{}^3}} \tag{9.7}$$

$$\frac{m_U}{m_F} = r' = \frac{1 - \frac{\sum q_{Fi} x_i{}^3}{\sum q_{Oi} x_i{}^3}}{\frac{\sum q_{Fi} x_i{}^3}{\sum q_{Ui} x_i{}^3} - \frac{\sum q_{Fi} x_i{}^3}{\sum q_{Oi} x_i{}^3}} = \frac{\frac{1}{\sum q_{Fi} x_i{}^3} - \frac{1}{\sum q_{Oi} x_i{}^3}}{\frac{1}{\sum q_{Ui} x_i{}^3} - \frac{1}{\sum q_{Oi} x_i{}^3}} \tag{9.8}$$

$$\frac{m_O}{m_U} = \frac{\sum q_{Oi} x_i{}^3}{\sum q_{Ui} x_i{}^3} \times \frac{(\sum q_{Fi} x_i{}^3 - \sum q_{Ui} x_i{}^3)}{(\sum q_{Oi} x_i{}^3 - \sum q_{Fi} x_i{}^3)} \tag{9.9}$$

APPENDIX B – OBTAINING THE GRADE BY IMAGE ANALYSIS (IMGA)

In fact, samples of interest were put in the vials and once the sediment of minerals stick well to the bottom, photos were taken from the upside down vials in a symmetric arrangement (Figure 9.1). Later on, the photos were analyzed by the ImageJ software.

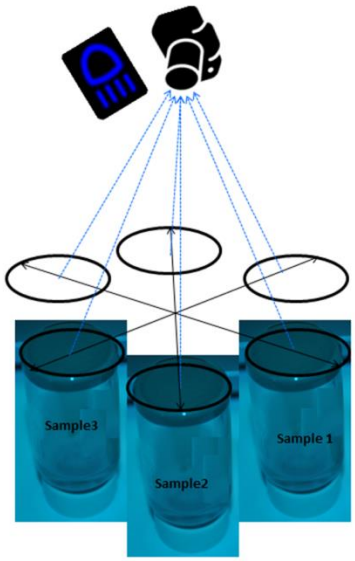

Figure 9.1 Mineral samples with symmetric arrangement in the upside down vials to take the photos

The ImageJ software provides the level of brightness in the RGB standard format which is a value between 0 and 256 for each red, green and blue pixel colors. Since the REE bearing minerals have specific light absorption behavior, i.e. wave length absorbance, the brightness level of samples differs via grade of the rare earth elements(Aneus 1965). In fact, a higher grade or concentration of REE bearing minerals results in a lower RGB brightness level for a given sample. Taking this behavior into account, brightness level of a sample of fresh ore (BFO) and brightness level of a concentrate of ore (BCO) were measured and a parameter called brightness level ratio (BLR) was defined (9.11). The grade of this concentrate was obtained by NAA and in fact considered as a calibrated indicator for extreme of beneficiation. In other words, a BLR value close to 100% indicates that the experimental sample had a low grade close to CSF of fresh ore. Figure 4.21 compares REE grade data of the three feeds with a -37 µm size by NAA versus their estimated BLR values. As expected, BLR varied in opposite to the trend of REE grade. We calibrate the IMGA method for any unknown samples using NAA results. A linier function was

observed (Figure 4.22). Thus, the preliminary calibration was performed between F.O and concentrated ore of 7% TREE whereas both come from physical beneficiation and their BLRs show a linier function versus concentration. To justify the approach, the upper and lower concentration points were always indicated by NAA on which the middle point were estimated by IMGA. This quick and simple approach establishes a quantitative method to estimate the grade in an unknown sample.

$$\frac{(\mathrm{B.F.O.}-\mathrm{B.S.}) \times (\mathrm{E.C.O.}-\mathrm{E.F.O.})}{\mathrm{B.F.O.}-\mathrm{B.C.O.}} + \mathrm{E.F.O.} = \mathrm{E.S.} \qquad 9.10$$

Where B.F.O. is level of brightness emitted from fresh ore, B.S. is level of brightness emitted from the sample, B.C.O. is level of brightness emitted from calibrated sample ore, E.C.O. is elemental assay of calibrated sample ore, E.F.O. is elemental assay of fresh ore and E.S. is elemental assay of the sample:

$$\frac{\mathrm{B.F.O.}-\mathrm{B.S.}}{\mathrm{B.F.O.}-\mathrm{B.C.O.}} = \text{Brightness level ratio "BLR"} \qquad 9.11$$

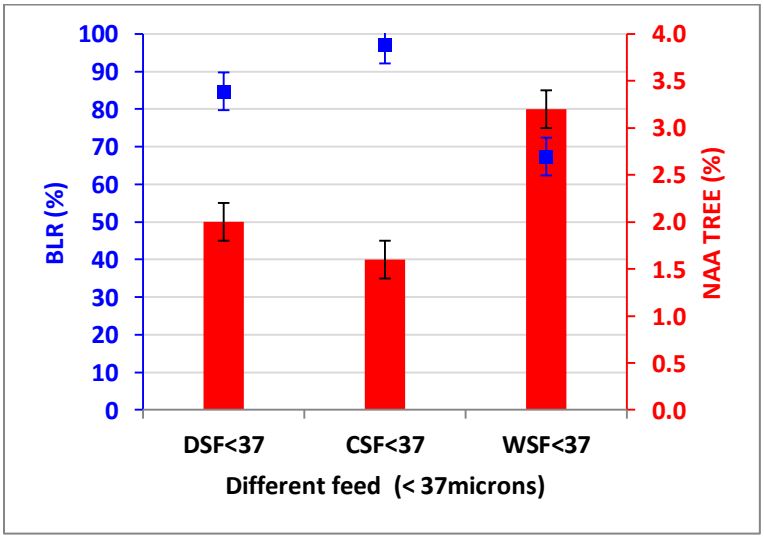

Figure 9.2 Obtaining the grade by IMGA when compared with NAA results

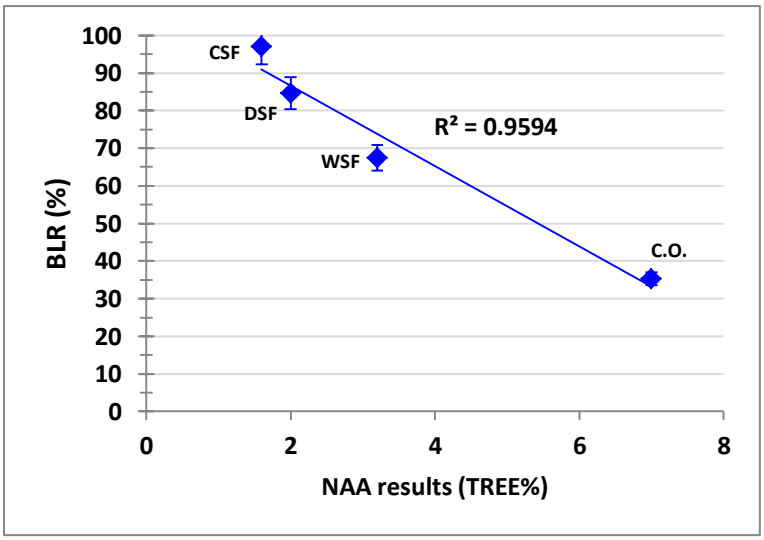

Figure 9.3 Correlation of IMGA results with NAA, the first three points from DSF, CSF and WSF feed samples and 4th point is the concentrated ore from emulsification

APPENDIX C –PARTICLE SIZE CLASS ATTACHMENT

Feed size fewer than -63µm was prepared to investigate the mass fractions of each particle size class attached into the interface. The all size classes belong to feed -63µm and the mass fractions of each size intervals were calculated based on the mass distribution balance (Appendix A). The mass of particles of cut size interval (i) in the overflow (particles attached to the droplets) over the mass of the same size interval (i) in the feed is shown as function of each cut size. Figure 4.23 clearly indicates that lower size has tendency to attach more into the oil droplet interface. The trend for DSF and CSF at -37µm is interesting when compared with WSF. There are fine particles accumulated in WSF under -37µm while the fine particles which are remained attached to coarse particles makes the differences for DSF and CSF at bigger cut sizes.

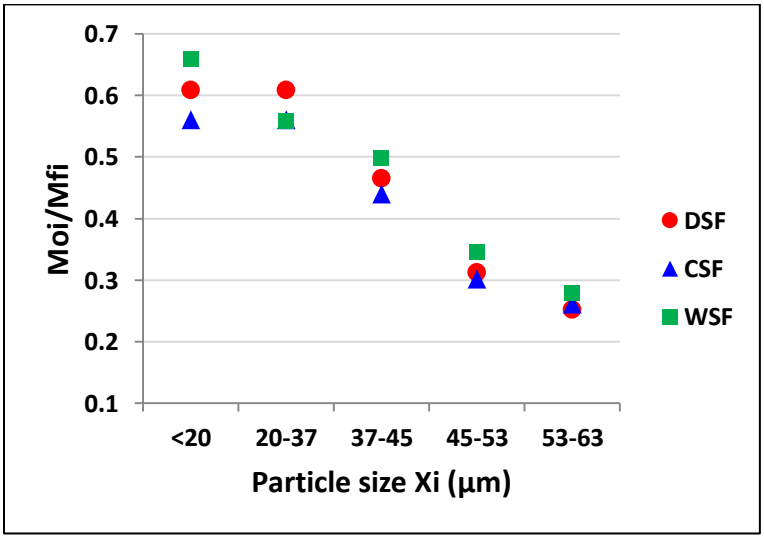

Figure 9.4 Overflow particle size attachment, ($Feeds\ are - 63\ \mu m, \Phi_d$=9%, PDMS oil 50 cSt, Ms=5%, 15minPBT@1000 rpm)

APPENDIX D – QEMSCAN NIOBEC ORE

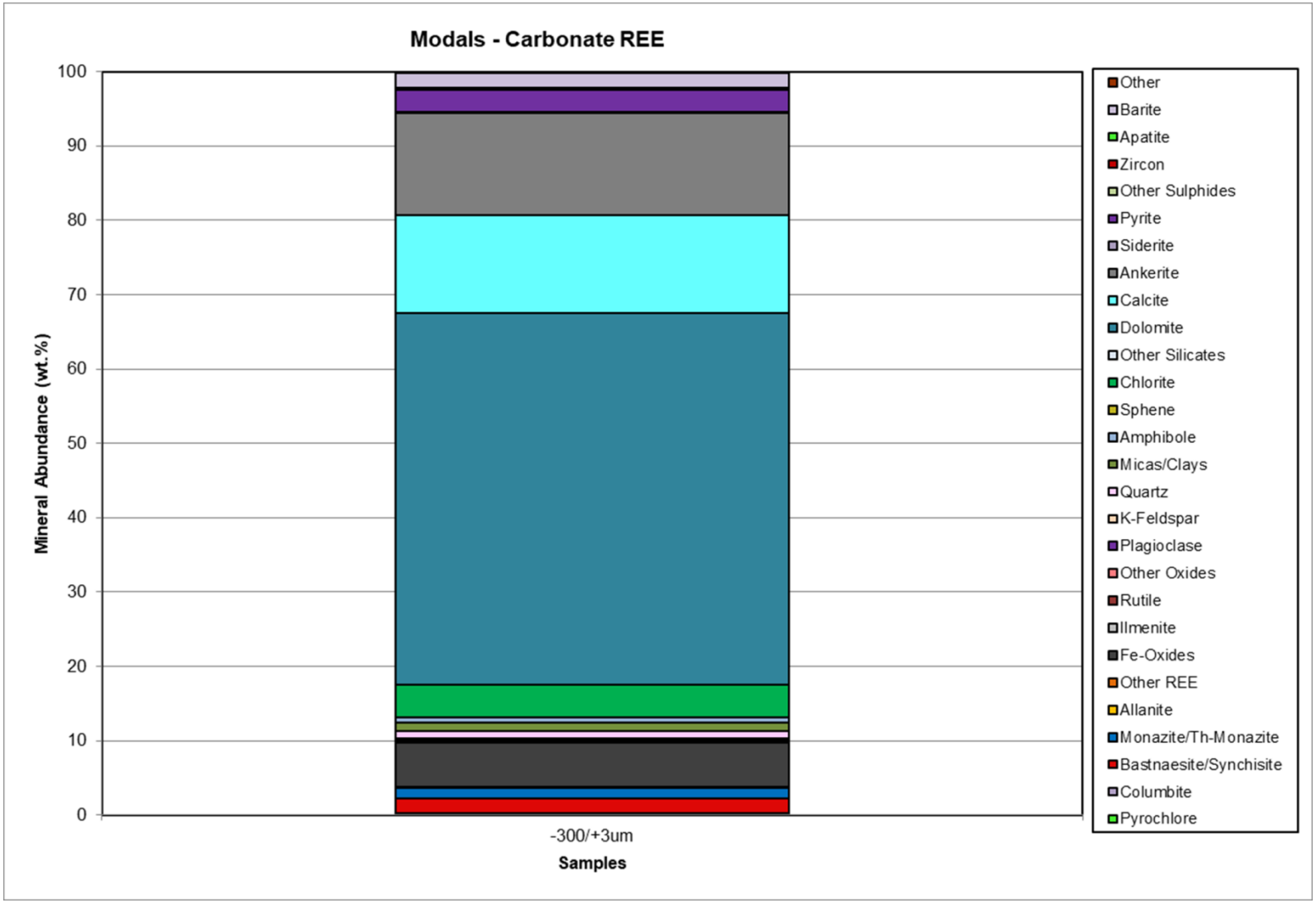

Monazite Association

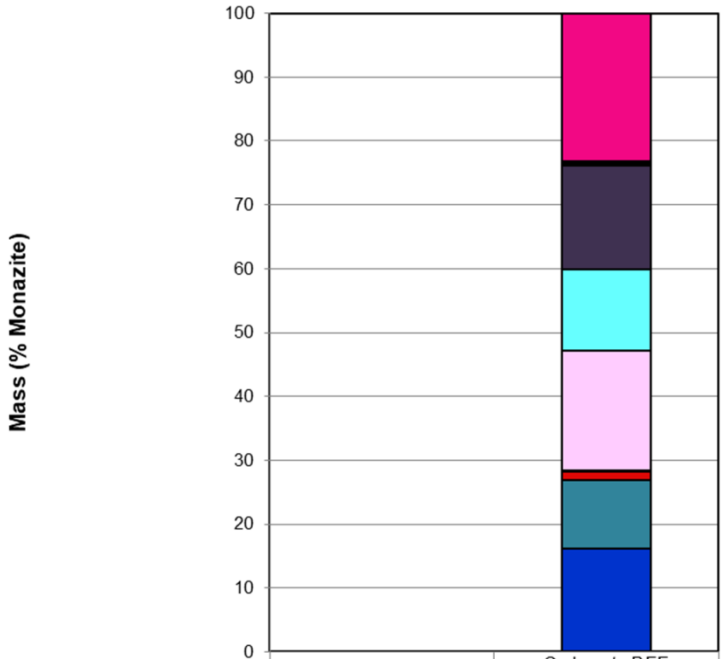

		Carbonate REE
Monazite Complex		23.2
Monazite:Other		0.00
Monazite:Zircon		0.01
Monazite:Barite		0.36
Monazite:Sulphides		0.30
Monazite:Apatite		0.04
Monazite:Carbonates:Silicates		16.2
Monazite:Carbonates		12.7
Monazite:Silicates		18.7
Monazite:Ti-Oxides		0.04
Monazite:Fe-Oxides		0.06
Monazite:Other REE		0.03
Monazite:Allanite		0.05
Monazite:Bastnaesite/Synchisite		1.33
Monazite:Nb-Minerals		0.05
Liberated Monazite		10.6
Free Monazite		16.2

Bastnaesite Association

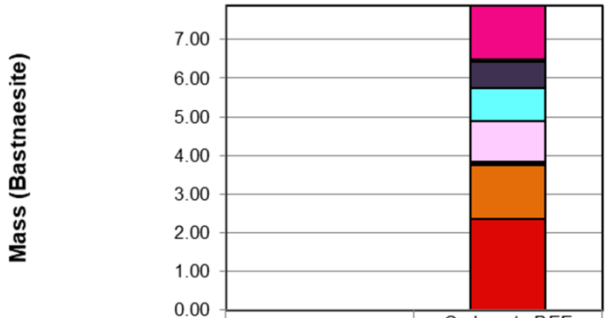

		Carbonate REE
Bastnaesite Synchisite Complex		1.42
Bastnaesite Synchisite :Other		0.00
Bastnaesite Synchisite:Zircon		0.00
Bastnaesite Synchisite:Barite		0.03
Bastnaesite Synchisite:Sulphides		0.03
Bastnaesite Synchisite:Apatites		0.00
Bastnaesite Synchisite :Carbonates:Silicates		0.67
Bastnaesite Synchisite :Carbonates		0.85
Bastnaesite Synchisite :Silicates		1.06
Bastnaesite Synchisite :Ti-Oxides		0.00
Bastnaesite Synchisite :Fe-Oxides		0.01
Bastnaesite Synchisite :Other REE		0.00
Bastnaesite Synchisite :Monazite/Th-Monazite		0.07
Bastnaesite Synchisite :Allanite		0.01
Bastnaesite Synchisite :Nb-Minerals		0.00
Liberated Bastnaesite Synchisite		1.38
Free Bastnaesite Synchisite		2.36